

SHEAR STRENGTH AND DETERIORATION OF SHORT
LIGHTWEIGHT REINFORCED CONCRETE COLUMNS
UNDER CYCLIC DEFORMATIONS

APPROVED:

In loving memory
of
my father

SHEAR STRENGTH AND DETERIORATION OF SHORT
LIGHTWEIGHT REINFORCED CONCRETE COLUMNS
UNDER CYCLIC DEFORMATIONS

BY

MARK EDWARD MOORE, B.S.C.E.

THESIS

Presented to the Faculty of the Graduate School of
The University of Texas at Austin
in Partial Fulfillment
of the Requirements
for the Degree of

MASTER OF SCIENCE IN ENGINEERING

THE UNIVERSITY OF TEXAS AT AUSTIN

May 1982

A C K N O W L E D G M E N T S

The author wishes to express his sincere gratitude to Dr. J. O. Jirsa for his invaluable direction and assistance throughout the test program and the writing of this report, and also for his concerned guidance of the author's program of graduate study at The University of Texas. Dr. John E. Breen of the Civil Engineering faculty of The University of Texas also assisted in making many valuable comments on the preliminary draft of this report.

This report was funded by Grant No. ENV77-20816 from the National Science Foundation's Directorate for Applied Science and Research Applications, Division of Problem-Focused Research. The lightweight aggregate used in this project was provided by the Lightweight Processing Company of Glendale, California.

The author would like to extend his gratitude to Mr. Hideteke Umehara and Mr. Roberto Leon for their many valuable suggestions, endless encouragement and wonderful friendship throughout the test program. The author is indebted to his fellow graduate students, Jefferson Reeder, Paul Murray and Neil Cichy, who helped in so many ways during the course of this program, but most importantly provided the author with friendship and enthusiastic encouragement. Appreciation is expressed for the willing cooperation and helpful advice of the Ferguson Structural Engineering Laboratory staff.

The author is very grateful to his mother for her constant love and encouragement throughout his engineering studies.

Finally, the author would like to express his deepest love and gratitude to his wife Carrie, for her neverending love, patience and understanding.

M.E.M.
April 1982

T A B L E O F C O N T E N T S

Chapter		Page
1	INTRODUCTION	1
	1.1 Background	1
	1.2 Lightweight Concrete in Structures	2
	1.3 Short Columns in Structures	2
	1.4 Scope of This Study	3
2	EXPERIMENTAL PROGRAM	7
	2.1 Introduction	7
	2.2 Overall Program	7
	2.3 Test Specimen	9
	2.3.1 Design Requirements	9
	2.3.2 Specimen Detail	10
	2.3.3 Calculated Strength	12
	2.3.4 Specimen Fabrication	14
	2.4 Materials	14
	2.4.1 Lightweight Concrete	14
	2.4.2 Normalweight Concrete	18
	2.4.3 Reinforcing Steel	20
	2.5 Test Frame and Instrumentation	22
	2.5.1 Introduction	22
	2.5.2 Loading System	22
	2.5.3 Instrumentation	29
	2.5.4 Data Acquisition	29
	2.6 Loading Sequence	33
3	BEHAVIOR OF LIGHTWEIGHT SPECIMENS	35
	3.1 Introduction	35
	3.2 Description of Test Results	36
	3.2.1 Load-Deflection Curves	36
	3.2.2 Peak Lateral Forces	36
	3.2.3 Crack Patterns	43

Chapter	Page
4	BEHAVIOR OF NORMALWEIGHT SPECIMENS 48
4.1	Introduction 48
4.2	Description of Test Results 48
4.2.1	Load-Deflection Curves 48
4.2.2	Peak Lateral Forces 53
4.2.3	Crack Patterns 53
5	COMPARISON OF TEST RESULTS 60
5.1	Introduction 60
5.2	Test Results 60
5.2.1	Specimen Stiffness 60
5.2.2	Shear Strength and Deterioration due to Cycling 72
5.2.3	Crack Patterns 72
5.3	Discussion of Test Results 79
6	SUMMARY AND CONCLUSIONS 88
6.1	Summary of Study 88
6.2	Summary of Test Results 89
6.2.1	Lightweight Concrete Specimens 89
6.2.2	Normalweight Concrete Specimens 89
6.2.3	Comparison of Lightweight and Normalweight Tests 90
6.3	Conclusions 90
APPENDIX A	Peak Values LW1 92
APPENDIX B	Peak Values LW2 94
APPENDIX C	Peak Values NW1 96
APPENDIX D	Peak Values NW2 98
BIBLIOGRAPHY 100

L I S T O F T A B L E S

Table	Page
2.1 Concrete Properties	18
2.2 Steel Properties	20
5.1 Comparison of Initial Specimen Stiffness	83
5.2 Comparison of Normalized Peak Lateral Loads	85
5.3 Comparison of Normalized Peak Horizontal Shears	86

L I S T O F F I G U R E S

Figure	Page
1.1 Captive columns	4
1.2 Fixed end member	5
1.3 Failed columns at Misawa Commercial High School-- Tokachi-Oki Earthquake, Japan, 1968	6
2.1 Specimen details	11
2.2 Formwork assembly	15
2.3 Concrete compressive strength gain curve	17
2.4 Stress-strain relationship for lightweight concrete	19
2.5 Stress-strain curve for steel reinforcement	21
2.6 Floor-wall reaction system	23
2.7 Loading rams	24
2.8 Test setup	25
2.9 Restraining rams	27
2.10 Vertical and horizontal positioning system	28
2.11 Linear potentiometer locations	30
2.12 Linear potentiometer mounting frame	31
2.13 Strain gage locations	32
2.14 Lateral loading sequence	34
3.1 Load-deflection curve, test LW1 north-south direction	37
3.2 Load-deflection curve, test LW1 east-west direction	38
3.3 Load-deflection curve, test LW2 north-south direction	39
3.4 Load-deflection curve, test LW2 east-west direction	40
3.5 Envelopes of load-deflection, tests LW1 and LW2, north-south direction	41
3.6 Envelopes of load-deflection, tests LW1 and LW2, east-west direction	42
3.7 Shear deterioration, test LW1 and LW2	44
3.8 Crack patterns, test LW1 east face	45

Figure	Page
3.9 Crack patterns, test LW2 east face	46
4.1 Load-deflection curves, test NW1 north-south direction	49
4.2 Load-deflection curve, test NW1 east-west direction . .	50
4.3 Load-deflection curve, test NW2 north-south direction .	51
4.4 Load-deflection curve, test NW2 east-west direction . .	52
4.5 Envelopes of load-deflection, tests NW1 and NW2, north-south direction	54
4.6 Envelopes of load-deflection, tests NW1 and NW2, east-west direction	55
4.7 Shear deterioration, test NW1 and NW2	56
4.8 Crack pattern, test NW1	57
4.9 Crack patterns, test NW2	59
5.1 Load-deflection curves, tests LW1 and NW1, one cycle at $1\Delta_i$	61
5.2 Load-deflection curves, tests LW1 and NW1, three cycles at $1\Delta_i$	62
5.3 Load-deflection curves, test LW1 and NW1, one cycle at $2\Delta_i$	63
5.4 Load-deflection curves, tests LW1 and NW1, three cycles at $2\Delta_i$	64
5.5 Load-deflection curves, tests LW1 and NW1, one cycle at $3\Delta_i$ (0.60 in.)	65
5.6 Load-deflection curve, tests LW2 and NW2, one cycle at $1\Delta_i$	67
5.7 Load-deflection curve, tests LW2 and NW2, three cycles at $1\Delta_i$	68
5.8 Load-deflection curves, tests LW2 and NW2, one cycle at $2\Delta_i$	69
5.9 Load-deflection curves, tests LW2 and NW2, three cycles at $2\Delta_i$	70
5.10 Load-deflection curves, tests LW2 and NW2, one cycle at $3\Delta_i$ (0.60 in.)	71
5.11 Envelopes of load-deflection for LW1 and NW1, north-south loading	73

Figure		Page
5.12	Envelopes of load-deflection for LW1 and NW1, east-west loading	74
5.13	Shear deterioration for LW1 and NW1	75
5.14	Envelopes of load-deflection for LW2 and NW2, north-south loading	76
5.15	Envelopes of load-deflection for LW2 and NW2, east-west loading	77
5.16	Shear deterioration of LW2 and NW2	78
5.17	Crack pattern for LW1 and NW1	80
5.18	Crack pattern for LW2 and NW2	81

N O T A T I O N

a	Shear span, in.
A	Gross area of column cross section, in ² .
A_c	Area of concrete core, out-to-out of ties, in ² .
A_s	Area of longitudinal tension reinforcement, in ² .
A_v	Area of transverse reinforcement within a distance s_h , in ² .
b	Section width, in.
d	Distance from extreme compression fiber to the centroid of the tension reinforcement, in.
E_c	Young's modulus for concrete, psi
E_s	Young's modulus for longitudinal reinforcement, psi
f'_c	Concrete compressive strength, psi
f_{ct}	Average splitting tensile strength of concrete, psi
f_{yt}	Tensile yield strength of transverse reinforcement, psi
f_{su}	Ultimate tensile strength of longitudinal reinforcement, psi
L	Length of column, in.
L'	Reduced length of column, in.
M	Bending moment, lb.-in.
N	Applied axial compression, lbs.
P_b	Nominal axial load strength at balanced strain conditions, lbs.
V	Shear force on section, lbs.
V_c	Nominal shear strength provided by concrete, lbs.
V_n	Nominal shear strength in ACI 318-77, $V_c + V_s$, lbs.
V_s	Nominal shear strength provided by transverse reinforcement, lbs.

V_u Design shear force, lbs.
 Δ Deflection, in.
 ϵ_c Strain of concrete, in./in.
 ϵ_s Strain of reinforcement, in./in.
 ρ Ratio of longitudinal extreme tension reinforcement, A_s/bd
 ϕ Strength reduction factor

C H A P T E R 1

INTRODUCTION

1.1 Background

The use of lightweight concrete in earthquake resistant structures has often been proposed as an alternate to normalweight concrete because of the reduction in weight of the structure and the associated reduction of lateral forces under seismic excitation. In order to utilize lightweight concrete properly as a structural building material, an understanding of the performance of the material in structural applications must be made. To date there has been only a minimal amount of research conducted to study the structural behavior of lightweight concrete members subjected to simulated earthquake loadings. During a period of strong ground motions, column members are a critical part of the lateral load resisting mechanism of a structure. The random orientation of ground motions subjects column members to multidirectional cyclic lateral load variations. It has been previously assumed that bidirectional loading sequences can be accounted for by modeling the structure as a planar frame and considering each orthogonal direction independently. The use of the simplified design approach was justified by lack of information regarding structural behavior under two-dimensional lateral loadings and the complex and time consuming nature of a two-dimensional analysis of a multistory multibay structure. It was generally considered unlikely that maximum deformations or lateral forces would occur in orthogonal directions simultaneously.

Recently reported earthquake damage studies raised questions regarding present methods of design for columns. The San Fernando

1971 and Tokachi-Oki 1968 earthquakes provided full-scale tests of structural frames subjected to strong ground motions. Following the San Fernando earthquake, the damage to the Olive View Hospital was studied extensively.^{1,2,3,4,5,6} These studies showed that employing one-dimensional procedures did not explain the observed damage and that the behavior of lightweight concrete members was not accurately predicted using current methods based on normalweight concrete properties.^{7,8,9}

1.2 Lightweight Concrete in Structures

The use of lightweight aggregate and "all lightweight" concrete for structural components in seismic regions has been promoted because of the apparent advantages. The use of normalweight concrete in seismic regions has been criticized because of the materials' low strength-to-weight ratio. Lightweight concrete of equivalent strength offers a more desirable strength-to-weight ratio. Making use of lightweight concrete also reduces the total mass of a structure lessening the inertia forces that must be resisted due to a strong ground motion.

There are significant differences in the behavior of lightweight and normalweight concretes.^{8,10,11,12,13,14} The use of lightweight concrete in seismic regions without properly accounting for the differences in mechanical behavior might result in an unconservative design.

1.3 Short Columns in Structures

In general, the use of short columns likely to fail in shear should be avoided in seismic design because of poor load-deformation characteristics exhibited. Shear dominated behavior in columns is most common in members where the shear span-to-depth ratio is less than 2.5.^{15,16,17,18} Short columns are incorporated into structural

systems either as part of the original design or as a result of structural changes made during the life of the structure. Members originally designed as short columns generally may not pose significant problems when subjected to lateral loads because the designer should be aware of the geometry of the column. However, in many cases "unintentional" short columns are produced and can be termed "captive" columns.¹⁸ Captive columns result from the reduction of the clear column height due to stiff, often nonstructural members that restrict the lateral deformation of the column over a portion of its length. Figure 1.1 illustrates the concept of the captive column. The original column may have been properly designed to resist both moment and shear forces by insuring that the flexural capacity of the member is developed before shear failure occurs. The shear and moment are related by the length of the member as shown in Fig. 1.2. A captive column is likely to fail in shear if not properly designed to resist the shear force associated with the members flexural capacity and reduced length. Structural investigations conducted following many earthquakes report failures of columns restrained by other elements (often nonstructural) over some portion of the original design length.^{5,6,19} Figure 1.3 illustrates the failure of a short column.

1.4 Scope of This Study

The objective of this study is to evaluate the shear strength and response of lightweight reinforced concrete short columns subjected to cyclic bidirectional lateral loads. Results of the lightweight concrete columns are compared to similar test specimens constructed with normalweight concrete. Variations in ultimate lateral capacity, stiffness and deterioration due to cycling are examined. Tests are conducted on specimens both with and without an axial compressive load.

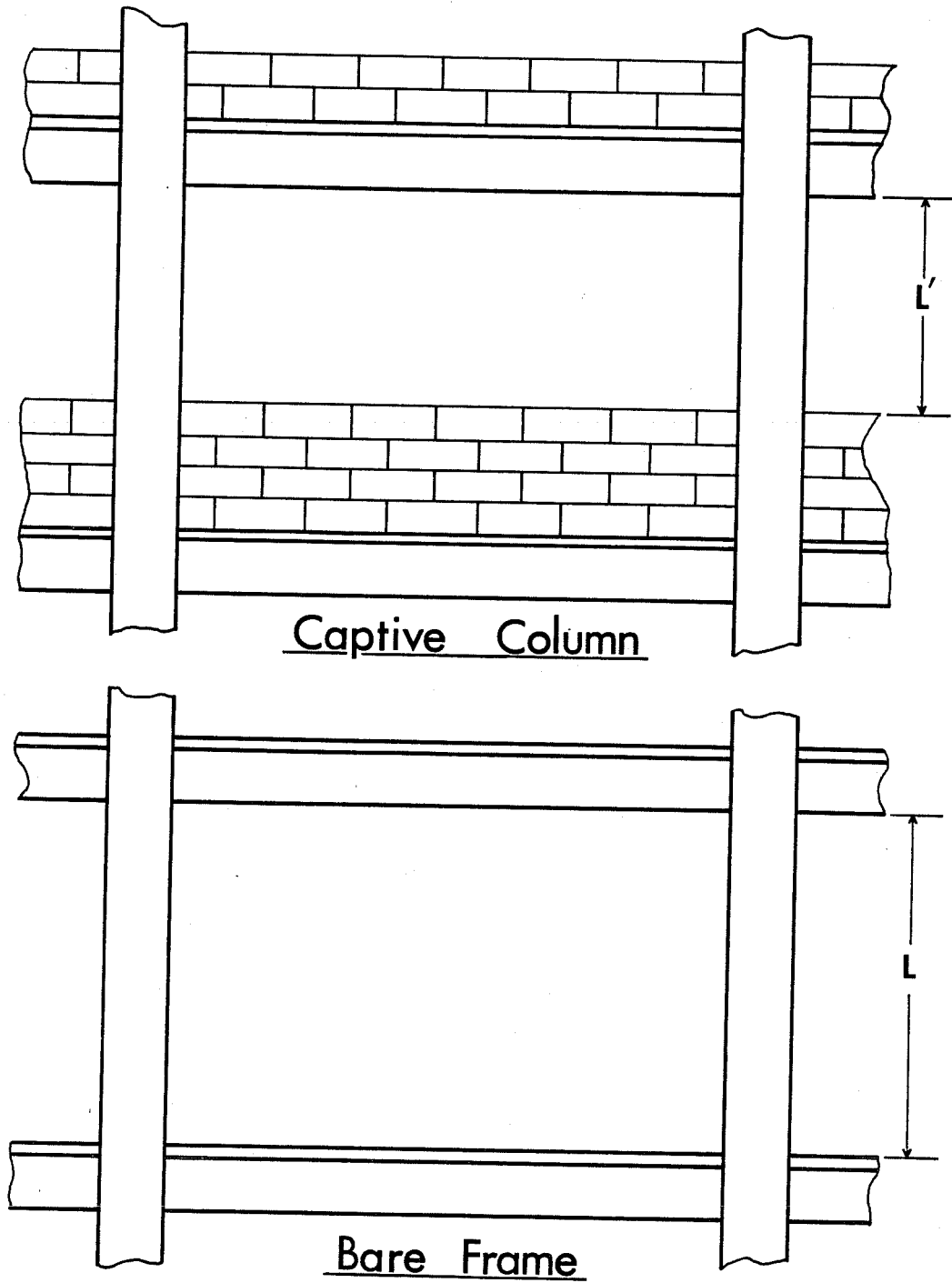
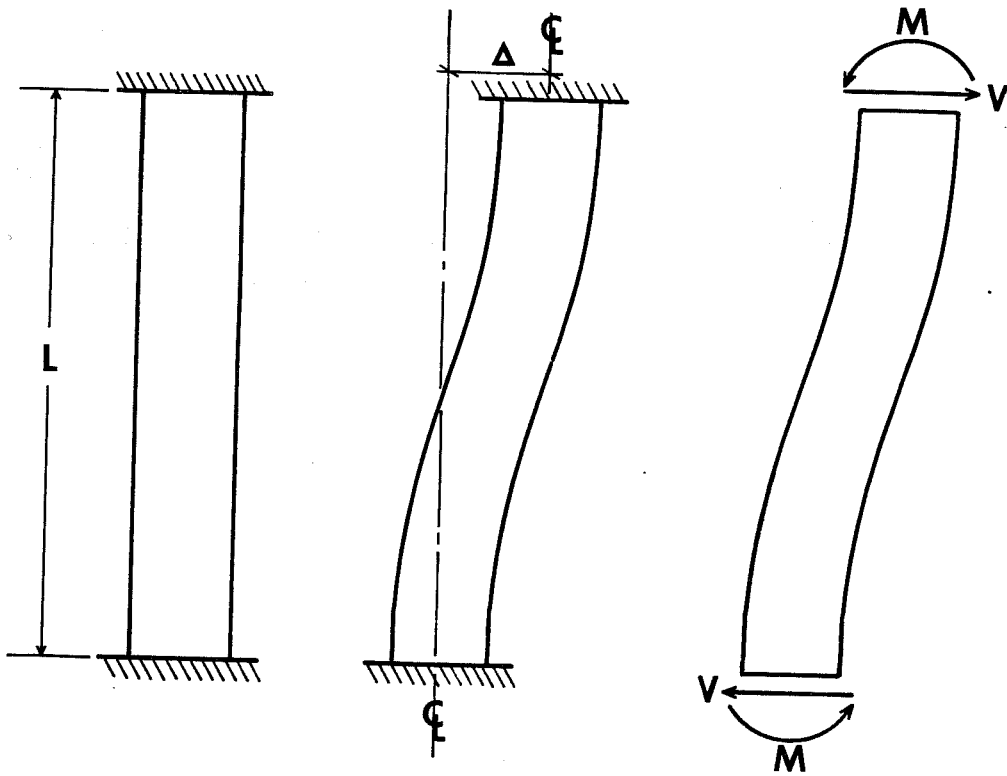


Fig. 1.1 Captive column concept



$$V = \frac{2M}{L}$$

Fig. 1.2 Column forces

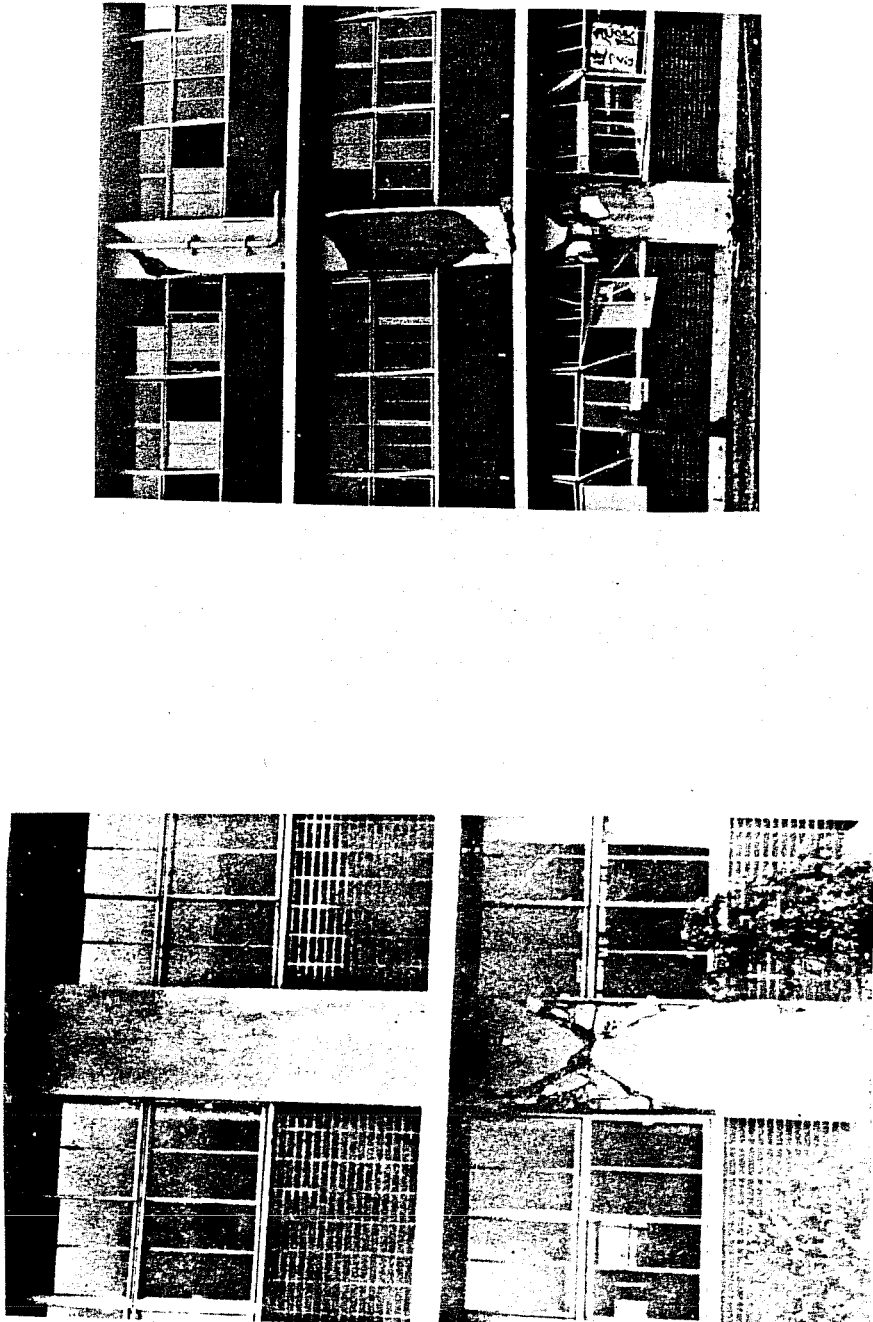


Fig. 1.3 Failure of short columns, Tokachi-Oki earthquake, 1968

C H A P T E R 2

EXPERIMENTAL PROGRAM

2.1 Introduction

The purpose of this study was to evaluate the shear strength and response of lightweight reinforced concrete short columns subjected to bidirectional lateral loads. Two test specimens were constructed using lightweight concrete and tested under bidirectional lateral loads. Primary objectives of this test program were:

- (1) to study the effect of axial load on the strength and response characteristics of lightweight reinforced concrete short columns.
- (2) To compare the strength and response characteristics of lightweight reinforced concrete short columns to similar tests conducted using normalweight concrete.

2.2 Overall Program

The current study was part of a larger study of the behavior of reinforced concrete frame elements subjected to cyclic bidirectional deformations. The test program was conducted at the Ferguson Structural Engineering Laboratory of The University of Texas at Austin. The main emphasis of the study was on the behavior of frame elements under large lateral deformations. The frame elements under study were beam-column joints and short columns. The study reported herein deals only with short columns.

Although many studies have been conducted on the behavior of short columns, most have considered only unidirectional deformations. In this project reversed bidirectional cyclic

deformations better reflect the general nature of seismic action. The deformations were applied slowly. Dynamic loading effects were not considered.

The first phase of the project was reported by Jirsa and Maruyama.¹⁶ The principle objective was the development of a behavioral model which accounted for the effects of deformation path on the response of the column. Deformation paths included in the study ranged from simple unidirectional deformations along only one axis to more complex paths involving deformations along the diagonals of the column. The size of the column, the amount of longitudinal reinforcement and the amount of transverse reinforcement was the same for all tests. No axial load was applied to the column. These tests provided valuable information concerning the effects of multidirectional loadings on the behavior of short columns.

Using columns with the same geometry, the effect of axial load was investigated by Ramirez in the second phase of the project.¹⁷ Axial loadings ranged from constant tension or compression to reversals of axial load. Both unidirectional and bidirectional lateral loadings were used.

In the third phase of the project, Woodward investigated other types of behavior.¹⁸ In Phases 1 and 2, the column was purposely underdesigned in shear if the provisions of the 1977 ACI Building Code were applied.²⁰ In both Phases 1 and 2, the behavior of the column was generally controlled by shear. To completely understand the entire range of behavior of short columns, the geometry of specimens in Phase 3 was modified to obtain response controlled by flexure. The boundary between flexural and shear dominated behavior was investigated by varying the amount of longitudinal and transverse reinforcement in the columns. The loading history was kept constant for all tests in Phase 3.

In the fourth phase of the project, the behavior of unsymmetric, rectangular sections was reported by Umehara.²¹ Previous studies dealt only with square symmetric column cross sections. The shear behavior of columns with rectangular cross sections may be different from that of columns with square cross sections. The loading histories ranged from simple unidirectional load paths to bidirectional load paths skewed with respect to the principle axis of the cross section. Tests were conducted with and without axial compressive loads.

2.3 Test Specimen

2.3.1 Design Requirements. The objective of the overall project was to study the behavior of reinforced concrete columns failing in shear. It was necessary to design the test specimen as a short stiff column that could be used in all phases of the project. Based on a review of available test results, a shear span-to-depth ratio of less than 2.5 was needed to ensure a shear failure.^{15,16,17,18} Provisions were made to apply bidirectional lateral loads and axial loads in both tension and compression. Based on these requirements, the prototype test specimen selected was a short column framing into enlarged end blocks. The enlarged end blocks provided for both attachment of the test specimen to the test frame and anchorage of the longitudinal column reinforcement.

The prototype column was designed as an 18 in. (45.7 cm) square section with a height of 4.5 ft. (1.37 m), meeting the requirements of ACI 318-77.²⁰ The shear span-to-depth ratio for the prototype was 1.5. Excessive fabrication costs for the test specimens and test frame made it necessary to scale down the prototype column design. A two-thirds scale was chosen to provide a column economical to fabricate using deformed reinforcement. The two-thirds scale also permitted a reduction in the applied loads without scale effects becoming a problem. The test specimen used

in this study was identical in detail to the specimens tested by Maruyama¹⁶ and Ramirez.¹⁷

2.3.2 Specimen Detail. Details for the test specimen are shown in Fig. 2.1. The prototype column was an 18 in. (45.7 cm) square section, 4.5 ft. (1.37 m) in height. The two-thirds scale model was a 12 in. (30.5 cm) square section, 3.0 ft. (0.92 m) in height. The prototype column design contained eight #9 longitudinal bars ($\rho_g = 0.025$) and #3 bars for transverse reinforcement. The cover on the prototype is 1.5 in. (3.81 cm). The two-thirds scale test column contained eight #6 longitudinal bars and special 6 mm deformed bars for transverse reinforcement. The cover was reduced to 1 in. and the column height was reduced to 36 in. (0.92 m).

The spacing of the transverse reinforcement was critical to developing shear dominated failure. The spacing was selected to be typical of existing structures. Such structures are often provided with insufficient transverse reinforcement and are dominated by shear.

With $f_y = 60$ ksi and $f'_c = 5$ ksi, the calculated moment capacity of the column section is 1000 in.-k. Ignoring second-order effects, the shear force V for a given moment M is given by $V = M/a$ where "a" is the shear span. For the 36 in. column, the shear span is 18 in. To develop the total moment capacity of the column, a shear force of about 56 kips is required. Using Chapter 11 of ACI 318-77, the required shear reinforcement can be determined using:

$$A_v = \frac{(V_u - V_c) b s}{f_y}$$

With 6 mm bars, the required spacing of transverse reinforcement to prevent a shear failure is 1.7 in.

Appendix A (Seismic Design) of ACI 318-77 specifies confinement reinforcement to be continued into the column from the ends.

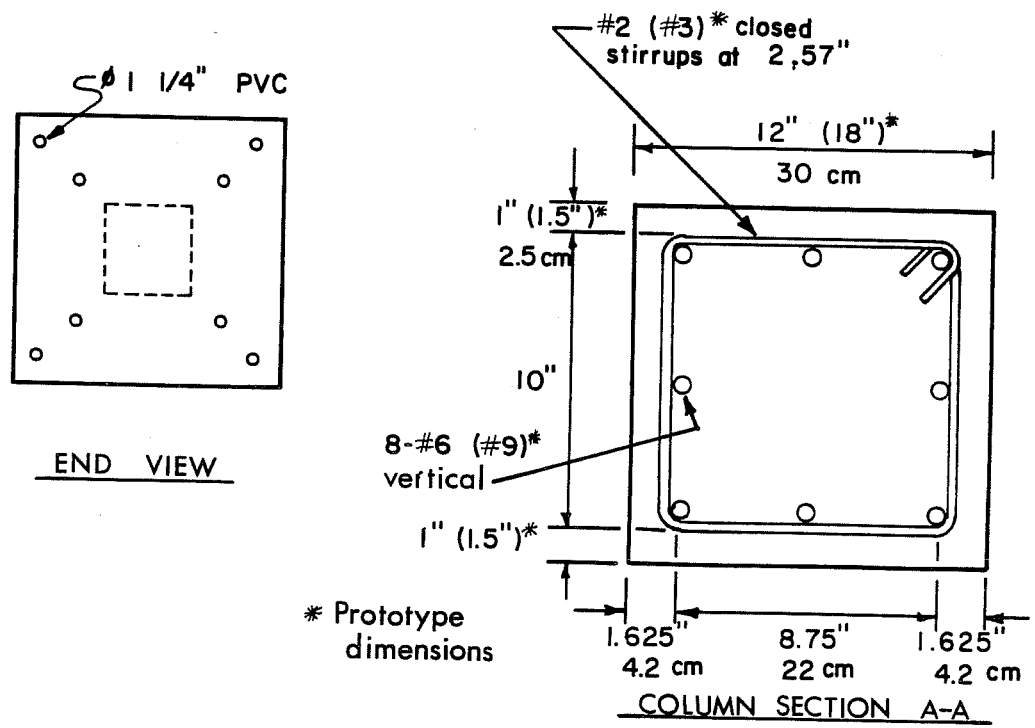
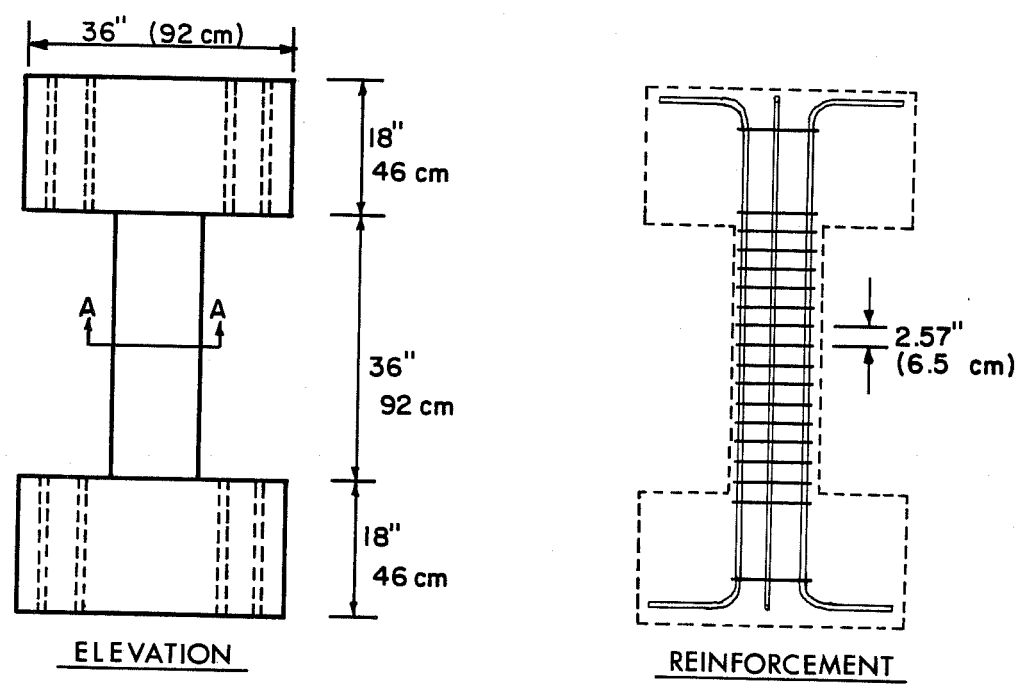


Fig. 2.1 Specimen details

Sections A.5.9 and A.6.3 require that for members subjected to low axial loads ($< 0.4P_b$), the column be designed as a flexural member with the transverse reinforcement spacing less than $d/4$ within a distance of four times the effective column depth from the ends of the member. For axial loads greater than $0.4P_b$, Section A.6.4 requires that confining reinforcement be supplied above and below connections over a minimum length of not less than the overall greatest column depth or $1/6$ the clear height of the column, whichever is greater. The maximum spacing of confinement reinforcement according to Section A.6.5.3 is 2.7 in. for the two-thirds scale test column. Using Section A.5.12, the required spacing is 2.4 in., and using Section A.5.11, the spacing is 2.59 in. Considering the various code requirements and the project objective that the column fail in shear, the spacing of stirrup ties was set at 2.5 in. (6.35 cm) for the two-thirds scale test column.

2.3.3 Calculated Strength. The ultimate moment capacity of the test specimen is about 1000 in.-k with no axial load. The lateral force required to develop this moment is about 56 kips for a column height of 36 in. Although the moment capacity can be estimated with fairly good accuracy, the shear strength capacity is difficult to predict. Using ACI 318-77, the shear strength may be calculated as follows:

$$V_u = \phi V_n$$

$$V_n = V_s + V_c$$

where

V_u = ultimate shear strength

V_n = nominal shear strength

V_s = shear strength provided by transverse reinforcement

V_c = shear strength provided by concrete

$\phi = 1.0$; assumed because of controlled laboratory testing conditions,

and

$$V_s = \frac{A_v f_y d}{s} = \frac{0.10 \times 60 \times 10.4}{2.5} = 25 \text{ kips}$$

The shear strength provided by the concrete may be estimated by several different approaches. Chapter 11 of ACI 318-77 specifies that V_c may be taken as $2\sqrt{f'_c} bd$ for normalweight concrete members with large shear span-to-depth ratios subjected to shear and flexure only. For members with short shear span-to-depth ratios (deep beams), ACI 318-77 permits shear stresses up to $6\sqrt{f'_c}$. Based on Chapter 11 of ACI 318-77, V_c may range from 16 to 50 kips. Using Eqs. (11-3) and (11-4) of Section 11.3.1, V_c for the specimen with no axial load is 17 kips and 24 kips for the specimen with 120 kips of axial compression. A strength reduction factor of 1.0 is used because of the controlled laboratory test conditions. Therefore, $V_u (= V_c + V_s)$ is 42 kips for the test with no axial load and 49 kips for the test with 120 kips of axial compression.

Section 11.2.1.2 of ACI 318-77 recommends that for "sand-lightweight" concrete a 15 percent reduction in concrete shear stresses be applied to all strength calculations. "Sand-lightweight" concrete is concrete produced with lightweight aggregate and normal-weight sand. For lightweight concrete produced with both lightweight aggregate and sand, a 25 percent reduction in concrete shear stresses is recommended for all shear calculations. For the test specimen constructed of sand-lightweight concrete, V_c is 14.5 kips for the specimen with no axial load and 20.5 kips for the specimen with 120 kips axial compression. The ultimate strength of the specimens is 39.5 kips for the test with no axial load and 45.5 kips for the specimen with an axial compressive load of 120 kips.

The calculated strength values for both the normalweight and lightweight concrete test specimens are based on static loads. ACI-ASCE Committee 426²² addresses the effects of various types of loading. According to the report of Committee 426, the ultimate shear strength under repeated loadings is 50-70 percent of the static strength. The committee also reports that uncertainty exists concerning the effects of load reversals on the ultimate shear strength.

2.3.4 Specimen Fabrication. The dimensions of the end block were based on the requirements for attaching the test specimen to the loading heads and for adequately anchoring the longitudinal column reinforcement. Details of the end-block reinforcement and provisions for attachment to the loading frame are included in Ref. 15.

The specimens were cast in one operation. Special formwork details were developed to ensure proper concrete compaction in the column and the end blocks.¹⁵ Figure 2.2 illustrates the specimen formwork.

2.4 Materials

2.4.1 Lightweight Concrete. Lightweight aggregate was obtained from a commercial supplier. The mix proportions were as follows:

Lightweight Concrete Mix Design ($f'_c = 5000$ psi)

Proportions for 1 cu. yd.

Water	264 lbs.	} w/c = 0.47 by weight
Cement	564 lbs.	
Fine Aggregate	1700 lbs.	
Coarse Aggregate ($\frac{1}{2}$ in.)	704 lbs.	

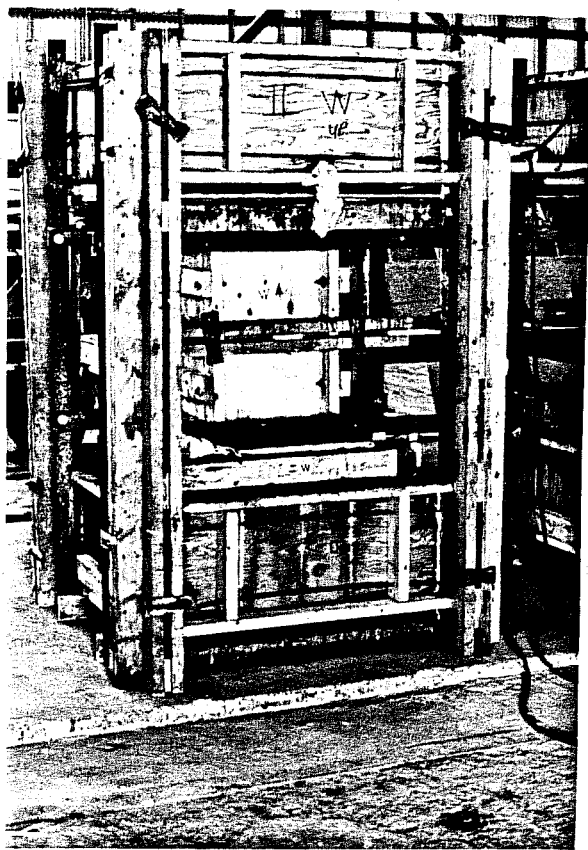


Fig. 2.2 Formwork assembly

The lightweight aggregate was "Rocklite" manufactured by Lightweight Processing Company, Glendale, California. Rocklite is manufactured by mining a sedimentary bentonitic clay stone and expanding the shale by firing in a rotary kiln. The final product, an expanded shale aggregate with a honeycombed inner structure, has the following gradation and physical properties:

Rocklite Aggregate ($\frac{1}{2}$ in.)

Sieve Size	% Passing
3/4 in.	100
1/2 in.	93
3/8 in.	64
No. 4	0
No. 8	0
Dry loose unit weight	45.7 p.c.f.
Oven dry specific gravity	1.29
One hour absorption	9.9% (by weight)
Resistance to abrasion (ASTM C131)	
(a) 100 revolutions	6.6%
(b) 500 revolutions	29.5%

Normalweight sand was used in the lightweight concrete mix. The source of the fine aggregate was Colorado River sand. For the specimen casting, a slurry mix of sand, cement and water was obtained from a local ready-mix producer. After the slurry was delivered to the laboratory, the lightweight aggregate was added to the mix. Some of the mix water was withheld at the mix plant and adjusted at the laboratory to achieve the desired 6 in. (15.24 cm) slump. Twenty-four control cylinders were cast and cured with the specimens. Both specimens were cast in the same operation. The forms were stripped three days after casting. The specimens were moist-cured under polyethylene sheets for a total of seven days after casting. At the time of testing, the concrete strength was about 4600 psi (31.72 MP_a). Figure 2.3 illustrates the strength gain properties of the lightweight concrete. In addition to compressive

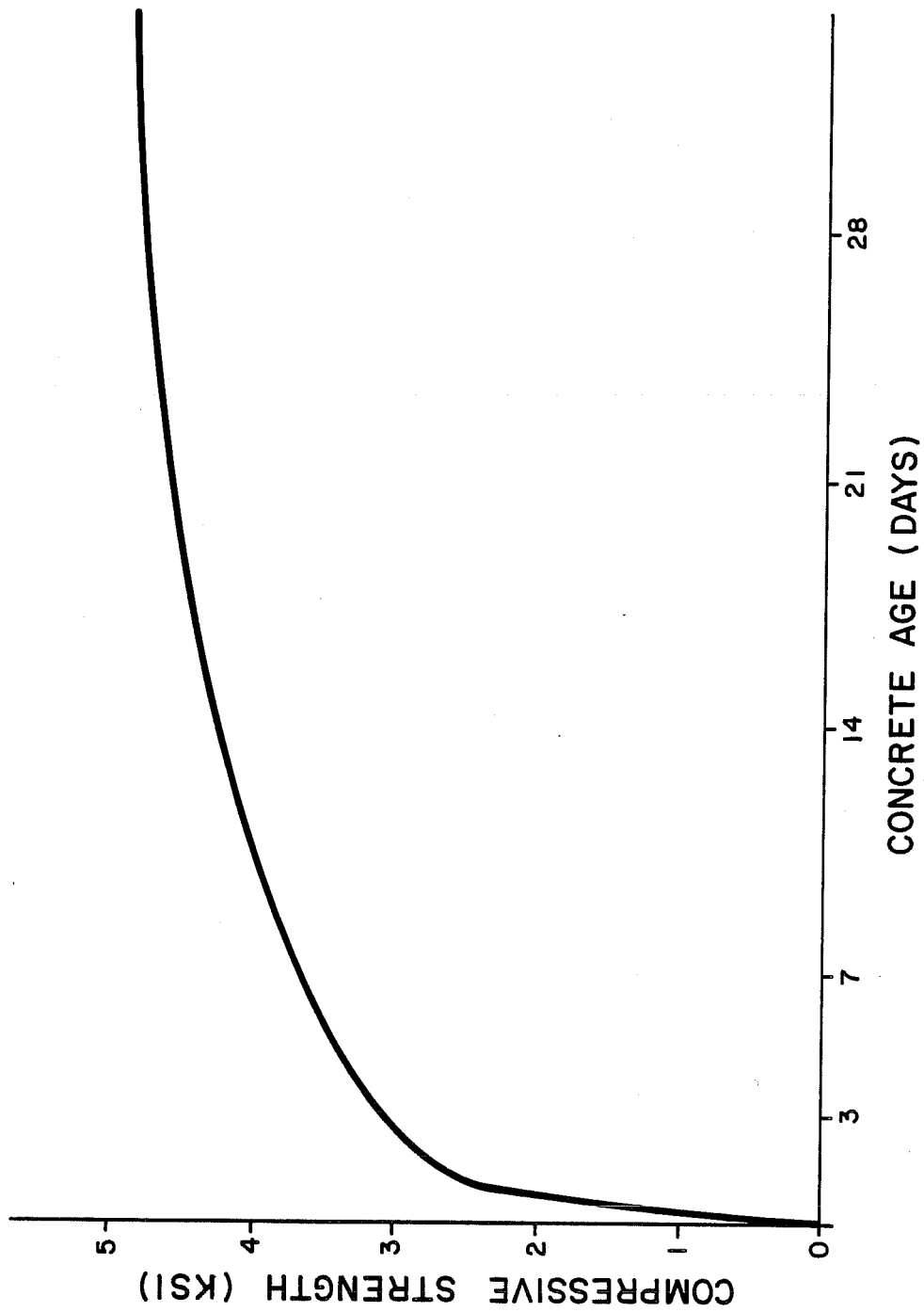


Fig. 2.3 Compressive strength gain curve for lightweight concrete

strength tests, split-cylinder tests were performed to evaluate the split tensile strength of the lightweight concrete. Table 2.1 summarizes the lightweight concrete properties.

TABLE 2.1 CONCRETE PROPERTIES

	f'_c Test (psi)	f_{ct} (psi)	Unit Weight (pcf)	E_c (ksi)
Lightweight Concrete	4600	455	108	2512.1
Normalweight Concrete	6000	490	145	4463.2

Standard tests were conducted in order to establish the physical properties of the lightweight concrete. The stress-strain curve for the lightweight concrete is shown in Fig. 2.4. Using the secant method, the modulus of elasticity for the lightweight concrete was 2820 ksi (19445.0 MP_a). The dry unit weight at 28 days was 108 lbs./c.f. (1730 kg/m³). Using Section 8.5.1 of ACI 318-77 the modulus of elasticity for the lightweight concrete was 2510 ksi (17320.0 MP_a). The modulus of elasticity for the normalweight concrete was 4465.0 ksi (30780.0 MP_a).

Strength reduction factors of 0.75 for "all-lightweight" concrete and 0.85 for "sand-lightweight" concrete are recommended by Section 11.2.1 of ACI 318-77. These reductions are to be applied to all values of $\sqrt{f'_c}$ for calculations pertaining to shear (V_c) and torsion (T_c) capacities of concrete. For specified values of f_{ct} , calculations of V_c and T_c are to be modified by substituting $f_{ct}/6.7$ for $\sqrt{f'_c}$.

2.4.2 Normalweight Concrete. Ready-mixed concrete was obtained from a local supplier for the normalweight concrete. The mix proportions for the normalweight concrete were as follows:

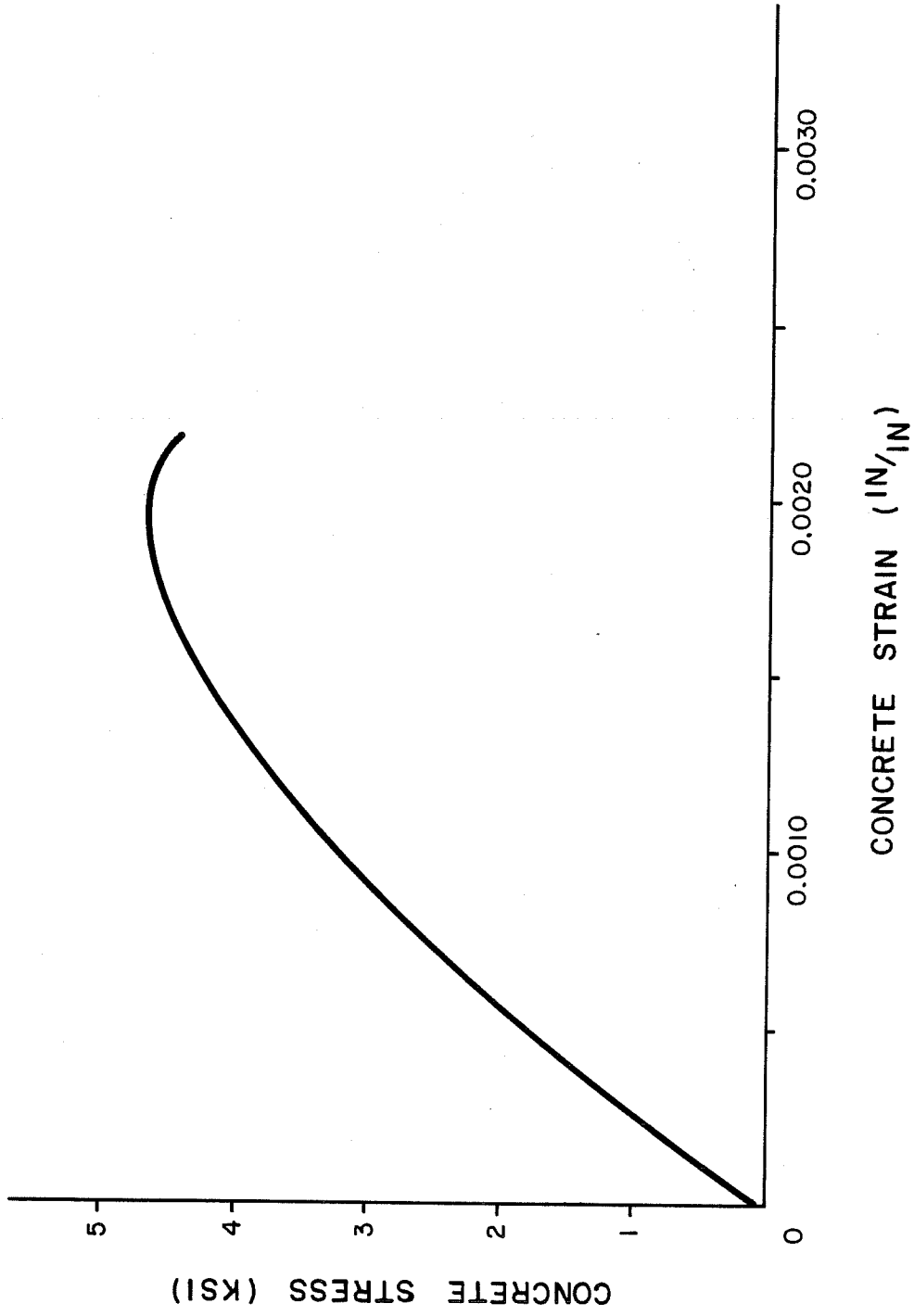


Fig. 2.4 Stress-strain relationship for lightweight concrete

Normalweight Concrete Mix Design (5000 psi)

Proportions for 1 cu. yd.

Water	312 lb.	} w/c = 0.6 by weight
Cement	520 lb.	
Fine Aggregate	2200 lb.	
Coarse Aggregate (3/8 in.)	3420 lb.	
Airsene (plasticizer)	25 oz.	

The aggregate was Colorado River sand and gravel. Some mix water was withheld at the plant and added to the mix at the laboratory to achieve the desired slump (6 in.). The casting and curing of the specimens was identical to that of the lightweight concrete specimen. Table 2.1 summarizes the normalweight concrete properties.

2.4.3 Reinforcing Steel. No. 6 deformed reinforcing bars were used for the longitudinal steel and 6 mm deformed bars were used for the transverse steel. All reinforcing steel conformed to ASTM A615-76a with a specified minimum yield strength of 40. Coupons of the deformed bars were tested to obtain the modulus of yield and ultimate for the steel. Stress-strain curves for reinforcement are shown in Fig. 2.5. The properties of the steel reinforcement used in both the normalweight and lightweight specimens are summarized in Table 2.2.

TABLE 2.2 STEEL PROPERTIES

		f_{yt} (ksi)	f_{su} (ksi)	E_s (ksi)
Lightweight Specimen	6 mm #6	62.0 53.0	82.0 90.0	30,400. 29,500.
Normalweight Specimen	6 mm #6	68.0 65.0	90.0 109.0	30,000. 30,000.

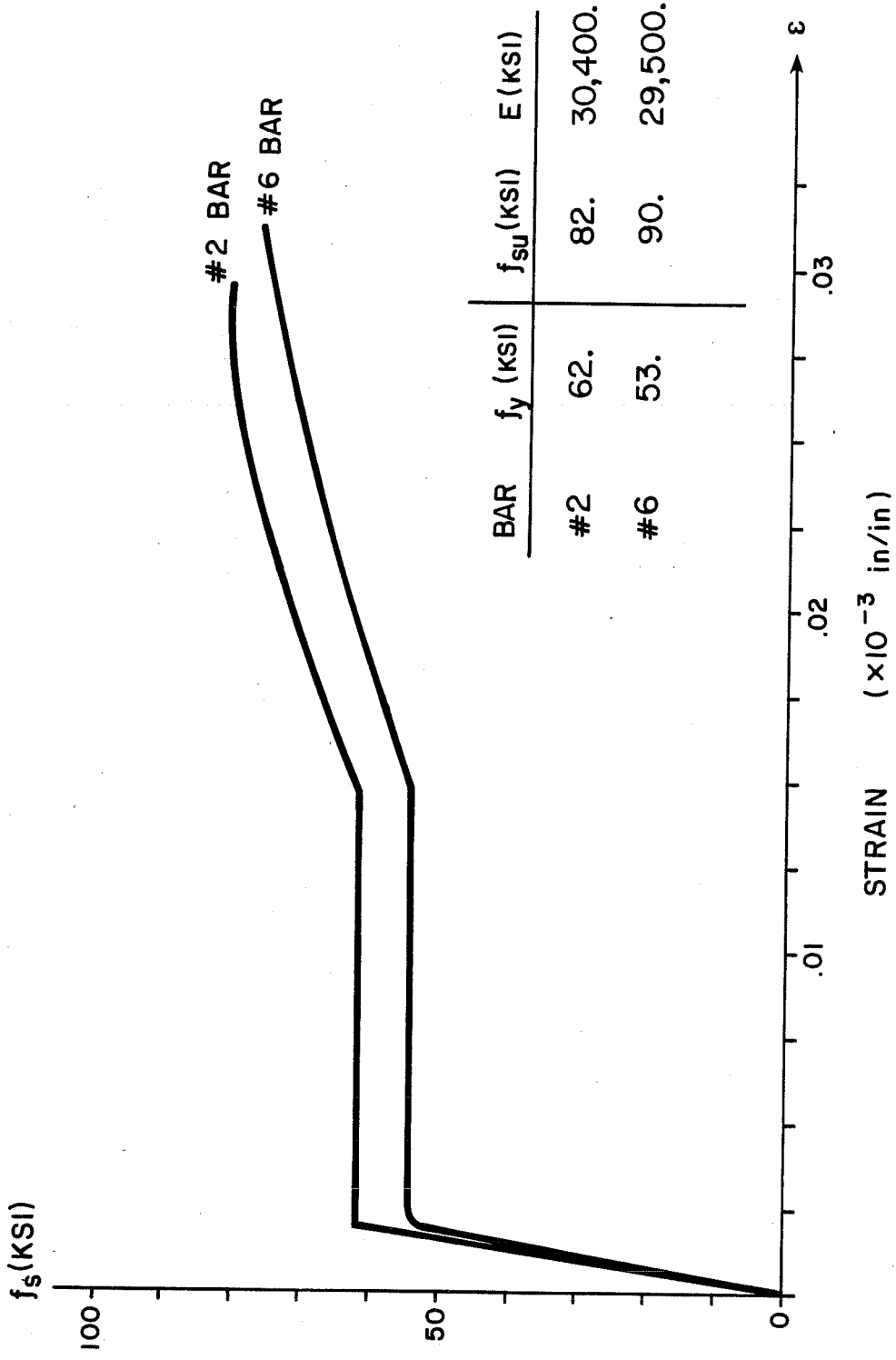


Fig. 2.5 Stress-strain curve for steel reinforcement

2.5 Test Frame and Instrumentation

2.5.1 Introduction. The objectives of the research program required that the loading system be capable of loading the specimen laterally in two independent, orthogonal directions and applying an axial load. The complexity and required capacity of the loading system utilized the reinforced concrete floor-wall reaction system (reaction wall) shown in Fig. 2.6. Detailed information on the floor-wall system can be found in Ref. 15.

2.5.2 Loading System. The loading system is made up of two independent components. The first subsystem is composed of a closed-loop, servo-controlled hydraulic system used to control the three active load components. The second subsystem is composed of cross-looped hydraulic rams whose function is to restrain the specimen ends from rotating during loading.

The closed-loop hydraulic system was made up of three rams, three accumulators, three servo-controllers and a central pump. The three rams; one for axial load, the other two for lateral loadings, were independently controlled by the servo-controllers. The feedback to the servo-controller is the output of either a load cell or a displacement transducer. By programming the servo-controller to monitor the electrical output of either the load cell or displacement transducer, each individual loading ram could be used in either the load control or displacement control mode. The position of each loading ram, relative to the test specimen is shown in Fig. 2.7. The axial load ram has a static capacity of 300 kips and a piston stroke of 6 in. The axial load ram was attached to the vertical reaction frame and the upper loading head on the specimen. The two lateral load rams each have a static capacity of 150 kips and a piston stroke of 12 in. The lateral rams were attached to the reaction wall and the upper loading head of the specimen. Figure 2.8 illustrates the arrangement of the loading rams and the test frame.

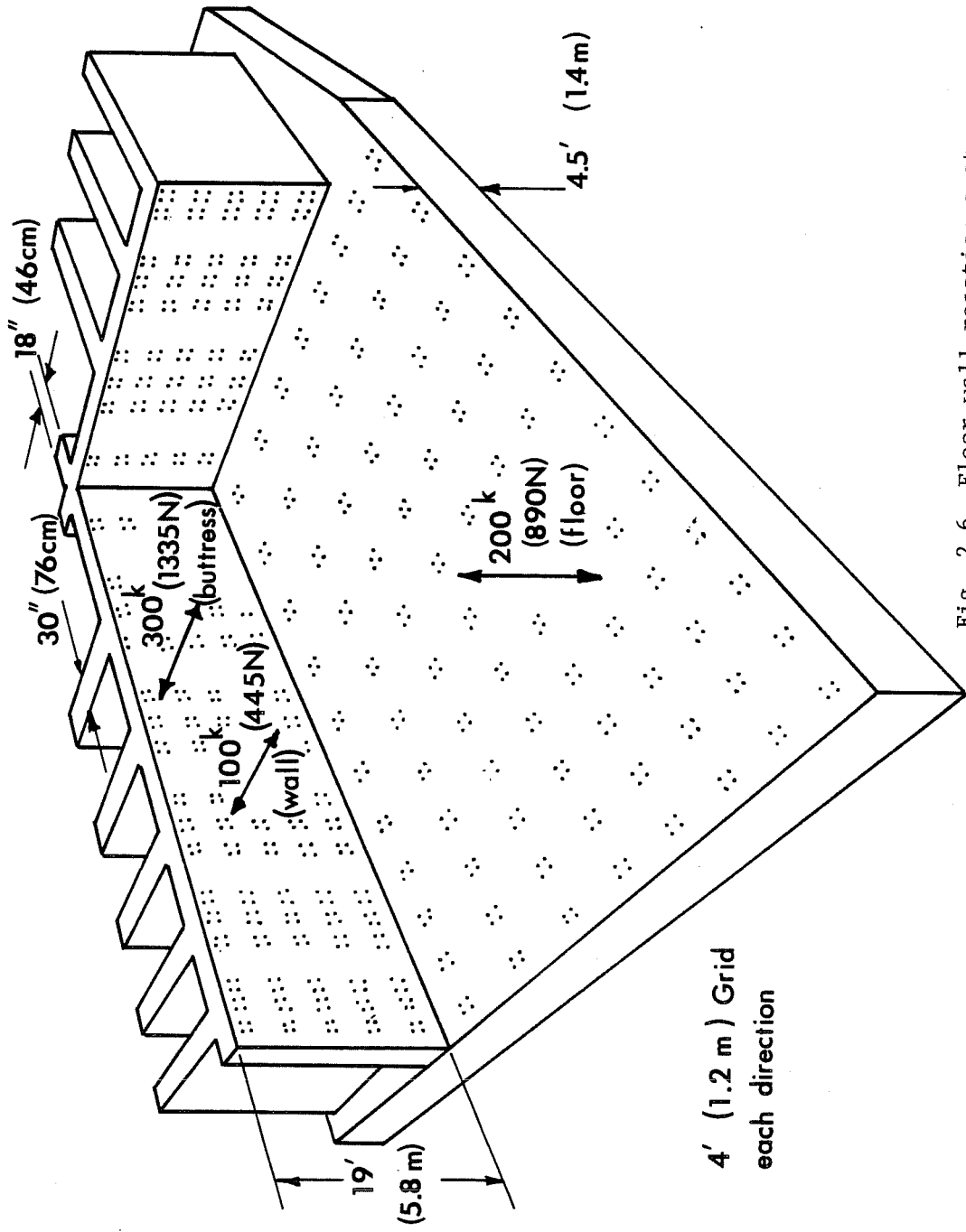


Fig. 2.6 Floor-wall reaction system

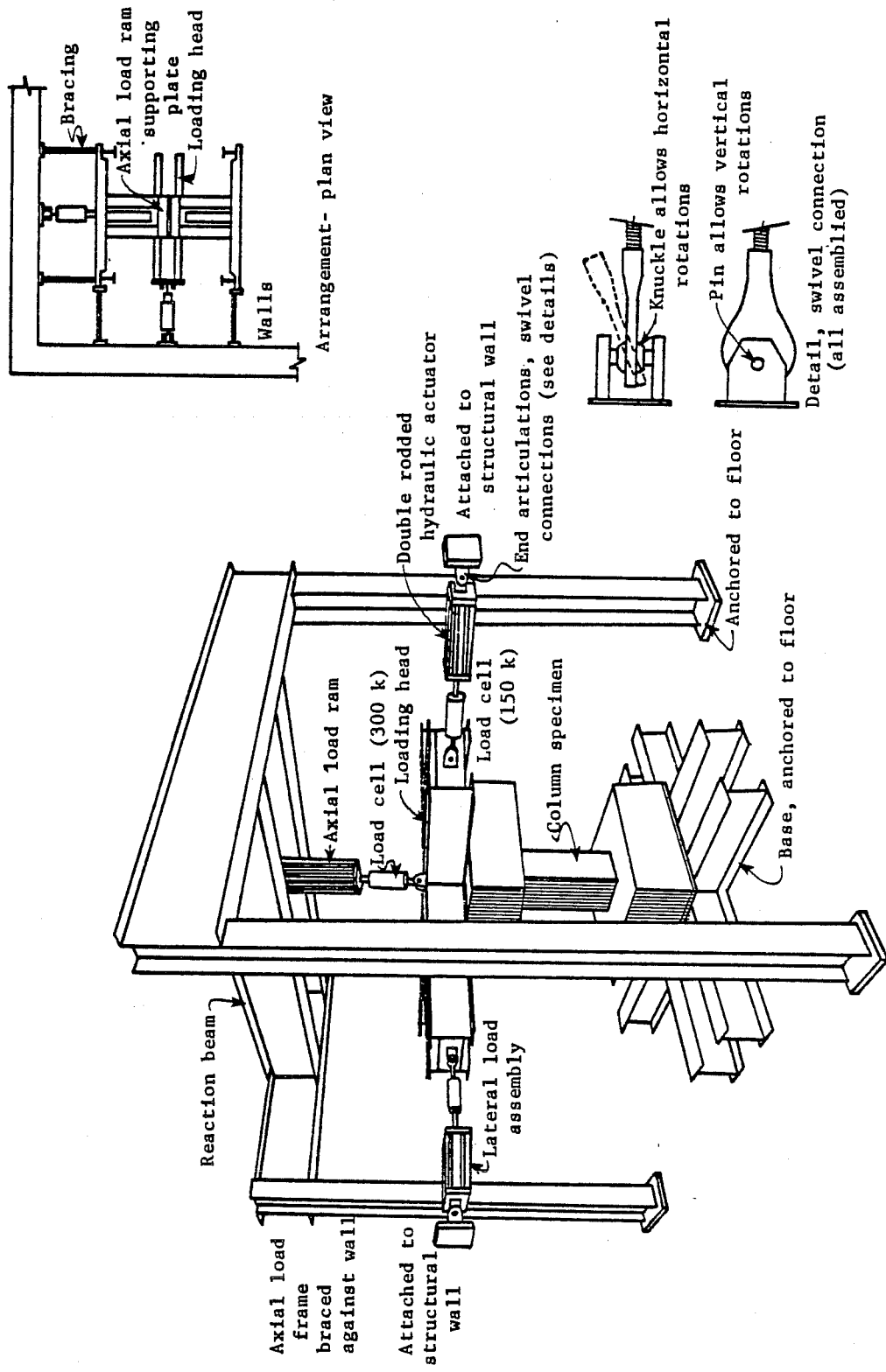


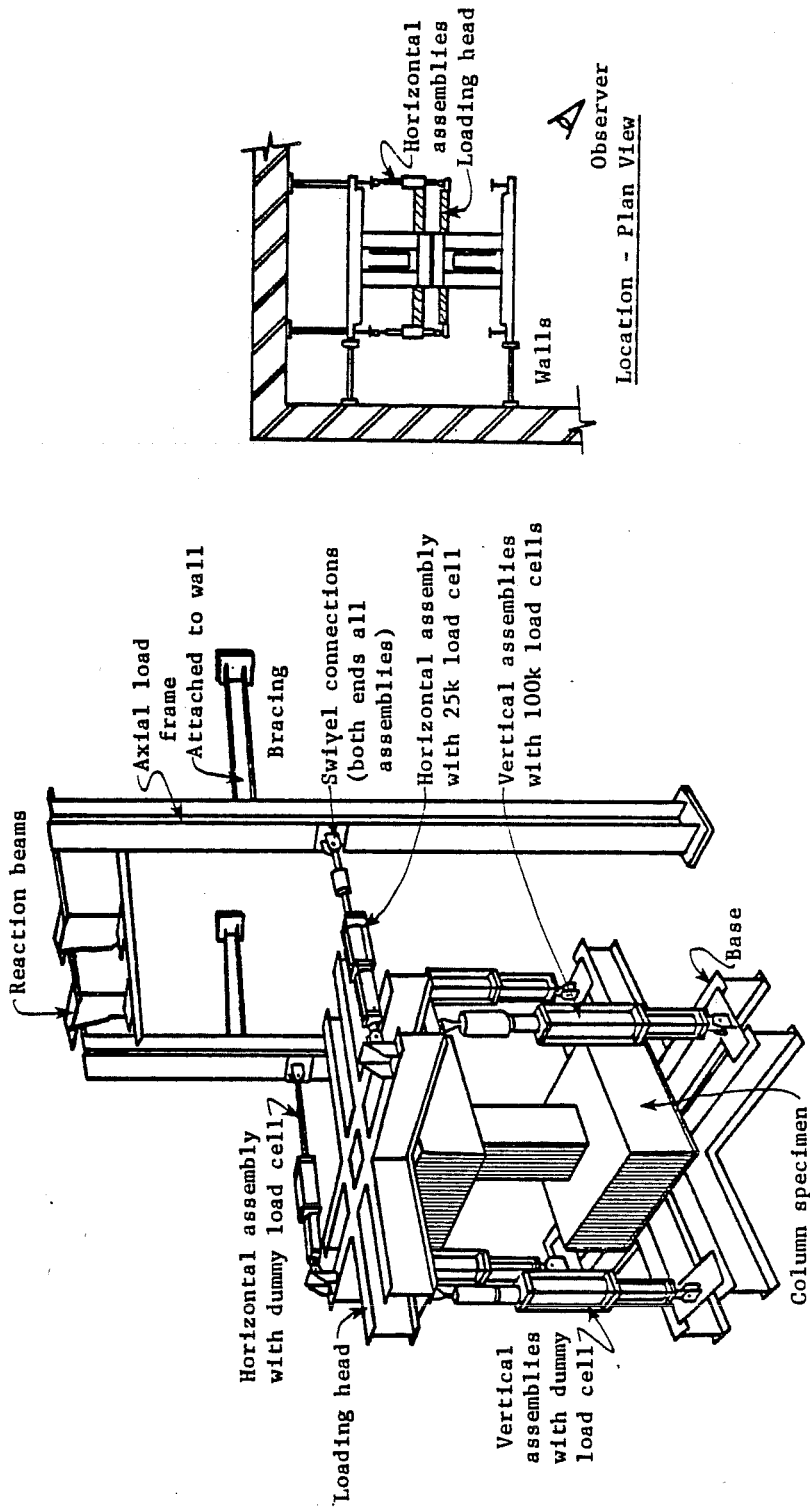
Fig. 2.7 Loading rams

The test specimen is bounded at each end by a loading head which is a welded assembly of wide flange members. The specimen was attached to the loading head by passing eight high-strength threaded rods through both the end block of the specimen and the loading head. Nuts are threaded on each end of the rod and tightened, clamping the loading head to the end block. A gypsum cement was placed between the loading head and the end block to ensure a smooth bearing surface. The base end block is bolted to the testing floor while the upper crosshead is free to translate in any direction.

The test specimen represents a column bounded by very stiff framing elements. To better model the condition of a fixed-end member, the upper loading head should be allowed to translate but not rotate. The rotation of the upper loading head is restrained by a system of cross-coupled hydraulic rams shown in Fig. 2.9. The upper loading head acts as a lever to decrease the load required in the rams to resist the rotation of the upper end block. The lower end block is prevented from rotation by secure anchorage to the floor slab.

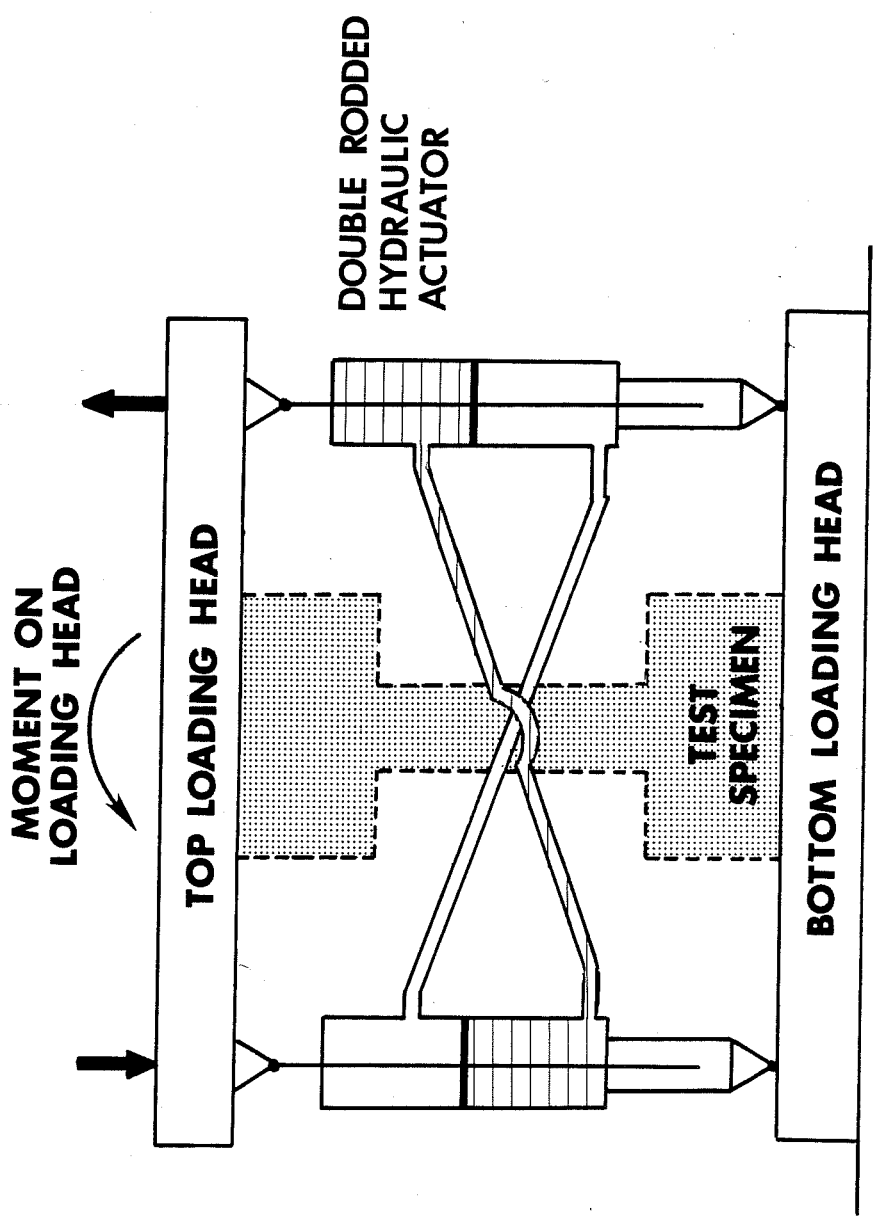
The rotation restraining system is composed of three pairs of cross coupled rams. Two pairs of the rams act vertically to restrain rotations of the upper head in two orthogonal vertical planes. One pair of rams is used to resist any tendency of the upper loading head to twist. By cross coupling a pair of double-action hydraulic rams, a downward force on one ram is counter-acted by an equivalent downward force in the opposite ram (Fig. 2.10).

Both rams may extend or retract equally, as in the case of vertical translation of the upper loading head. However, because of cross-coupling one ram in a pair cannot retract while the other ram extends. This resistance to differential displacements restrains rotation of the upper loading head. Three pairs of rams restrain rotation of the loading head in any direction.



Positioning System - Schematic

Fig. 2.9 Restraining rams



VERTICAL & HORIZONTAL POSITIONING SYSTEMS

Fig. 2.10 Vertical and horizontal positioning system

2.5.3 Instrumentation. Three types of measuring devices were used to monitor the performance of the specimen during testing: (a) load cells, (b) linear potentiometers, and (c) strain gages.

Load Cells. Load cells were mounted on each of the loading rams and on one ram in each pair of restraining rams. The load cells attached to the three loading rams contained double bridges. One bridge was used as feedback to the servo-controller and the other was used for data acquisition. Separate bridges were used to eliminate the possibility of the data acquisition system interfering with the servo-controller feedback signal. The signals from the lateral loading rams were also plotted on x-y recorders during the test.

Linear Potentiometers. Twelve potentiometers were used to monitor the deflection and rotation of the specimen end blocks. The location of the twelve potentiometers is illustrated in Fig. 2.11. The potentiometers were supported by a special frame independent of the loading frame as shown in Fig. 2.12. Deformations measured by the potentiometers were recorded by the data acquisition system. The signals from two lateral potentiometers, when used in conjunction with output from load cells on lateral loading rams, provided load-deflection plots along each of the two loading axes.

Strain Gages. Strain gages were attached to both tie and longitudinal reinforcement to provide an indication of the effect of external loading on the performance of the reinforcement. Strain gage locations are shown in Fig. 2.13 for a specimen with a tie spacing of 2.5 in. Gages were placed on all four legs of six ties and on the corner longitudinal bars at the intersection of the column and the end blocks.

2.5.4 Data Acquisition. The main component of the data acquisition system was a VIDAR Digital Data Acquisition System (DDAS). The VIDAR data scanner reads the analog output signal of each

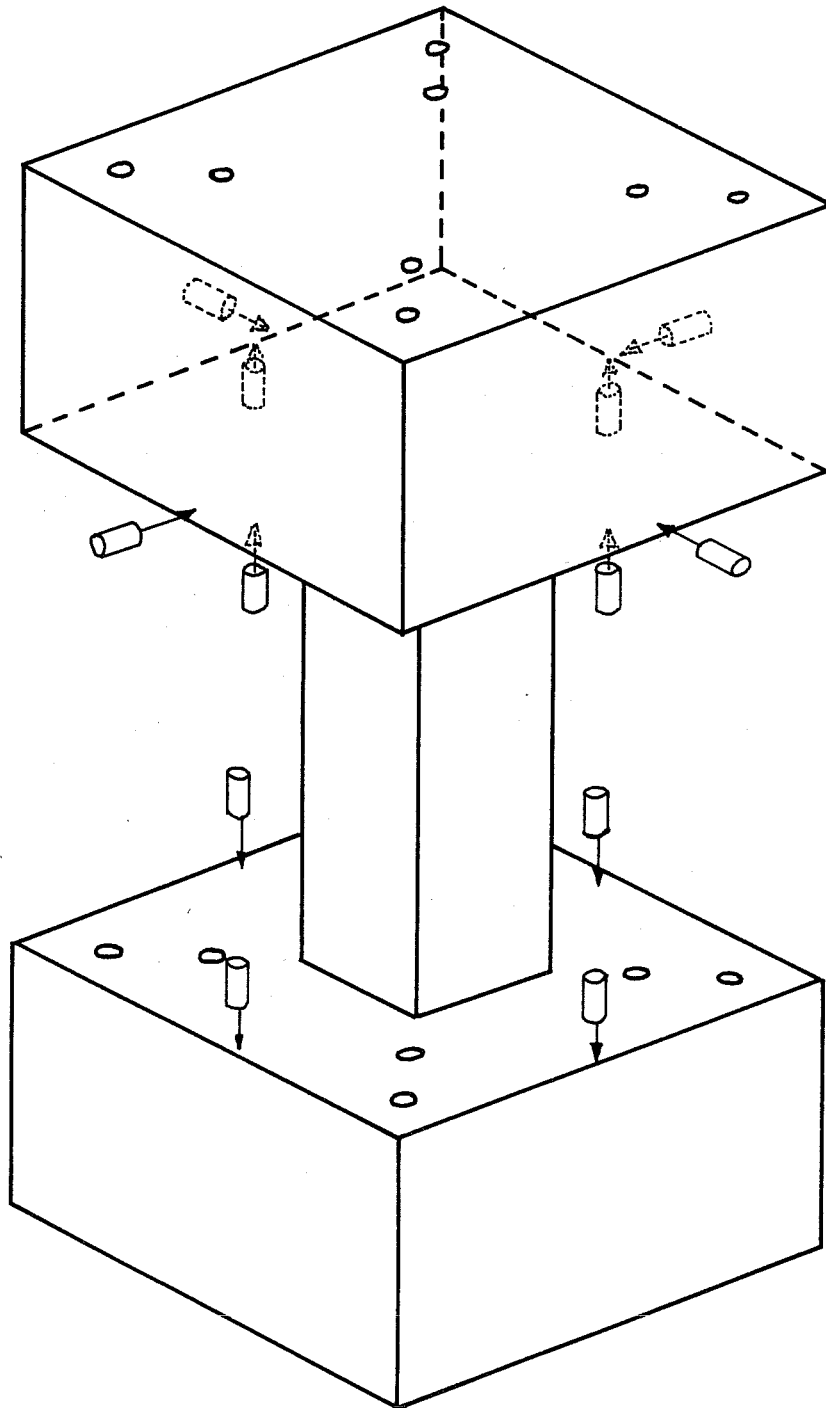


Fig. 2.11 Linear potentiometer locations

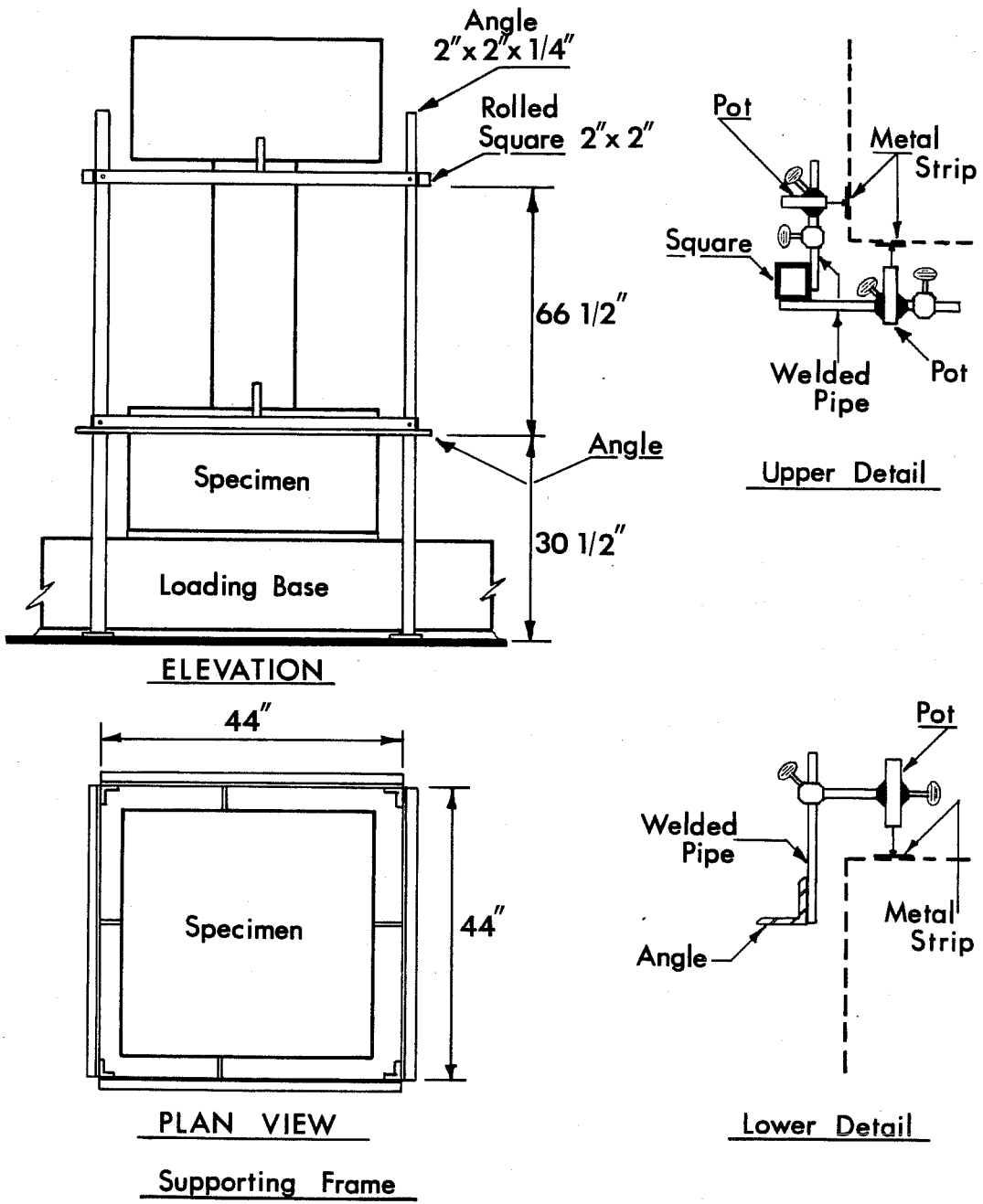


Fig. 2.12 Linear potentiometer mounting frame

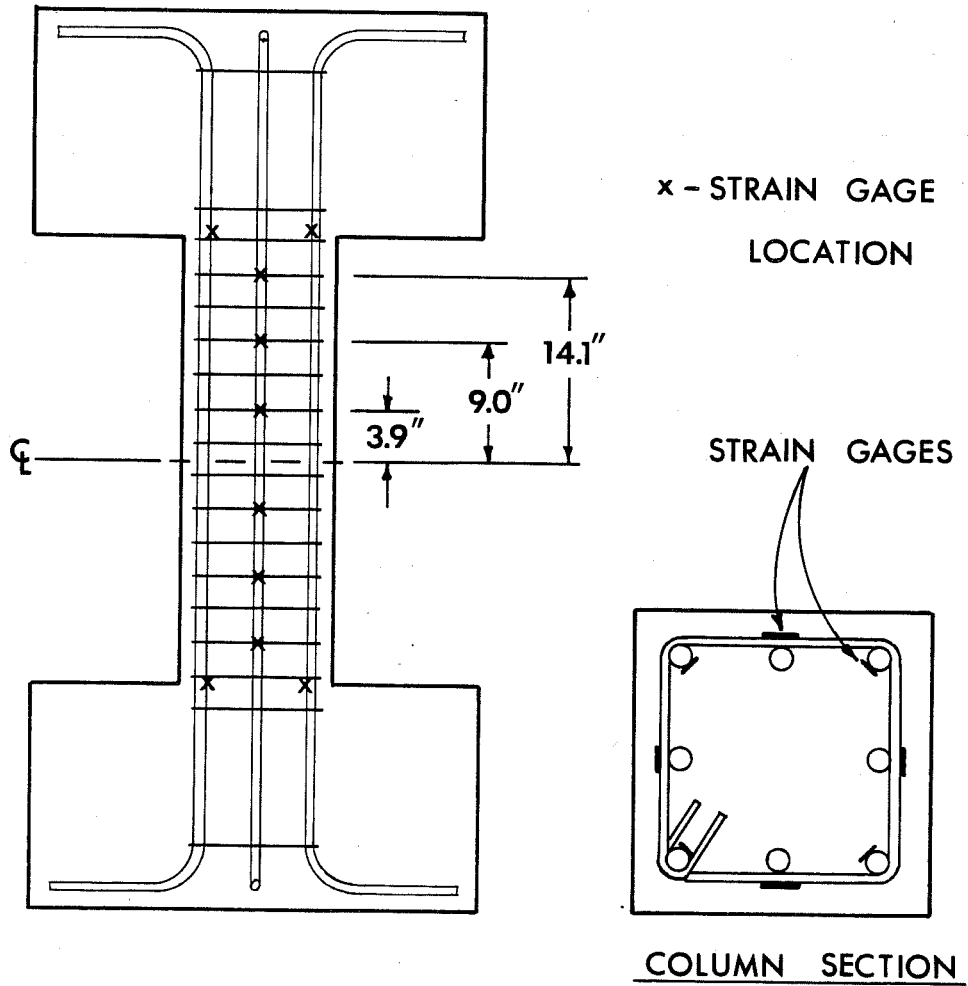


Fig. 2.13 Strain gage locations

instrument, converts it to a digital voltage and stores the information on magnetic tape. The VIDAR data scanner is started by the operator. Upon completion of the test, computer-based data reduction software was utilized to convert the raw digital voltage data to common engineering units. Data bases produced by the data reduction software allowed processed data to be plotted and/or tabulated efficiently.

2.6 Loading Sequence

In this study, the lateral loading pattern was identical for the two tests. The lateral history was controlled by deformation. The loading was alternated in both principle axes at each deflection level, as shown in Fig. 2.14. Three load cycles were applied in each direction at each deflection level. The peak deflections in each direction were equal. The load sequence chosen was identical to that used in earlier tests of otherwise identical test specimens constructed of normalweight concrete.^{16,17} For the purposes of comparison between behavior of lightweight concrete and normal-weight concrete columns, identical load histories were used. The deformation was increased in increments equal to Δ_i where Δ_i was determined in earlier tests as the deformation needed to produce first yielding in the longitudinal steel. The deformation increment, $\Delta_i = 0.20$ in., was determined under monotonic loadings without axial load.

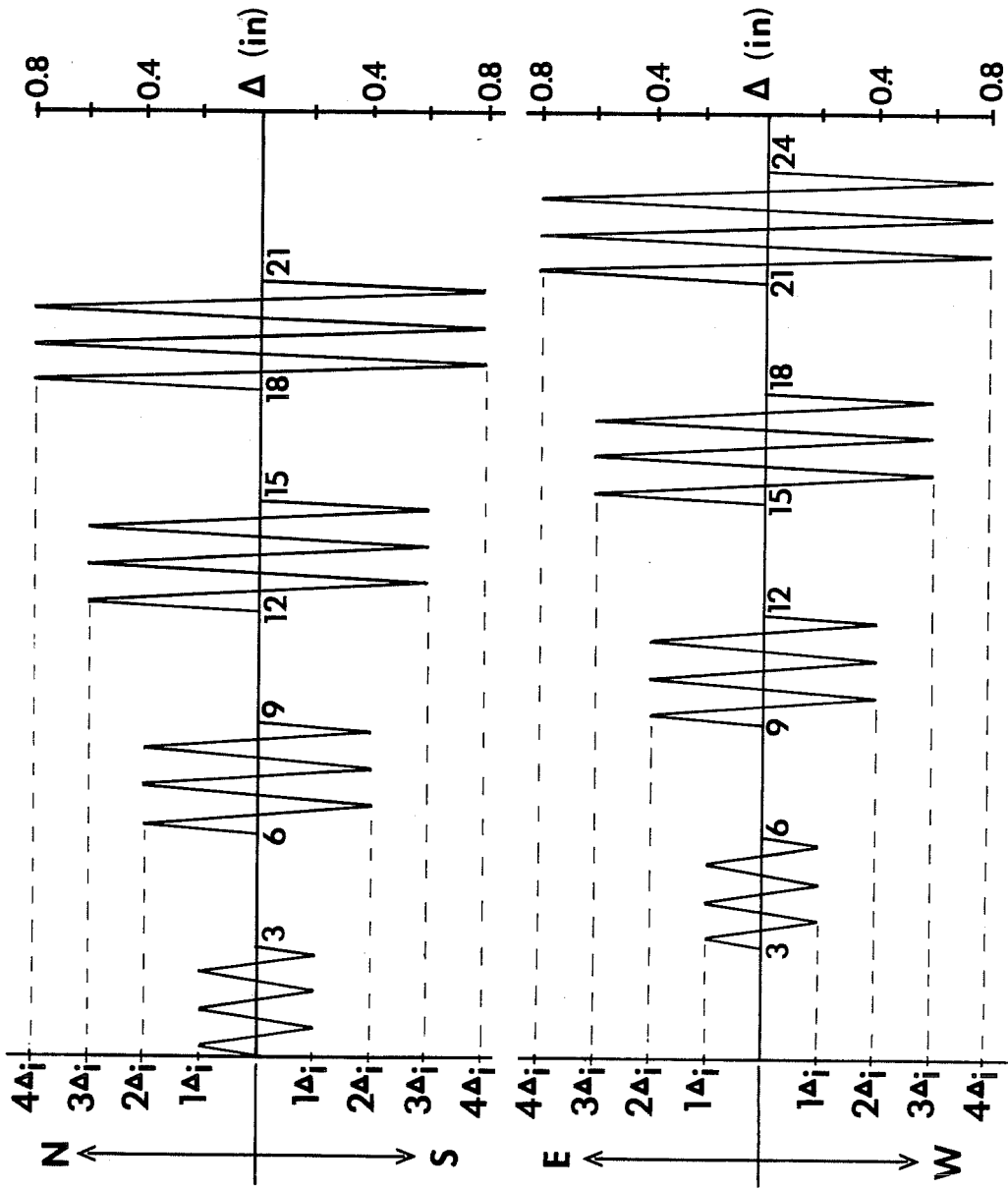


Fig. 2.14 Lateral loading sequence

C H A P T E R 3

BEHAVIOR OF LIGHTWEIGHT SPECIMENS

3.1 Introduction

Experimental test results for the lightweight concrete test specimens are reported in this chapter. Test results for the normal-weight concrete specimens are reported in Chapter 4. Basic data for each test consists of information recorded from strain gages, load cells and displacement transducers. Photographs were used to record crack patterns at each peak deflection.

The hysteretic behavior of the test specimens under the imposed cyclic deformations and axial loads are presented in terms of actual lateral load-deflection curves. Bidirectional tests require two load-deflection curves, one for each orthogonal direction, to describe the specimen behavior. Of particular interest is the stiffness of the specimen, the peak lateral capacity at a given deflection level, the loss of lateral capacity due to cycling at a deflection level and the overall shape of the hysteretic loop. The slope of the load deflection curve at any point represents the stiffness of the specimen. For direct comparison of test results, envelopes of peak lateral load-deflection values are used. The main objective in analyzing the test results is to study the difference in behavior between columns constructed of lightweight and normalweight concrete subjected to lateral loads. The comparison is based on tests conducted with and without axial loads using identical lateral loading patterns in all tests.

3.2 Description of Test Results

3.2.1 Load-Deflection Curves. The load-deflection curves for tests LW1 and LW2 are shown in Figs. 3.1 through 3.4. Hysteretic behavior is referred to as "stable" when only small changes in lateral capacity due to cycling are observed. Large losses in specimen stiffness are characterized by "pinching" of the hysteretic loops. Poor energy dissipating characteristics of a member are generally typified by nonstable hysteretic behavior with pinching. Peak envelope curves for tests LW1 and LW2 are shown in Figs. 3.5 and 3.6. The envelopes unite peak values of the load-deflection curve in the first and third cycles for each deflection level. Envelopes are used to obtain comparative hysteretic characteristics between different tests and to observe changes in lateral capacity with cycling at a given deflection level. As expected, the lateral load required to attain a displacement level of $1\Delta_i$ or $2\Delta_i$ was greater for LW2 (axial load) as compared to LW1 (no axial load). The pinching of the hysteretic loops appears to be more pronounced in LW1 than LW2, however, the loss of strength and stiffness in both cases is rapid once the peak load is reached. Pinching of hysteretic loops corresponds with cracking and spalling of concrete cover. The lateral load capacity of LW2 is observed to decay at a much greater rate, for deflections greater than $2\Delta_i$, as compared to LW1.

3.2.2 Peak Lateral Forces. Values of axial load, peak applied lateral load (or shear), normalized shear stress and actual lateral displacements are tabulated in Appendices A and B for test specimens LW1 and LW2, respectively. Normalized shear stresses were calculated by dividing the total applied lateral load by the core area of the column and the square root of the concrete compressive strength. The core area was used in this calculation because

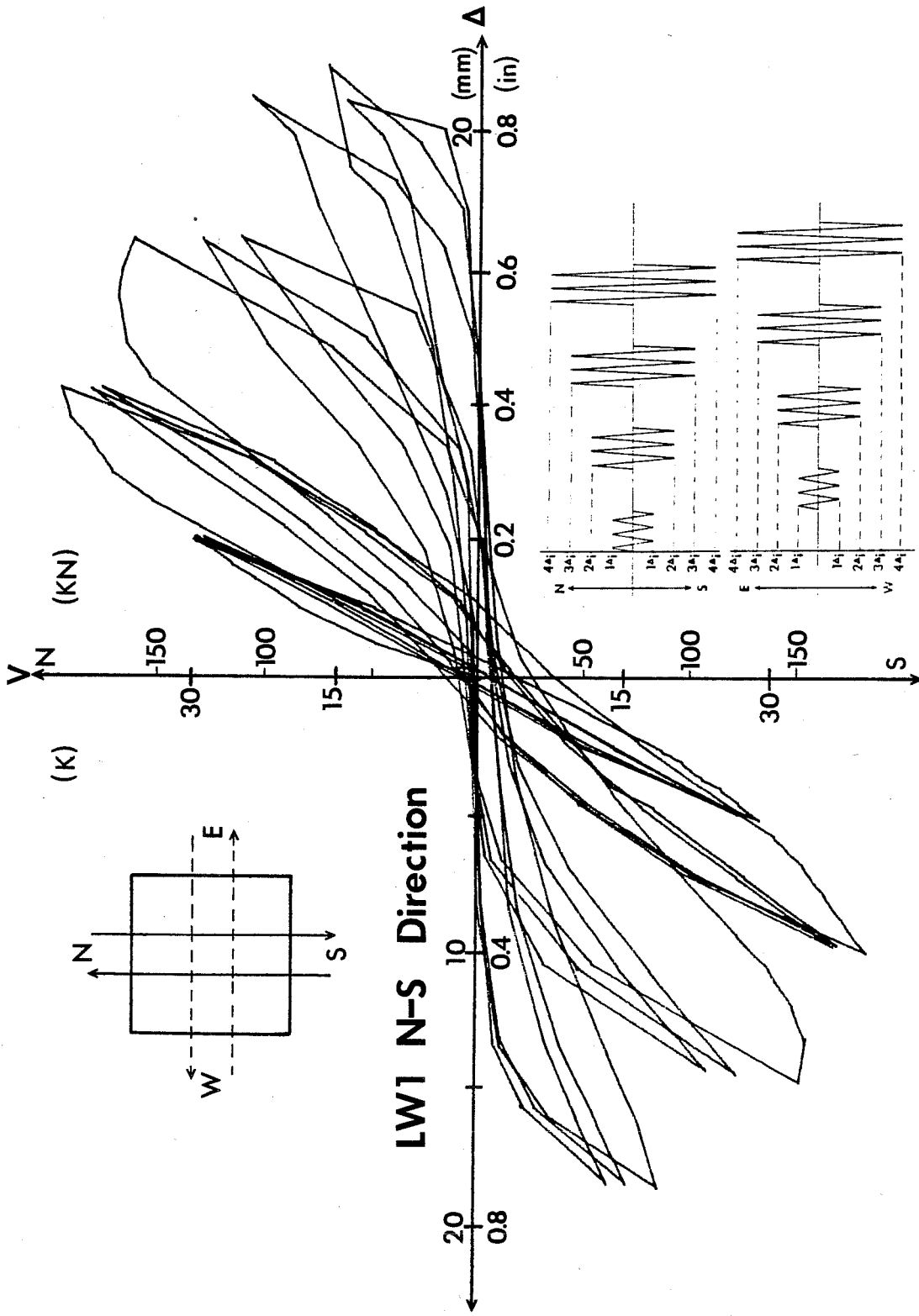


Fig. 3.1 Load-deflection curve, LW1 - N-S direction

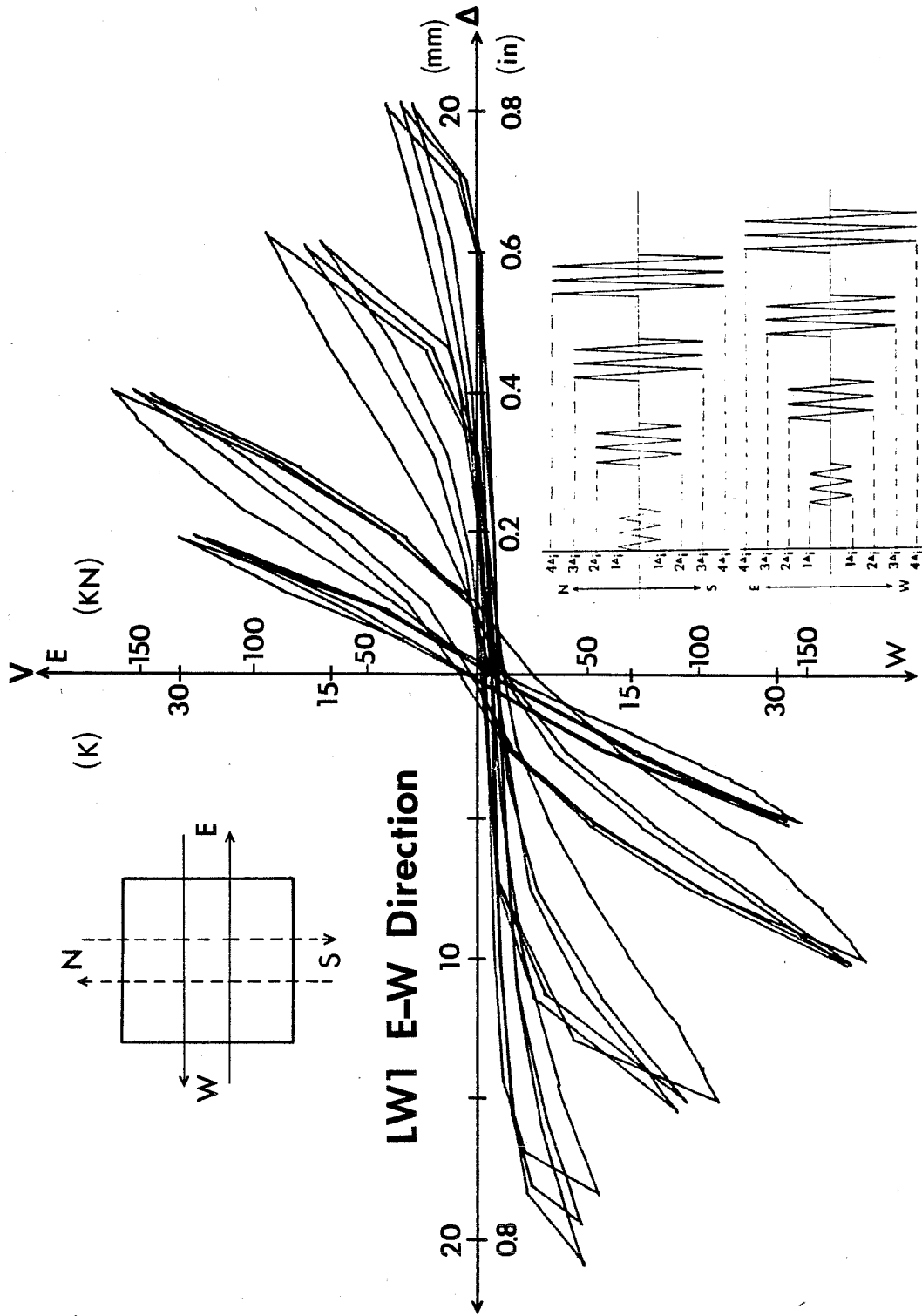


Fig. 3.2 Load-deflection curve, LW1 - E-W direction

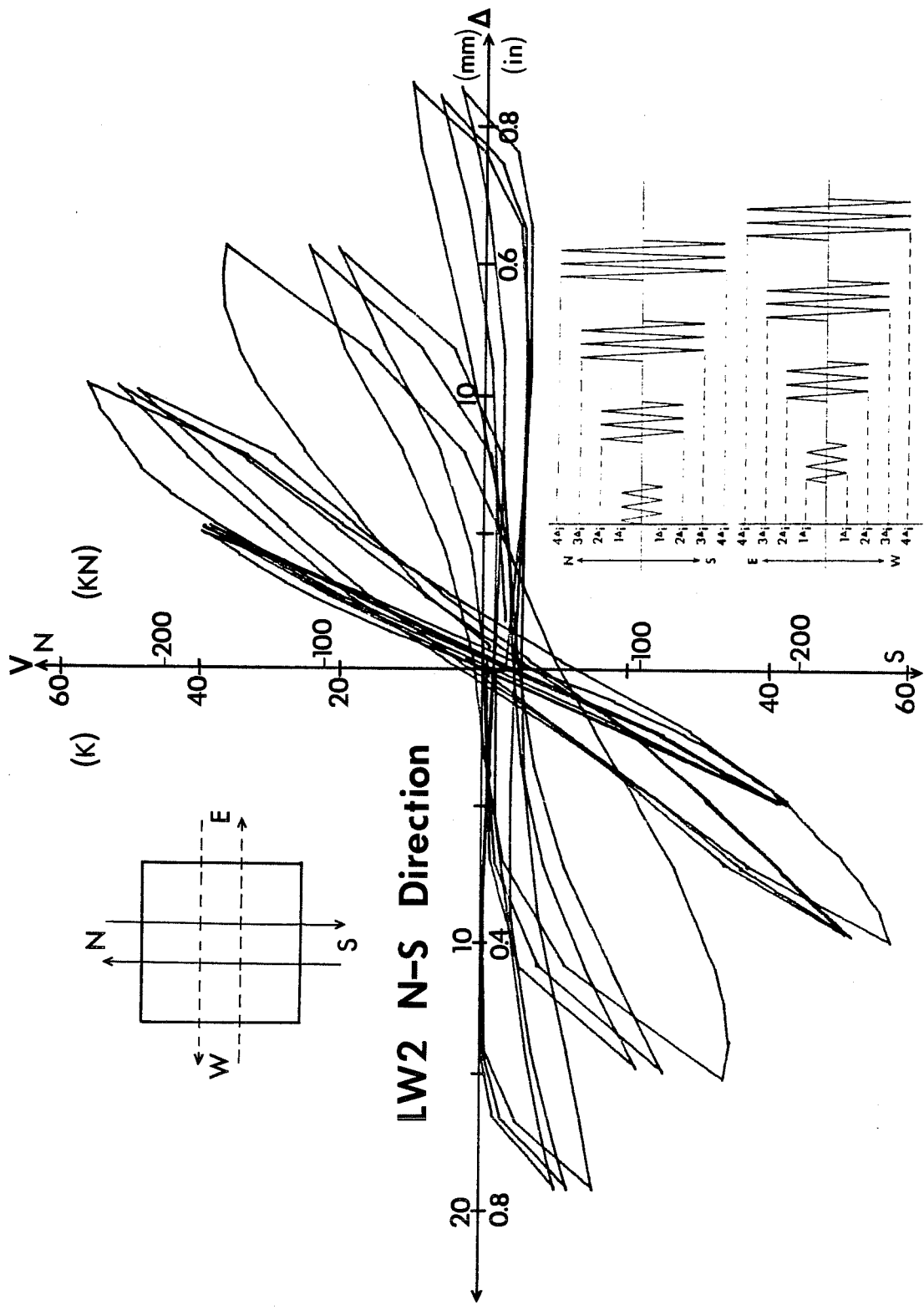


Fig. 3.3 Load-deflection curve, LW2 - N-S direction

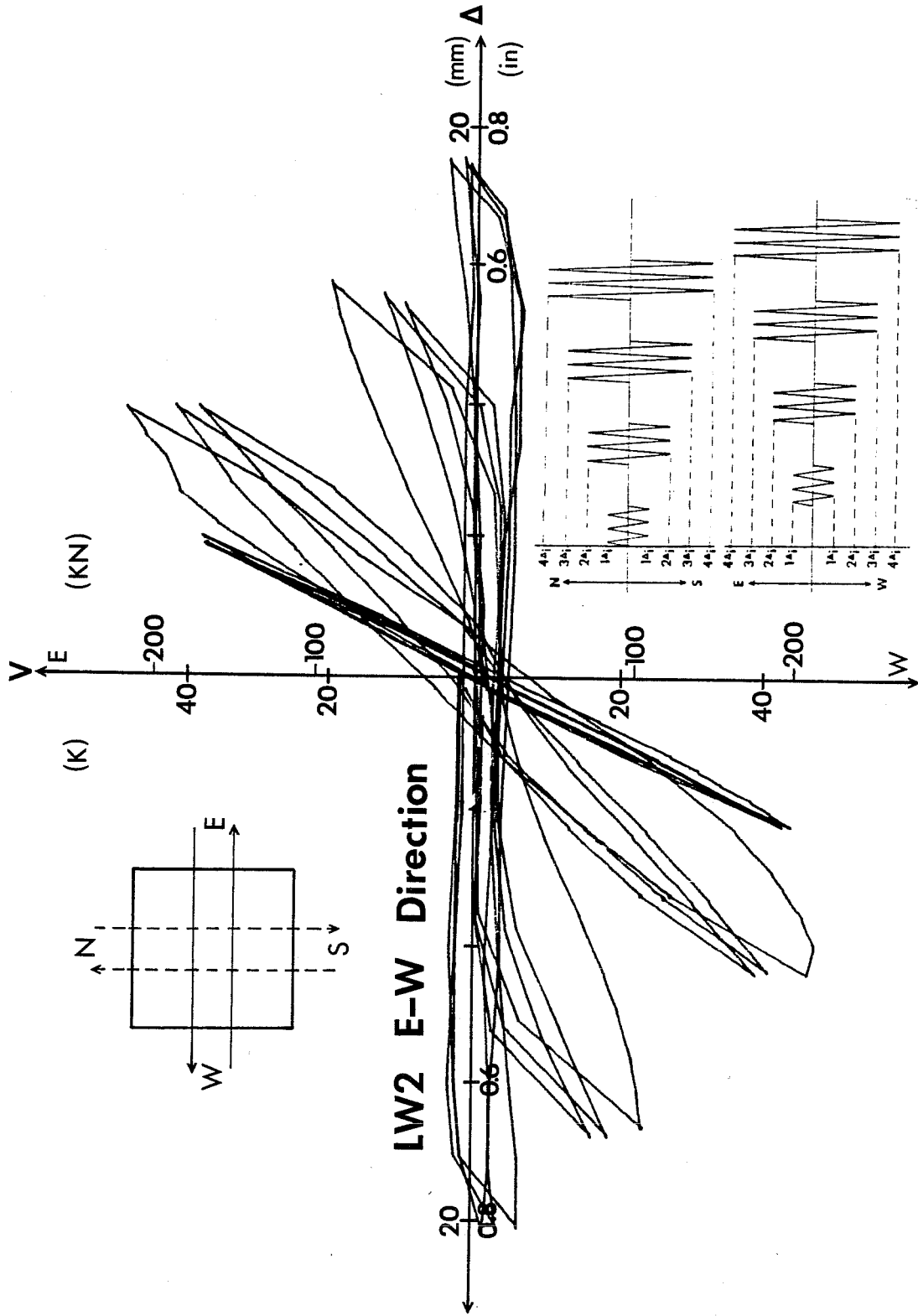


Fig. 3.4 Load-deflection curve, LW2 - E-W direction

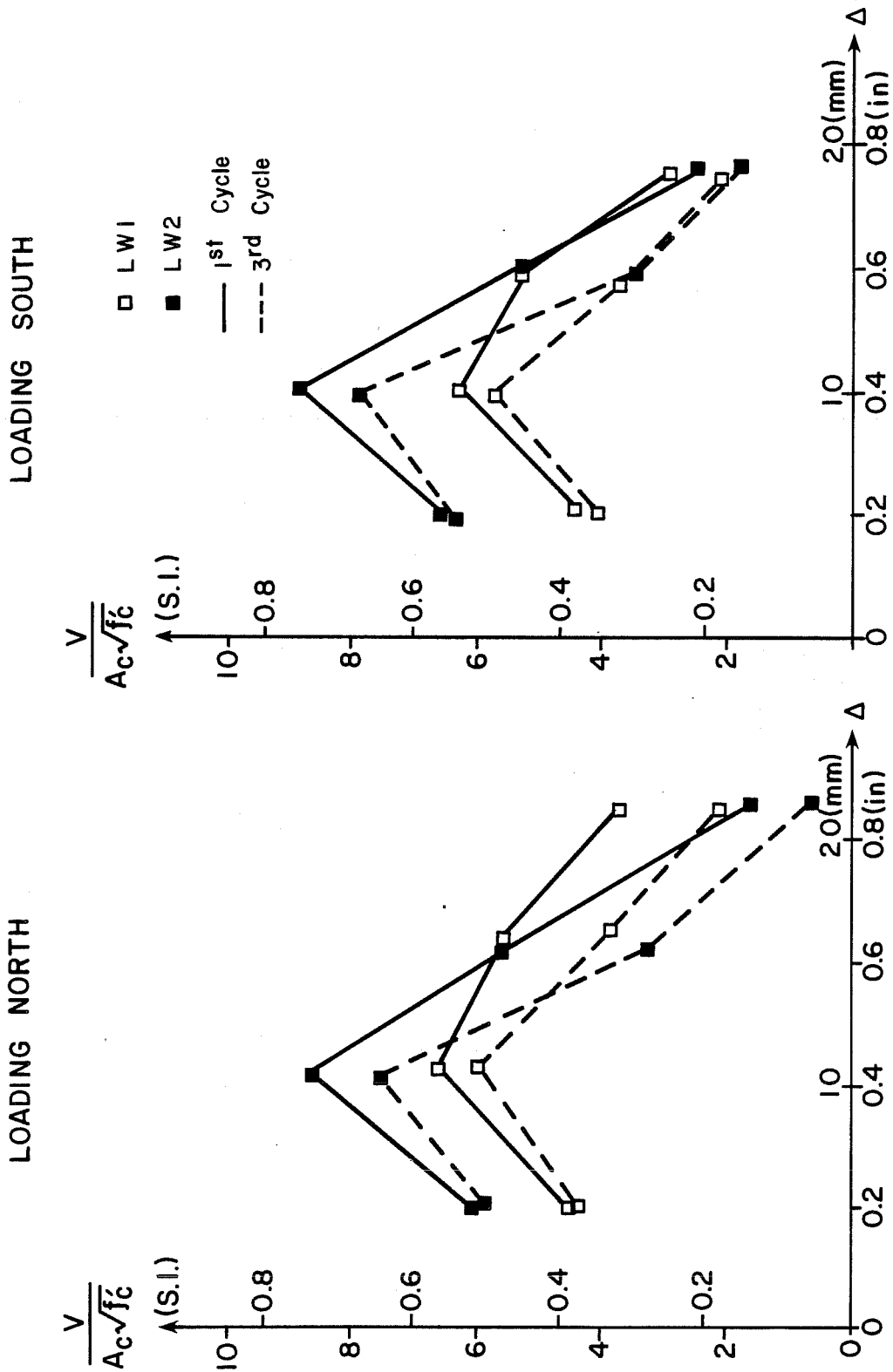


Fig. 3.5 Envelopes of load deflection, LW1 and LW2 - N-S direction

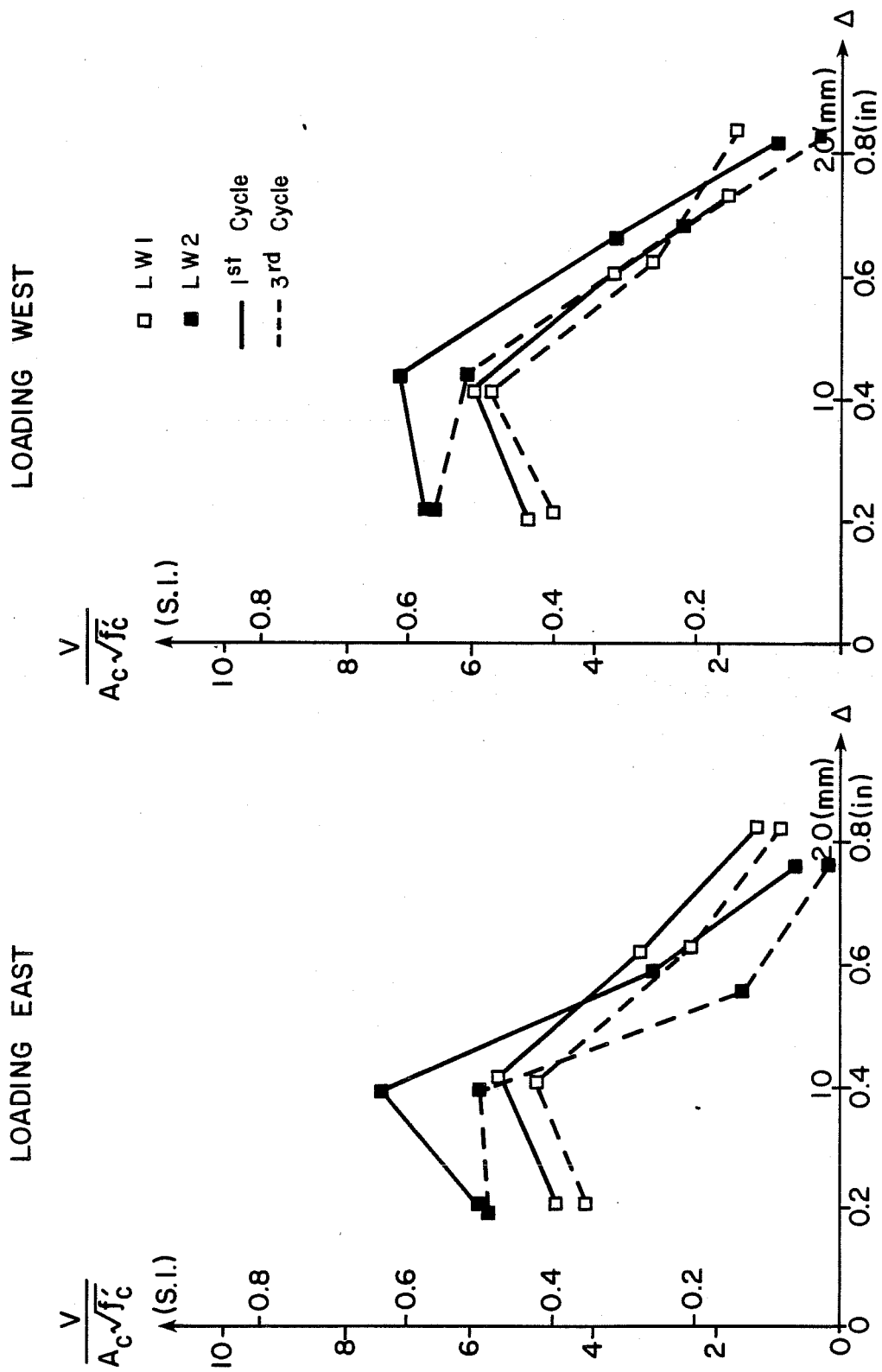


Fig. 3.6 Envelopes of load deflection, LW1 and LW2 - E-W direction

the contribution of the concrete shell to resist lateral load was low when extensive cracking and spalling has occurred.

Figure 3.7 illustrates the shear deterioration which took place in tests LW1 and LW2. For deformation levels greater than $2\Delta_i$, there is a larger difference between first and third peaks for tests LW2 than is observed in test LW1. The severe shear decay after the $2\Delta_i$ level in test LW2 is clearly shown, especially in the east-west direction. The most rapid shear decay from cycle to cycle occurred at the $2\Delta_i$ level for the east-west direction and at the $3\Delta_i$ level for the north-south direction.

3.2.3 Crack Patterns. Crack patterns for each of the tests were photographed at the end of each loading cycle. Figure 3.8 illustrates typical crack patterns for the east face of LW1 after three cycles at $1\Delta_i$, $2\Delta_i$, $3\Delta_i$, and $4\Delta_i$. At $1\Delta_i$, initial diagonal cracks originated at the end block and were inclined at 45° across the face of the column. Diagonal cracking was uniformly distributed across the column face at a deflection of $2\Delta_i$. Concrete spalling was observed at the column corners at $3\Delta_i$. The diagonal cracks were wider and extended into the core section of the column. At the end of the $4\Delta_i$ cycles, the majority of the concrete cover (shell) spalled off. Extensive diagonal cracking was observed in the core section.

Typical crack patterns for the east face of LW2 after three cycles at $1\Delta_i$, $2\Delta_i$, $3\Delta_i$, and $4\Delta_i$ are shown in Fig. 3.9. At $1\Delta_i$ only minor cracking was observed on the column face. Diagonal cracks inclined at 45° were located near the lower end block. Additional diagonal cracking was observed on the column face as the deflection increased to $2\Delta_i$. The orientation of the diagonal cracking at this level was about 30° , measured from vertical. At a deflection level of $3\Delta_i$, significant concrete spalling was observed along the column corners and partial spalling occurred on the column face at midheight. Diagonal cracking was observed to extend into the core section of

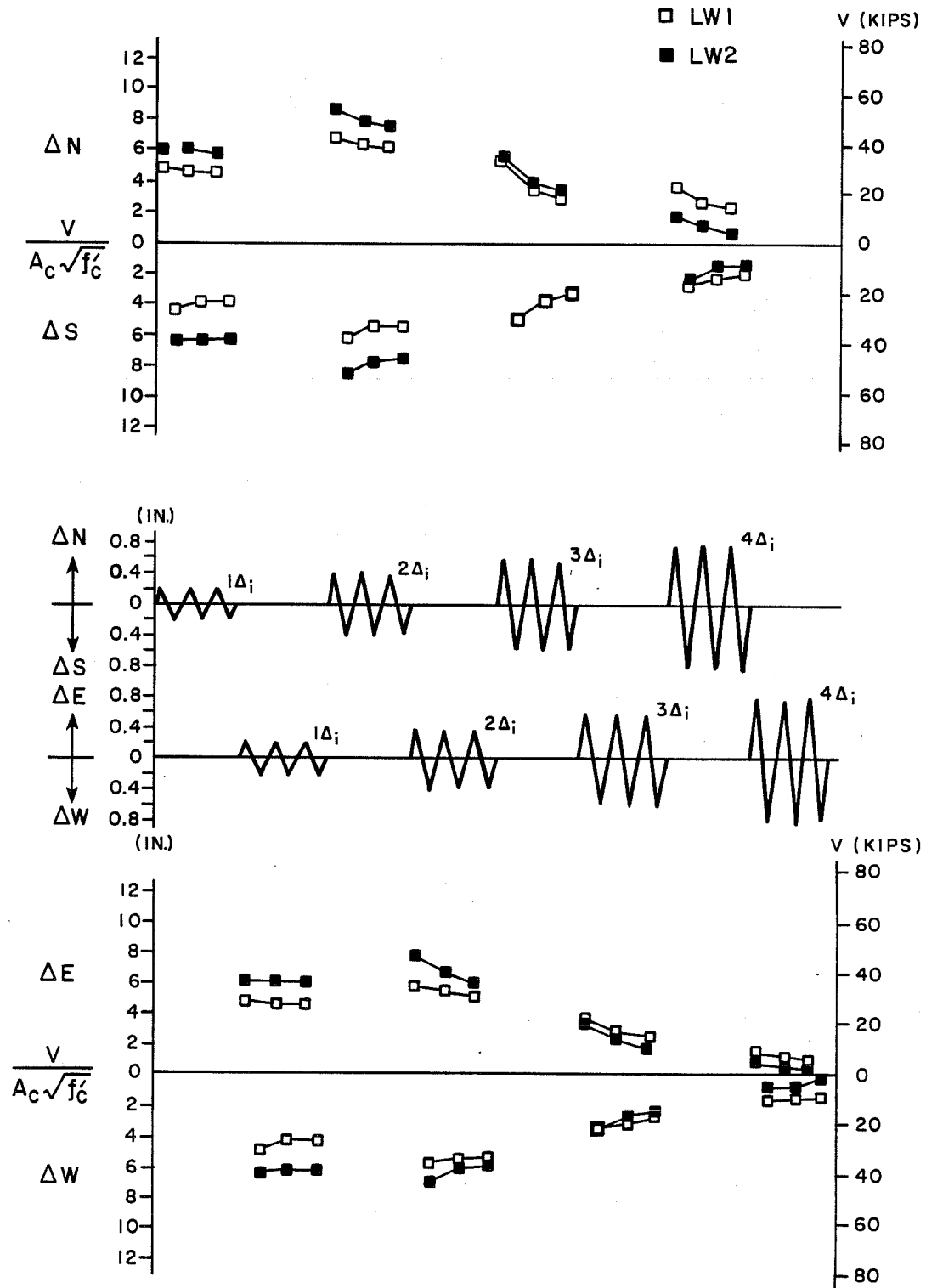
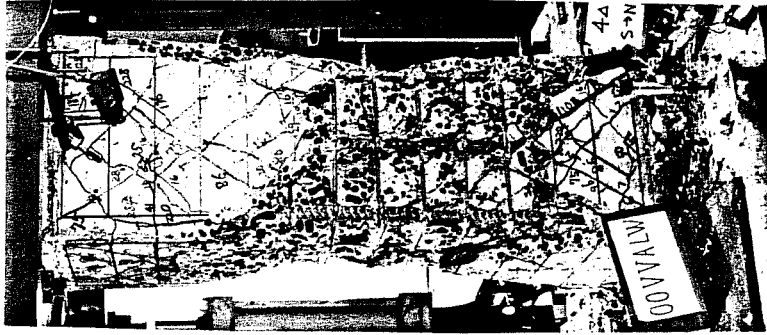
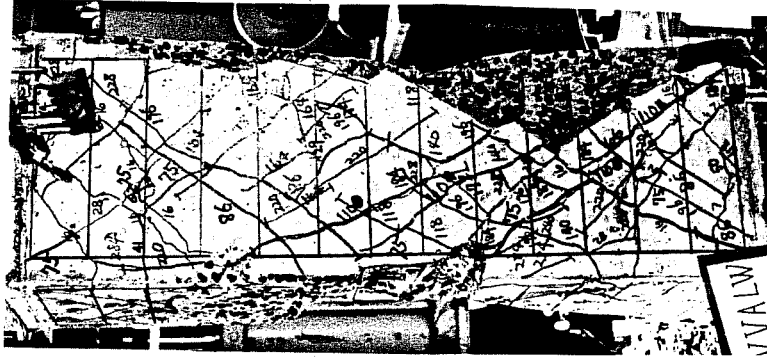


Fig. 3.7 Shear deterioration, tests LW1 and LW2



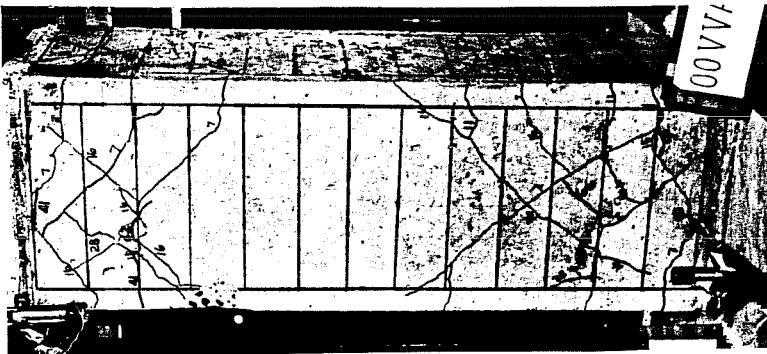
(a) $1\Delta_i$



(b) $2\Delta_i$

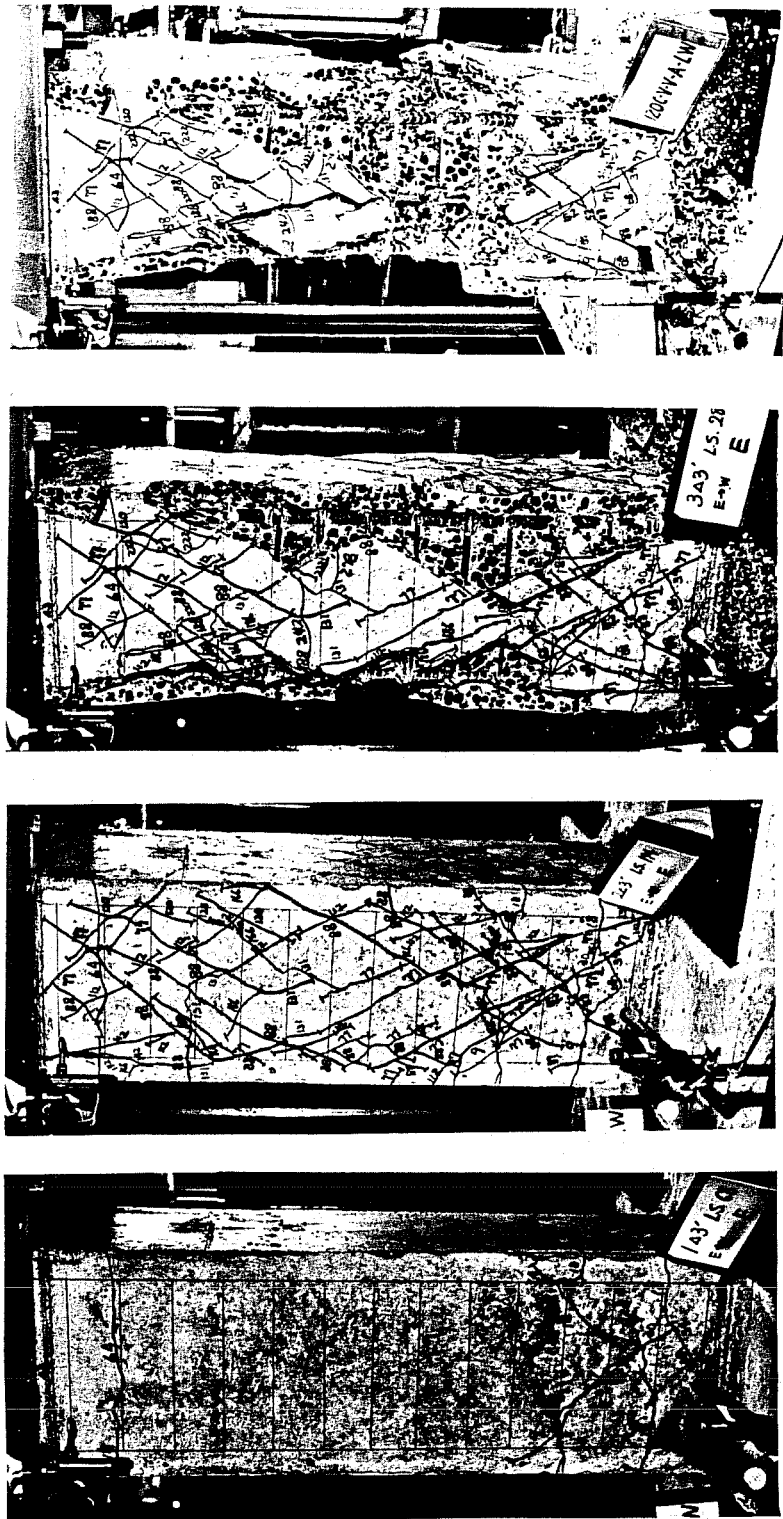


(c) $3\Delta_i$



(d) $4\Delta_i$

Fig. 3.8 Crack patterns, test LWI



(a) $1\Delta_i$ (b) $2\Delta_i$ (c) $3\Delta_i$ (d) $4\Delta_i$

Fig. 3.9 Crack patterns, test LW2

the column. At the end of the $4\Delta_i$ cycles, major spalling was observed throughout the midheight of the column face. Severe diagonal cracking was observed in the core section of the column. Crushing of the concrete core section and buckling of the longitudinal reinforcement were evident.

CHAPTER 4

BEHAVIOR OF NORMALWEIGHT SPECIMENS

4.1 Introduction

Two test specimens constructed with normalweight concrete were tested and reported by Ramirez¹⁶ and Maruyama.¹⁷ The lateral loading history was identical to the loading for the lightweight concrete specimens. One specimen was tested with no axial load and one was tested with a constant axial compression load of 120 kips ($0.12P_u$). As with the lightweight concrete test results, the behavior of the normalweight concrete test specimens was reported in terms of load versus deflection plots, shear deterioration plots, and tables and plots of peak lateral forces. Photographs were used to record crack patterns at each peak deflection.

4.2 Description of Test Results

4.2.1 Load-Deflection Curves. The load-deflection curves for the normalweight concrete test specimens NW1 and NW2 are shown in Figs. 4.1 through 4.4. Figures 4.1 and 4.2 show the load-deflection relationship for the test with no axial load, NW1. Figures 4.3 and 4.4 show the load-deflection relationship for the test with axial load, NW2. For deflections up to $2\Delta_1$, the lateral load associated with a given deflection is greater for the test with axial load, NW2. For both tests at deflection levels less than $2\Delta_1$, the behavior of the specimens is not greatly affected by previous loadings in the orthogonal direction. At deflection levels greater than $2\Delta_1$, the adverse effects of alternate application of lateral deformations are evident in the test with axial load.

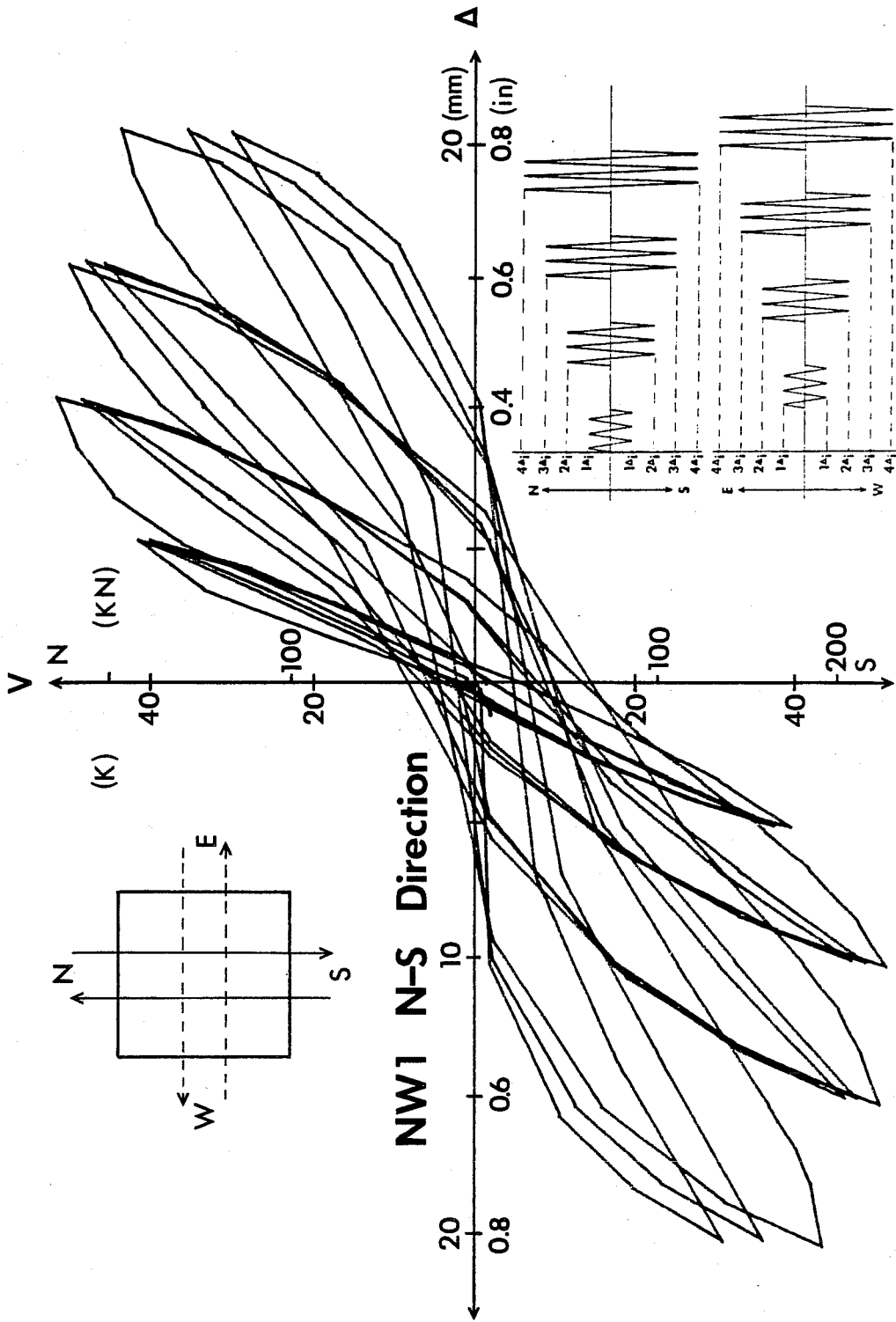


Fig. 4.1 Load deflection curve, NW1 - N-S direction

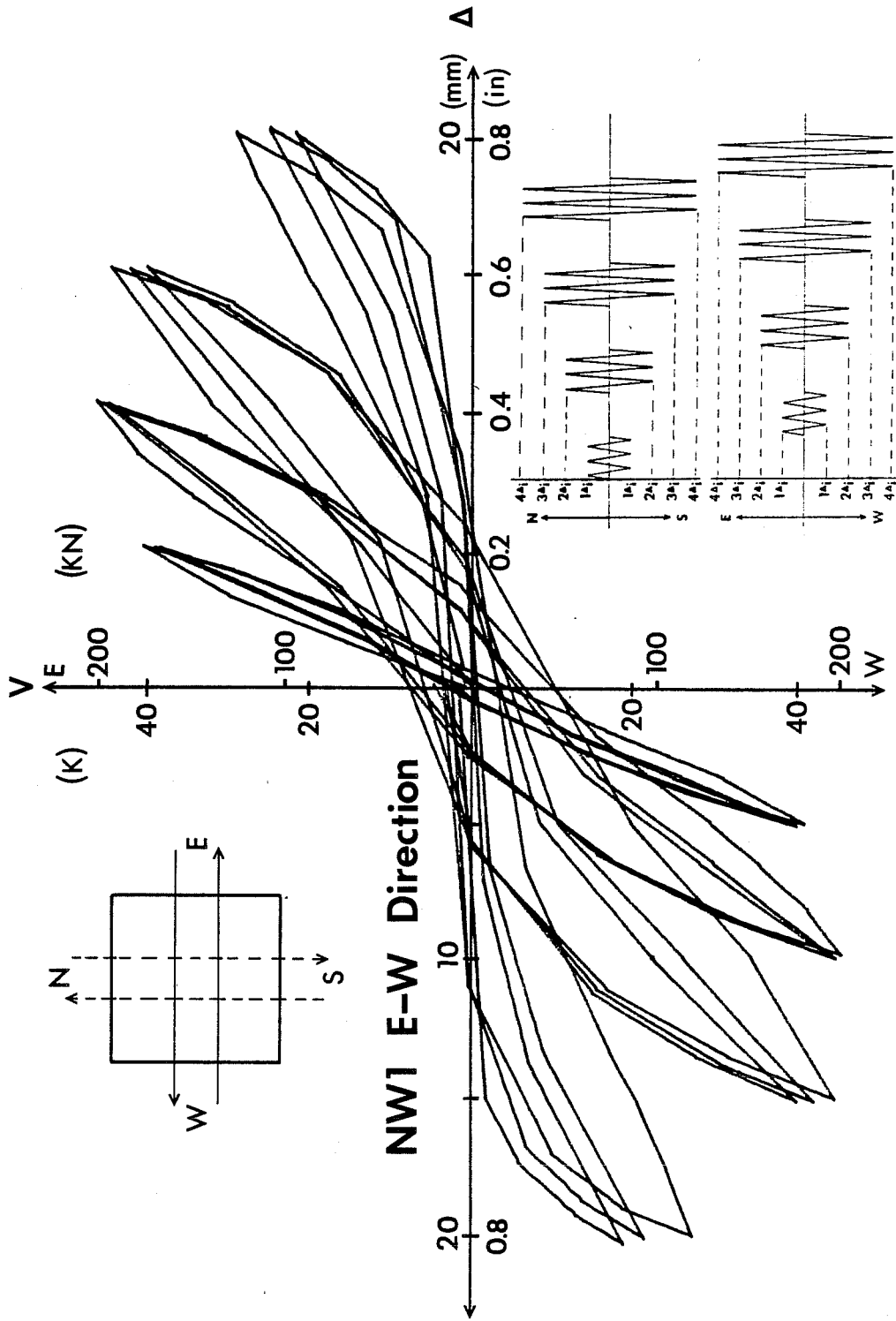


Fig. 4.2 Load deflection curve, NW1 - E-W direction

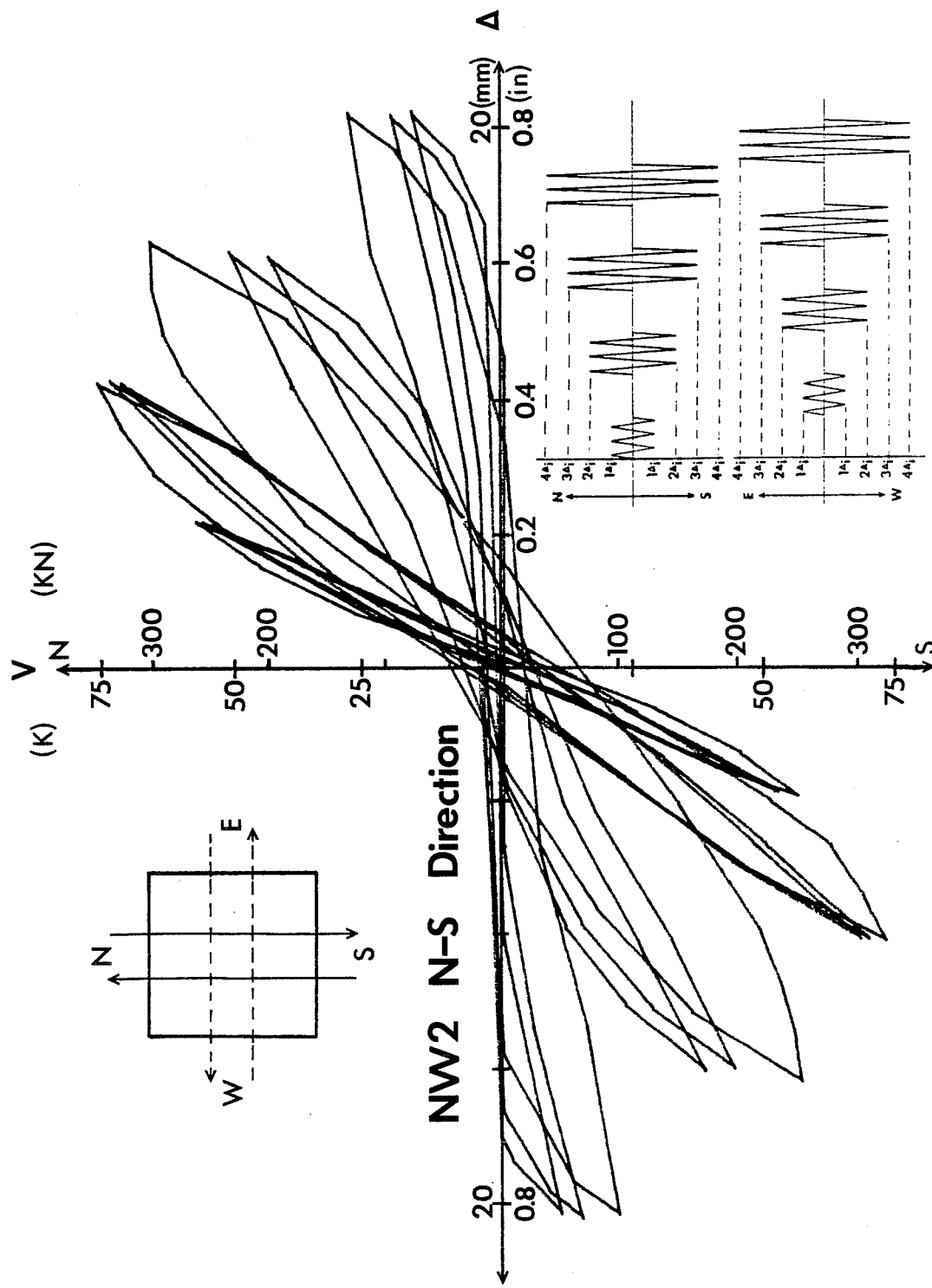


Fig. 4.3 Load deflection curve, NW2 - N-S direction

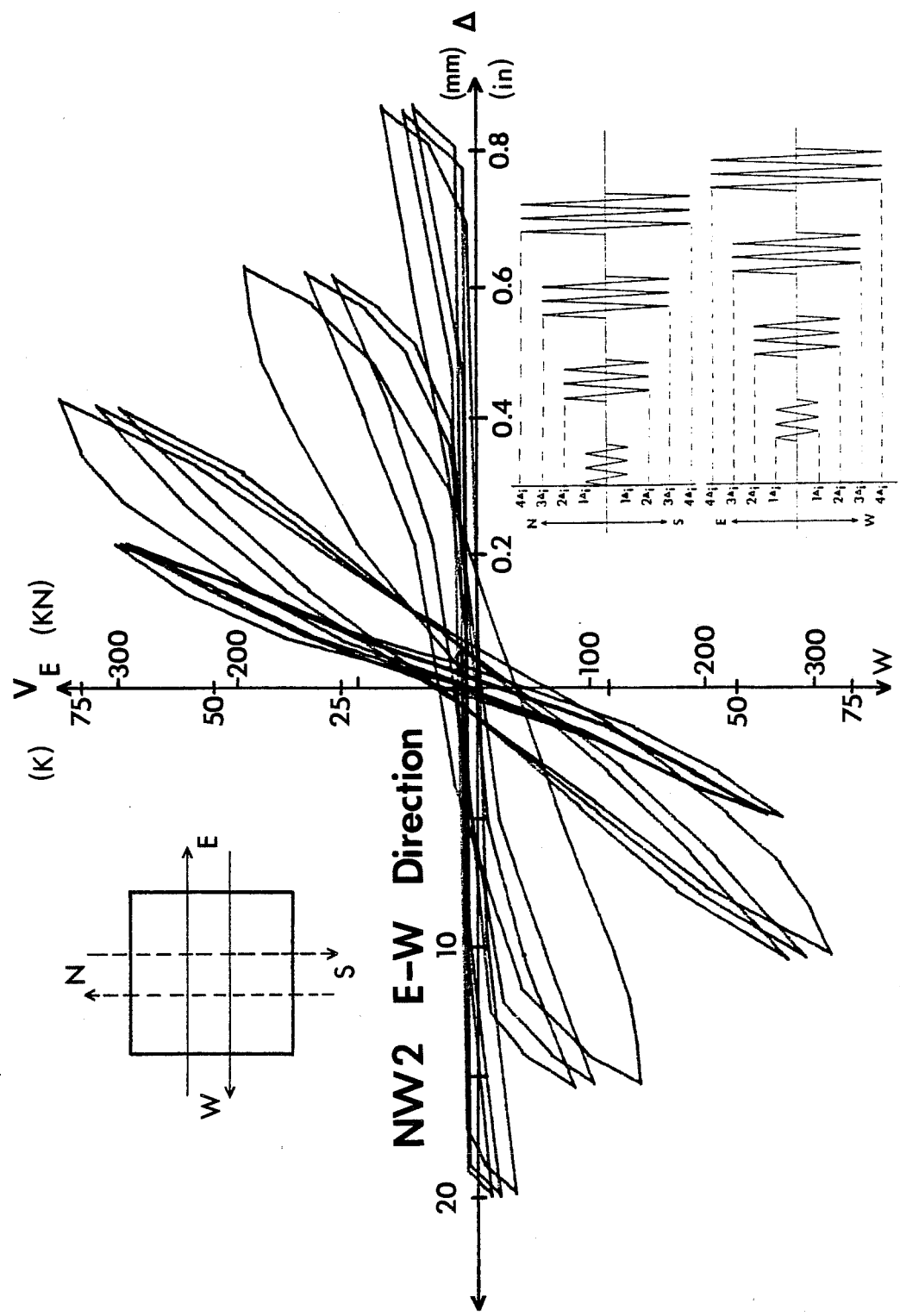


Fig. 4.4 Load deflection curve, NW2 - E-W direction

Significant losses in specimen strength and stiffness due to alternate application of lateral loads are not observed in test NW1. The pinching of the hysteretic loops appears to be more pronounced in test NW1 than NW2, however, the loss of strength and stiffness in both cases is rapid once the peak load is reached. Peak envelope curves for tests NW1 and NW2 are shown in Figs. 4.5 and 4.6. As expected, the lateral load required to attain displacement levels of $1\Delta_i$ or $2\Delta_i$ was greater for NW2 (axial load) as compared to NW1 (no axial load). At deflection levels greater than $2\Delta_i$, test specimens subjected to axial loads (NW2) showed significant losses of strength and stiffness as compared to tests with no axial load.

4.2.2 Peak Lateral Forces. Values of axial load, peak applied lateral load, normalized shear stress and lateral deflections are tabulated in Appendices C and D for test specimens NW1 and NW2, respectively. Figure 4.7 illustrates the shear deterioration that took place in the tests NW1 and NW2. For deformation levels up to $2\Delta_i$, the behavior of the two specimens was similar. The shear deterioration between the first and third cycles at $2\Delta_i$ is small for both NW1 and NW2. At a deflection $3\Delta_i$, the rate of shear deterioration for specimen NW2 greatly exceeds that of specimen NW1. Although the shear strength of NW2 is less than the shear strength of NW1 at a deflection of $4\Delta_i$, the rate of shear deterioration for the two test specimens is similar.

4.2.3 Crack Patterns. Figure 4.8 illustrates typical crack patterns for specimen NW1 at deflection levels $1\Delta_i$, $2\Delta_i$, $3\Delta_i$ and $4\Delta_i$. At a deflection of $1\Delta_i$, minor cracking is observed near the end blocks on all faces. Diagonal cracking is concentrated near the end blocks on all faces at a deflection level of $2\Delta_i$. The major cracks have an orientation of 30° , measured from vertical. At $3\Delta_i$ the diagonal cracking is increased and uniformly covers all faces of the column. At failure, diagonal cracks at an angle of 35° were dominant.

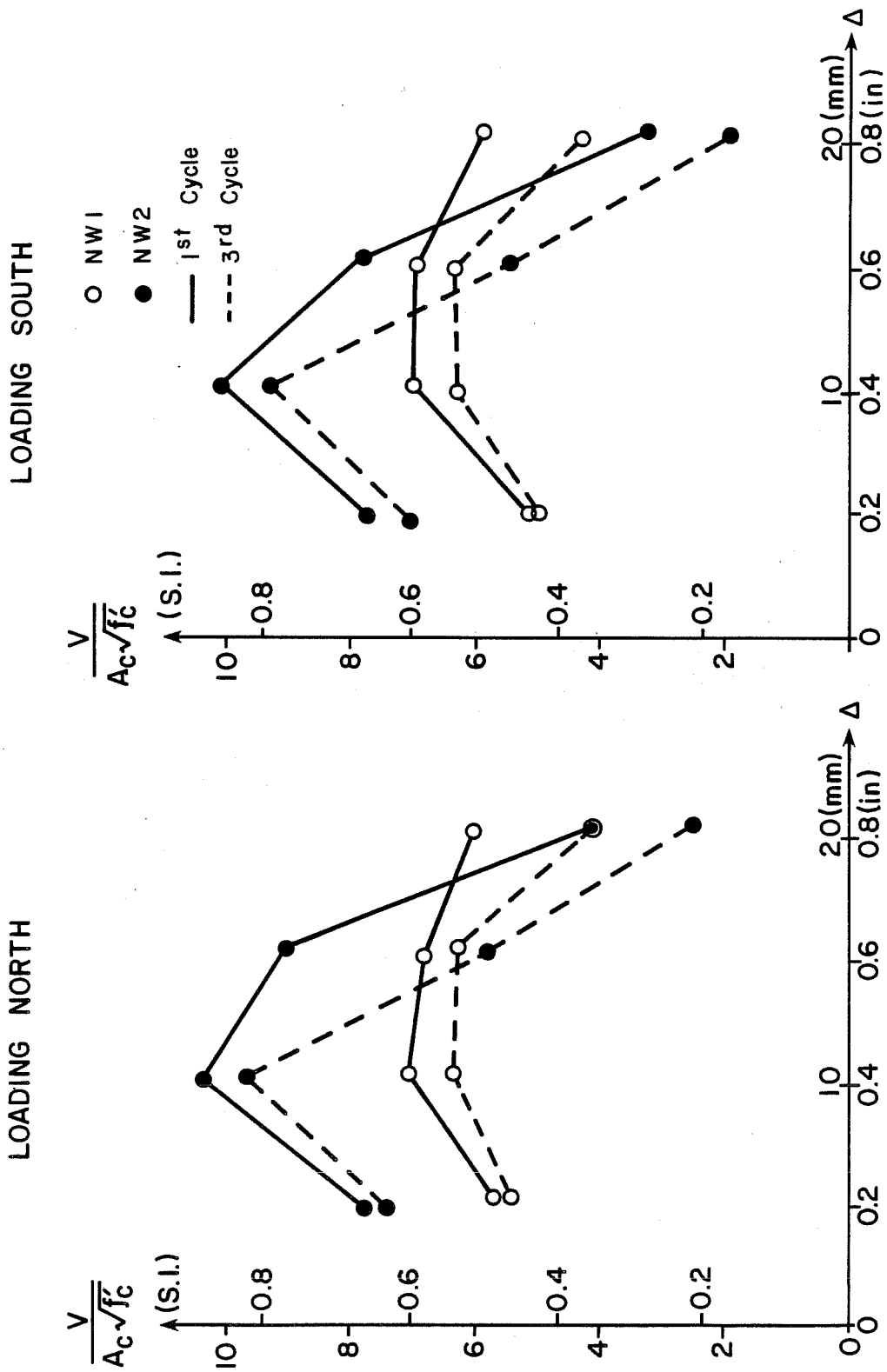


Fig. 4.5 Envelopes of load deflection, test NW1 and NW2 - N-S direction

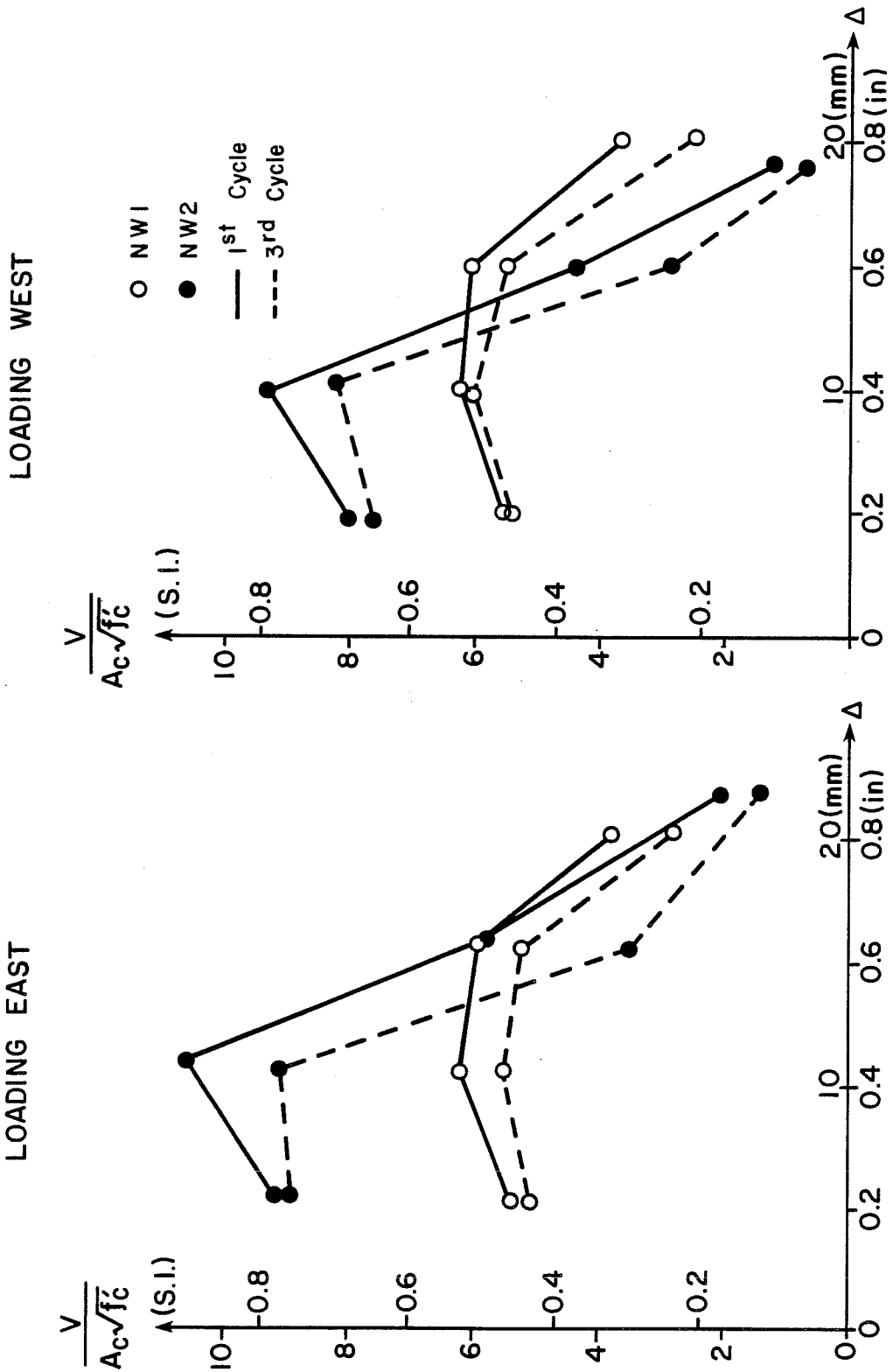


Fig. 4.6 Envelopes of load deflection, test NW1 and NW2 - E-W direction

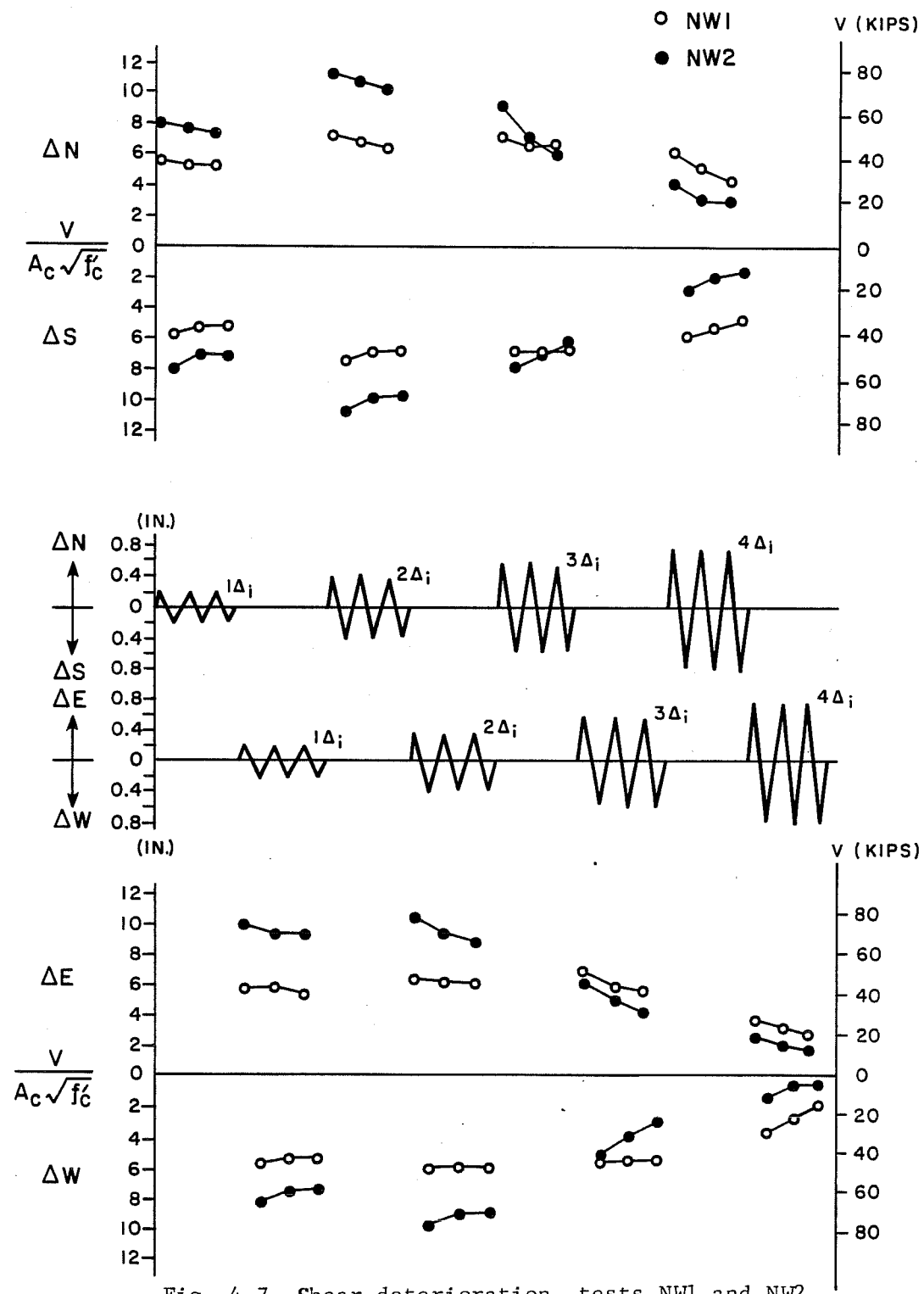
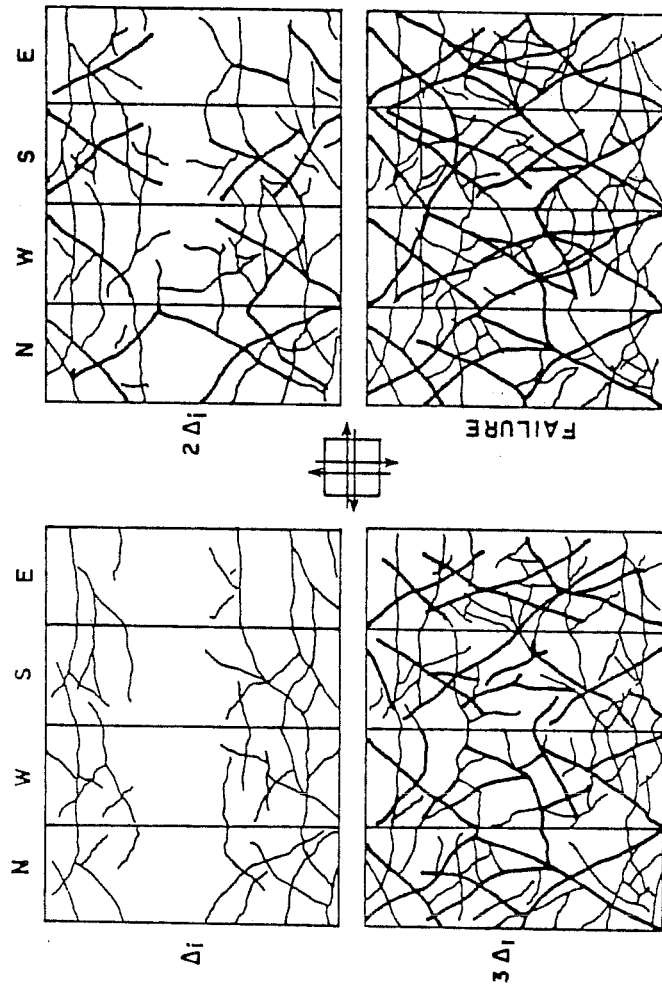
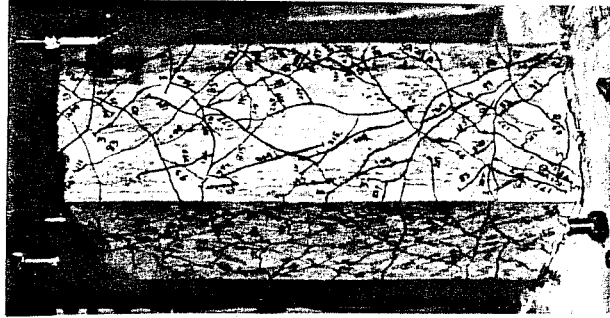


Fig. 4.7 Shear deterioration, tests NW1 and NW2



(a) Mapped cracks



(b) $2\Delta_i$

Fig. 4.8 Crack patterns, test NW1

Figure 4.9 shows the appearance of specimen NW2 at the completion of loading. Crack patterns very similar to those observed in test NW1 were observed. Minor spalling was observed at a deflection of $4\Delta_i$ in test NW2.

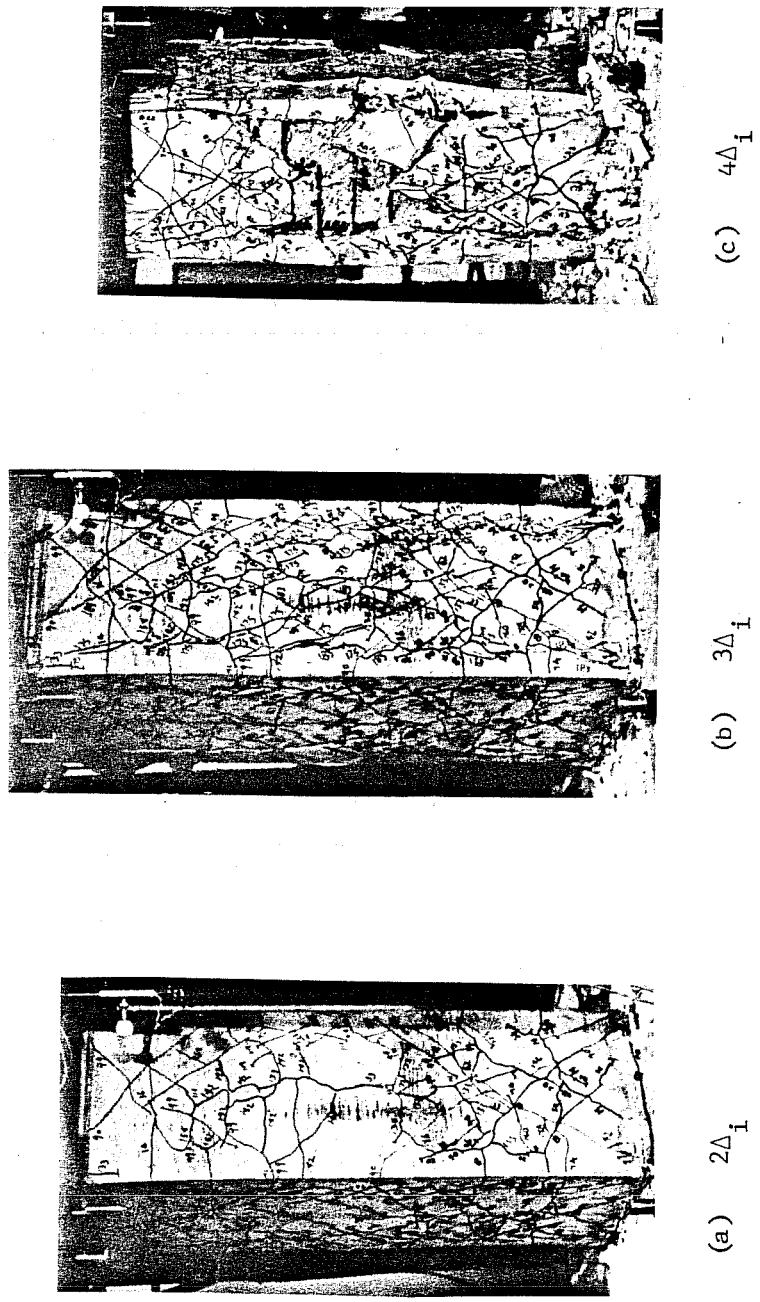


Fig. 4.9 Crack patterns, test NW2

C H A P T E R 5

COMPARISON OF TEST RESULTS

5.1 Introduction

In this chapter the behavior of test specimens constructed of lightweight and normalweight concrete will be compared. The behavior of two lightweight test specimens was reported in Chapter 3. The behavior of two normalweight test specimens was reported in Chapter 4. Identical lateral load histories were used for all tests. An axial compression of 120 kips was applied to one of the lightweight test specimens (LW2) and to one of the normalweight test specimens (NW2). The other two specimens were tested with no axial load (LW1 and NW1). All the test specimens used in this study were constructed using identical longitudinal and transverse reinforcement arrangements. Column cross-sectional dimensions were the same for all test specimens.

The behavior of the short columns is compared in terms of load-deflection curves, peak lateral force envelope curves, shear deterioration plots and cracking patterns.

5.2 Test Results

5.2.1 Specimen Stiffness. A comparison of load-deflection curves for selected cycles provides an indication of the stiffness of the lightweight concrete versus normalweight concrete columns. Load-deflection loops for tests LW1 and NW1 (no axial load) are shown in Figs. 5.1 through 5.5. In the first load cycle (Fig. 5.1), both the lightweight and normalweight concrete column specimens exhibited similar hysteretic behavior. Although differences in

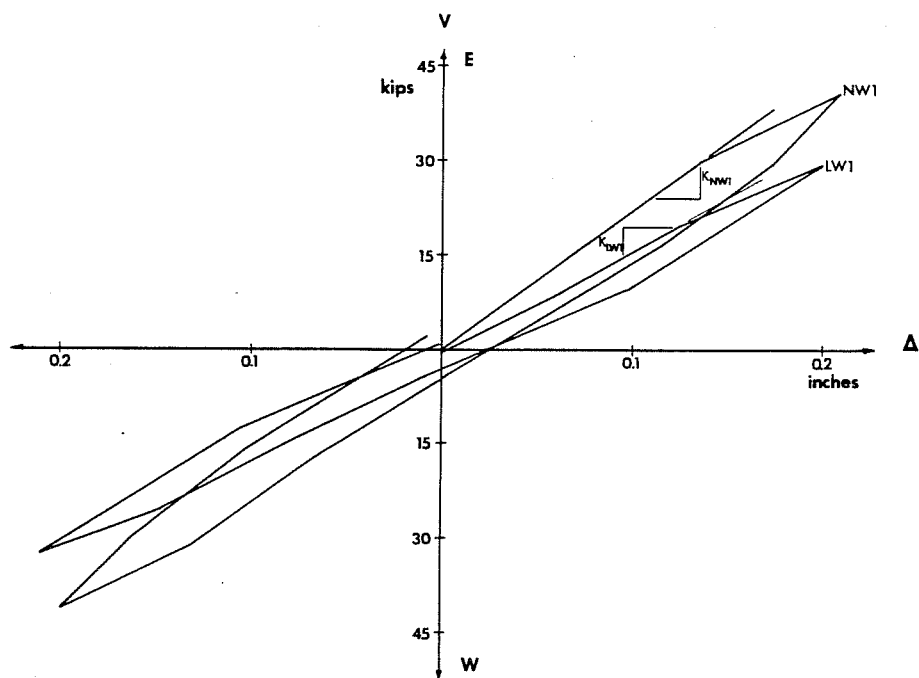
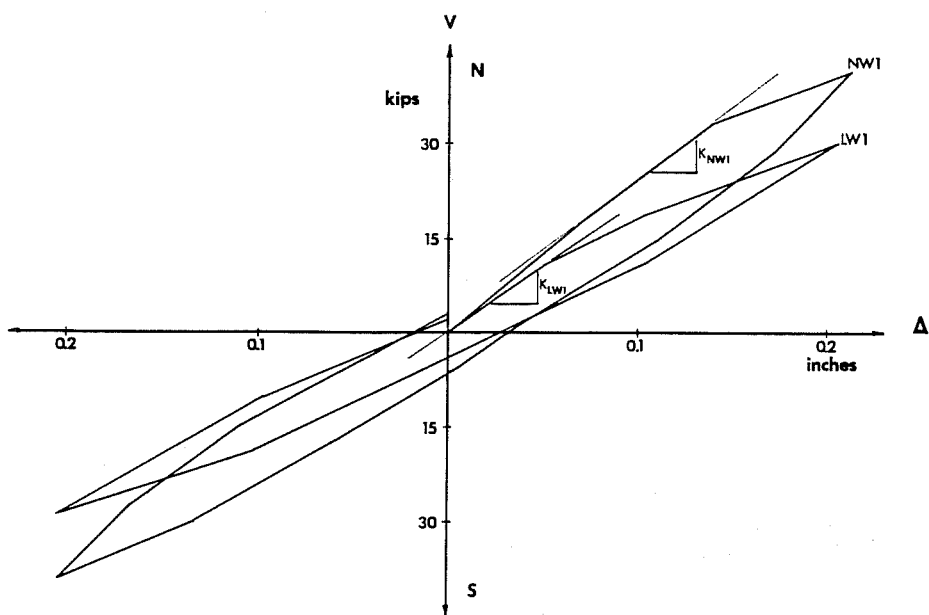


Fig. 5.1 Load deflection curves, tests LW1 and NW1, one cycle at $1\Delta_i$

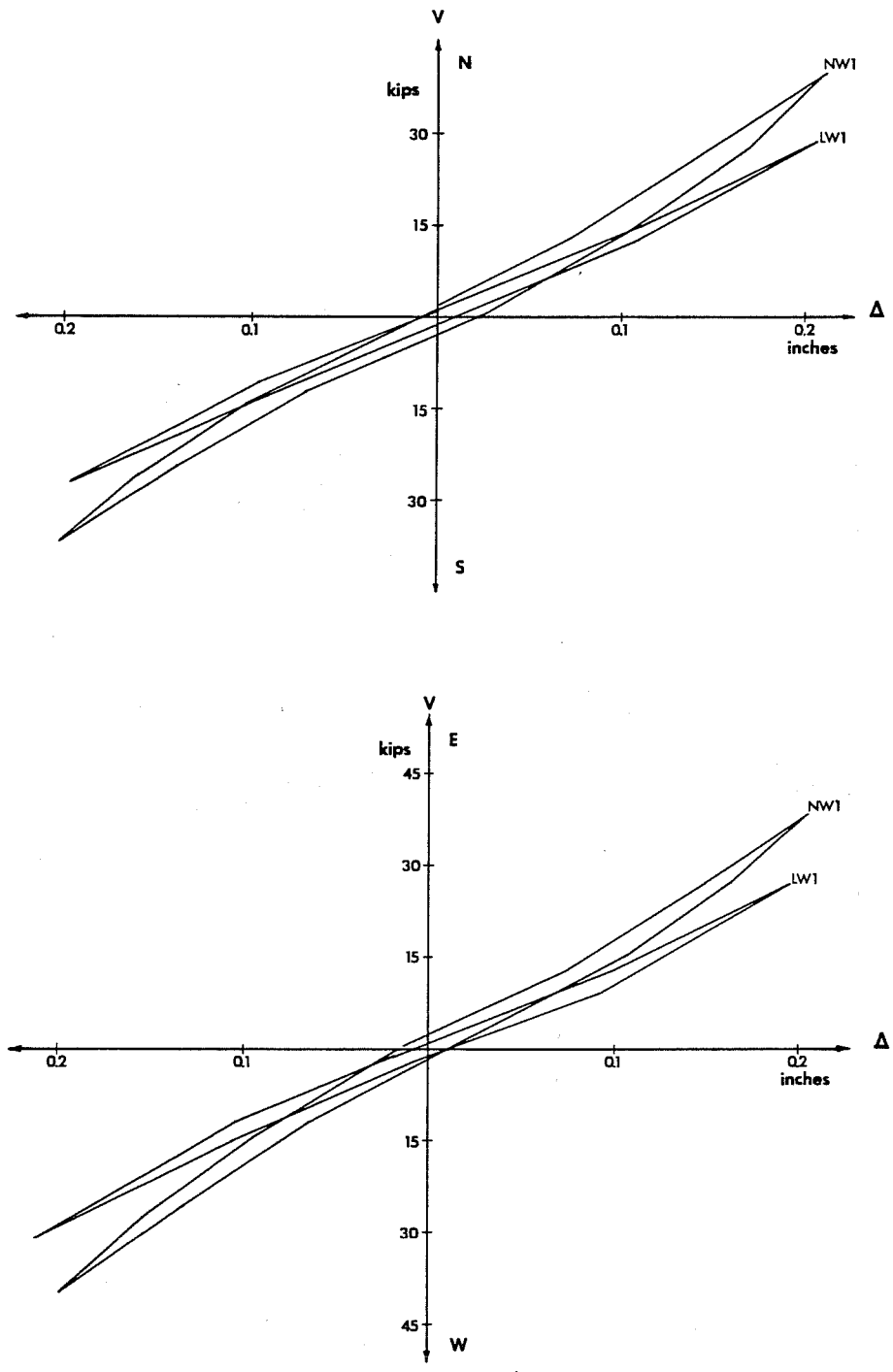


Fig. 5.2 Load deflection curves, tests LW1 and NW1, three cycles at $1\Delta_i$

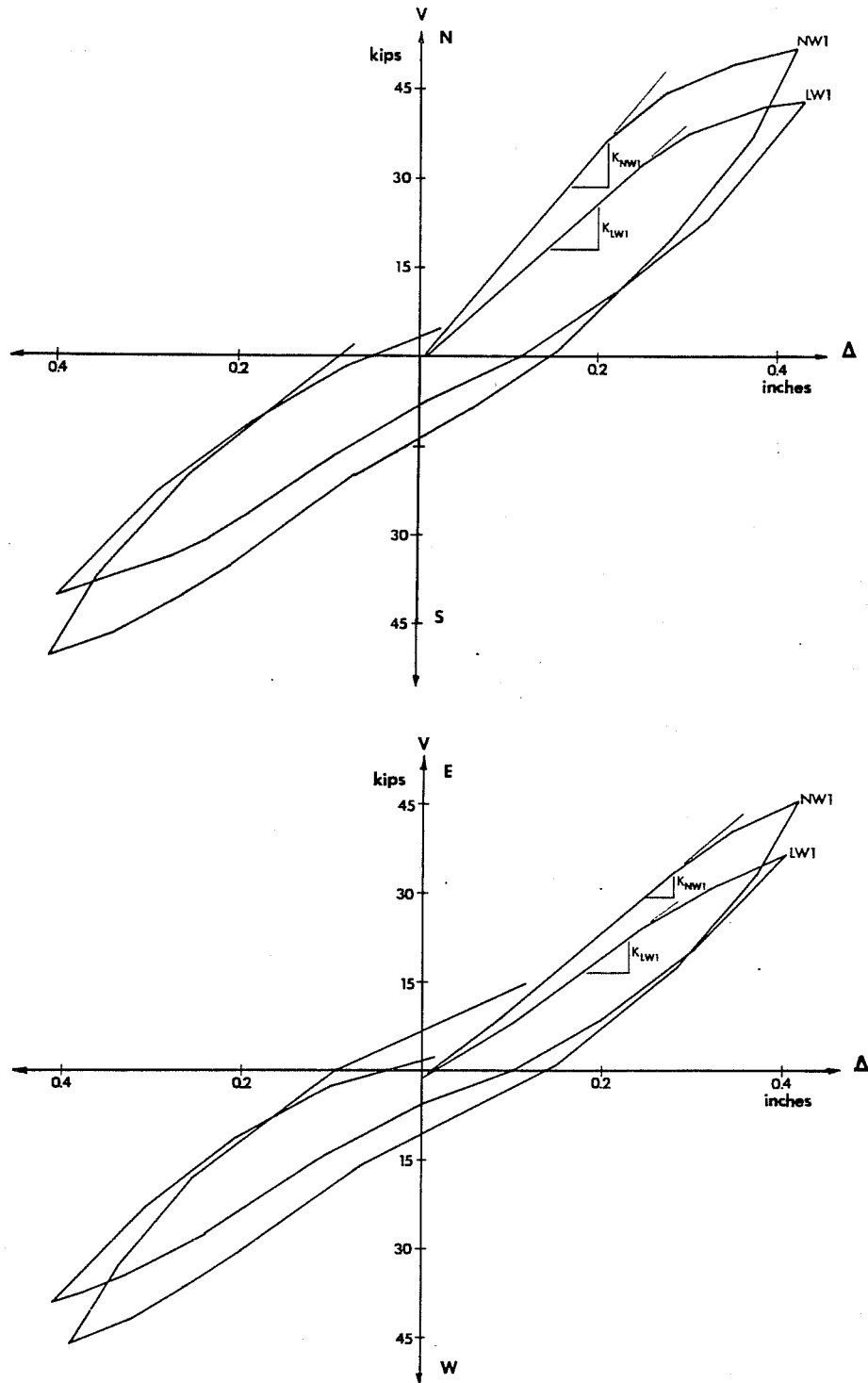


Fig. 5.3 Load deflection curves, tests LW1 and NW1, one cycle at $2\Delta_i$

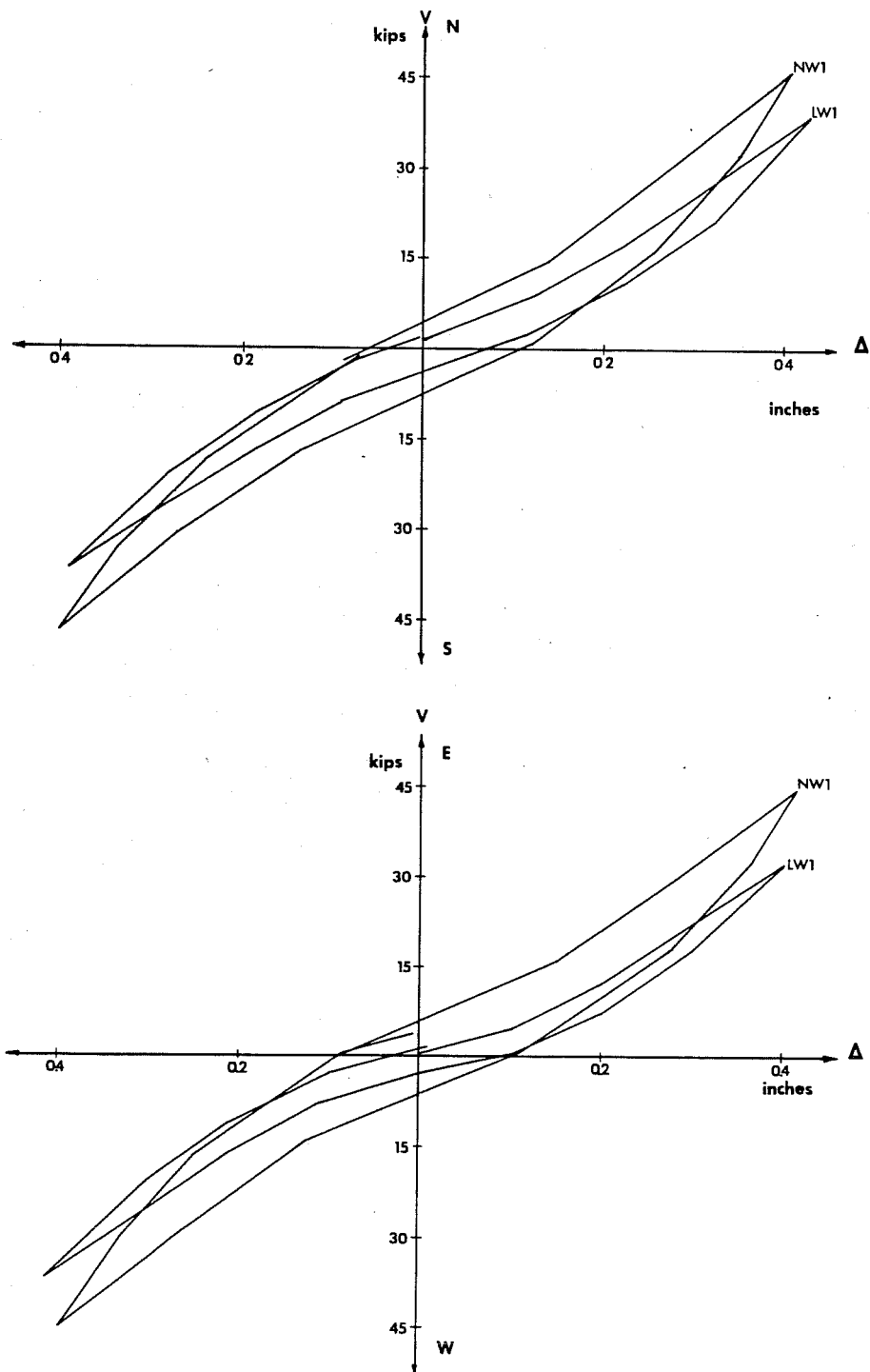


Fig. 5.4 Load deflection curves, tests LW1 and NW1, three cycles at $2\Delta_i$

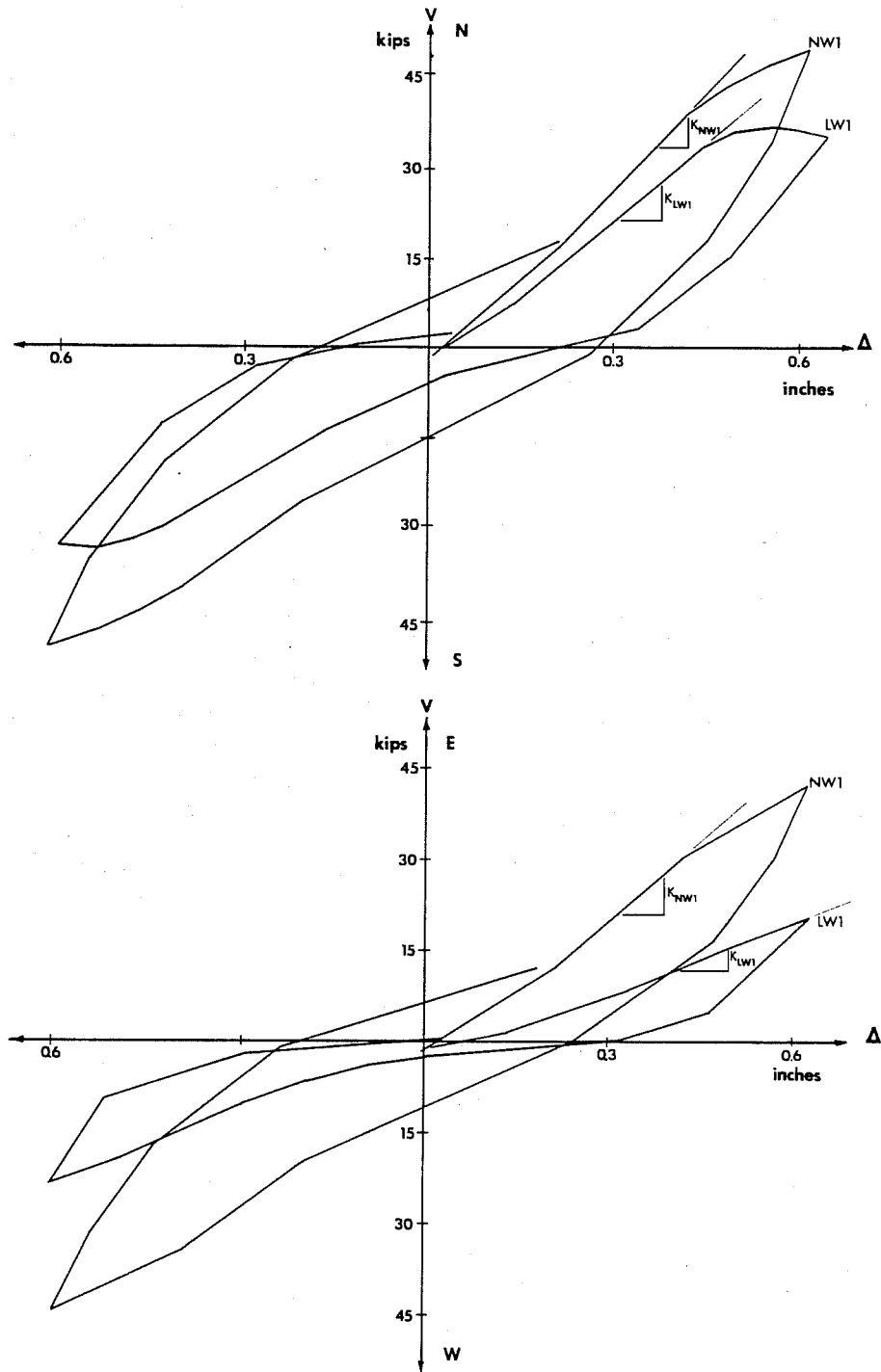


Fig. 5.5 Load deflection curves, tests LW1 and NW1, one cycle at $3\Delta_i$

stiffness were observed, there was very little pinching of the hysteretic loops in either test. During cycles to $2\Delta_i$ (0.40 in.), the stiffness of the lightweight specimen continued to be less than that of the normalweight specimen (Fig. 5.2). Although both specimens exhibited losses in stiffness due to the cyclic loading, pinching of the hysteretic loops for the lightweight specimen was more pronounced than was observed in the normalweight specimen (Fig. 5.3). Considerable losses of specimen stiffness were recorded for the lightweight specimen at a deformation of $3\Delta_i$ (0.60 in.). Pinching of the hysteretic loops was significant in the first deformation cycle at $3\Delta_i$ for the lightweight specimen. The normalweight specimen continued to exhibit stable hysteretic behavior through the $3\Delta_i$ deformation cycle (Figs. 5.4 and 5.5). At deformations greater than $3\Delta_i$, both the lightweight and normalweight specimens exhibited significant losses of stiffness and severe pinching of the hysteretic loops.

Figures 5.6 through 5.10 illustrate individual hysteretic load-deflection loops for tests conducted with an axial compressive load of 120 kips ($0.12P_u$), (LW2 and NW2). Stable hysteretic behavior was observed in both the normalweight and lightweight tests for deformations up to $2\Delta_i$ (0.40 in.). Initial losses in stiffness were observed in the lightweight test specimen after three load cycles at $2\Delta_i$. Figure 5.8 illustrates the stable hysteretic behavior of the normalweight specimen and the loss of stiffness (pinching) of the lightweight specimen. At a deformation of $3\Delta_i$ (0.60 in.), the normalweight specimen underwent only minor stiffness deterioration with cycling while the lightweight specimen continued to lose stiffness rapidly. At deformations greater than $3\Delta_i$, significant losses of stiffness were noted in both the lightweight and normalweight specimens. Nonstable degrading hysteretic behavior with pinching of the load-deflection curves was observed.

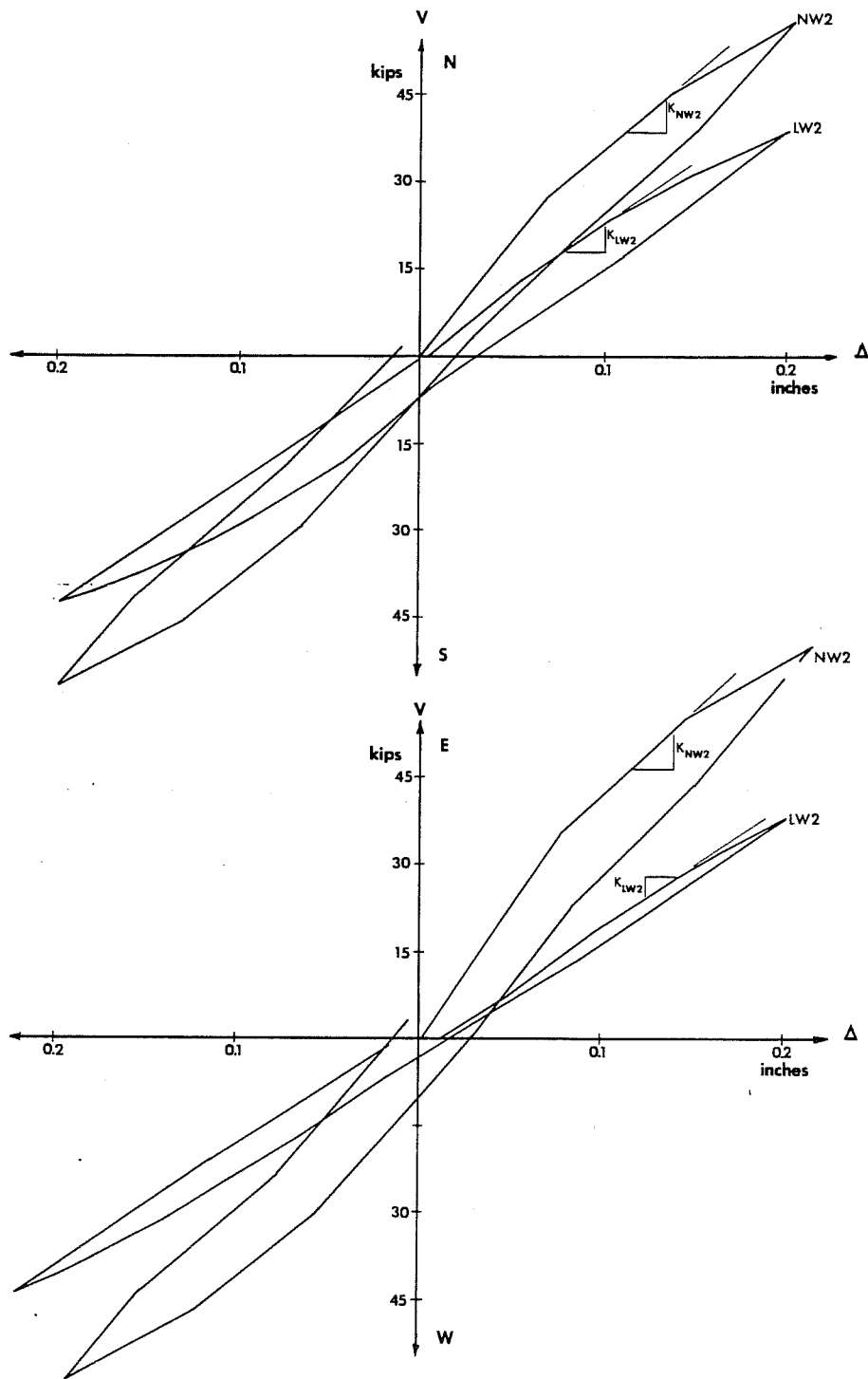


Fig. 5.6 Load deflection curves, tests LW2 and NW2, one cycle at $1\Delta_i$

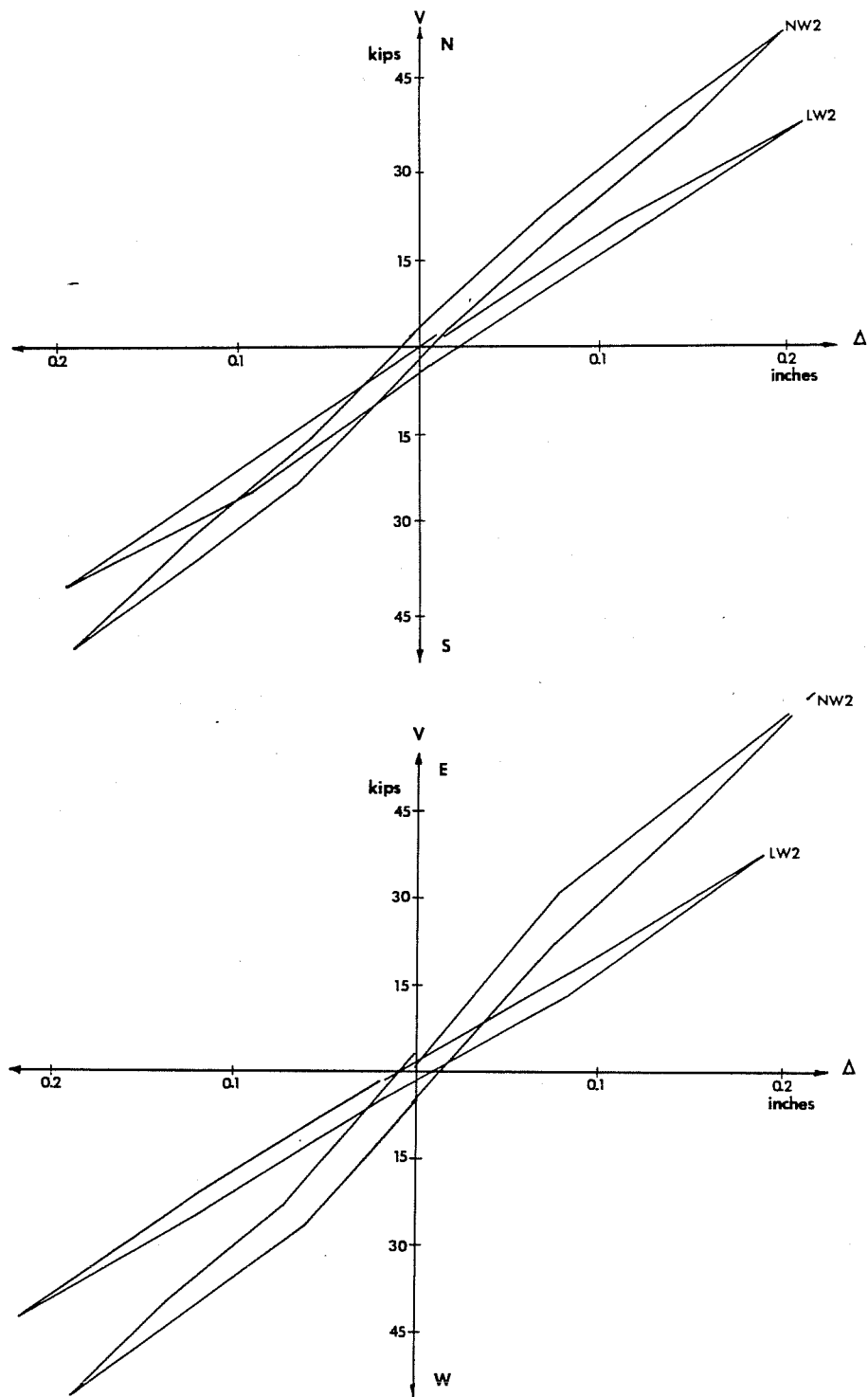


Fig. 5.7 Load deflection curves, tests LW2 and NW2, three cycles at $1\Delta_i$

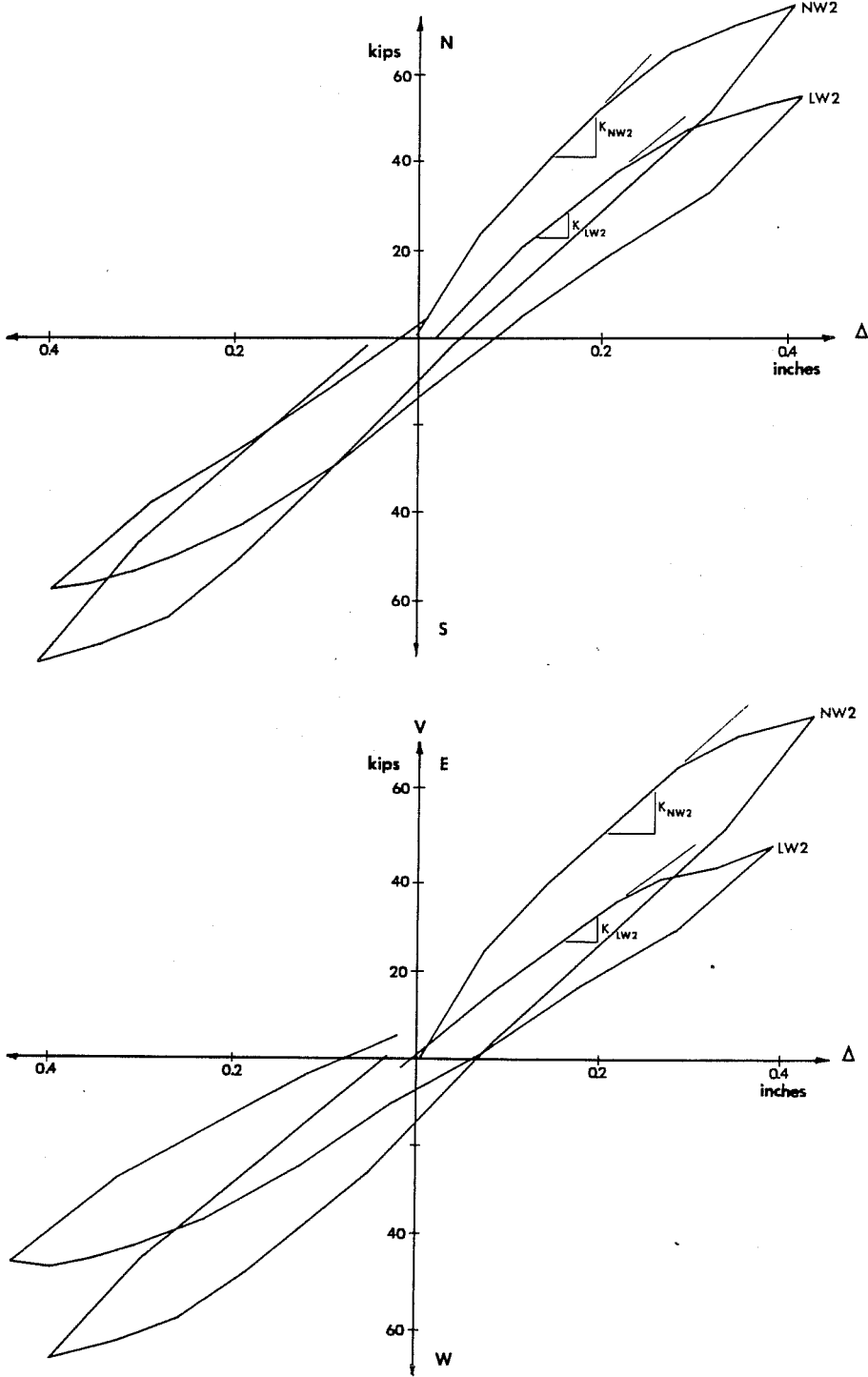


Fig. 5.8 Load deflection curves, tests LW2 and NW2, one cycle at $2\Delta_i$

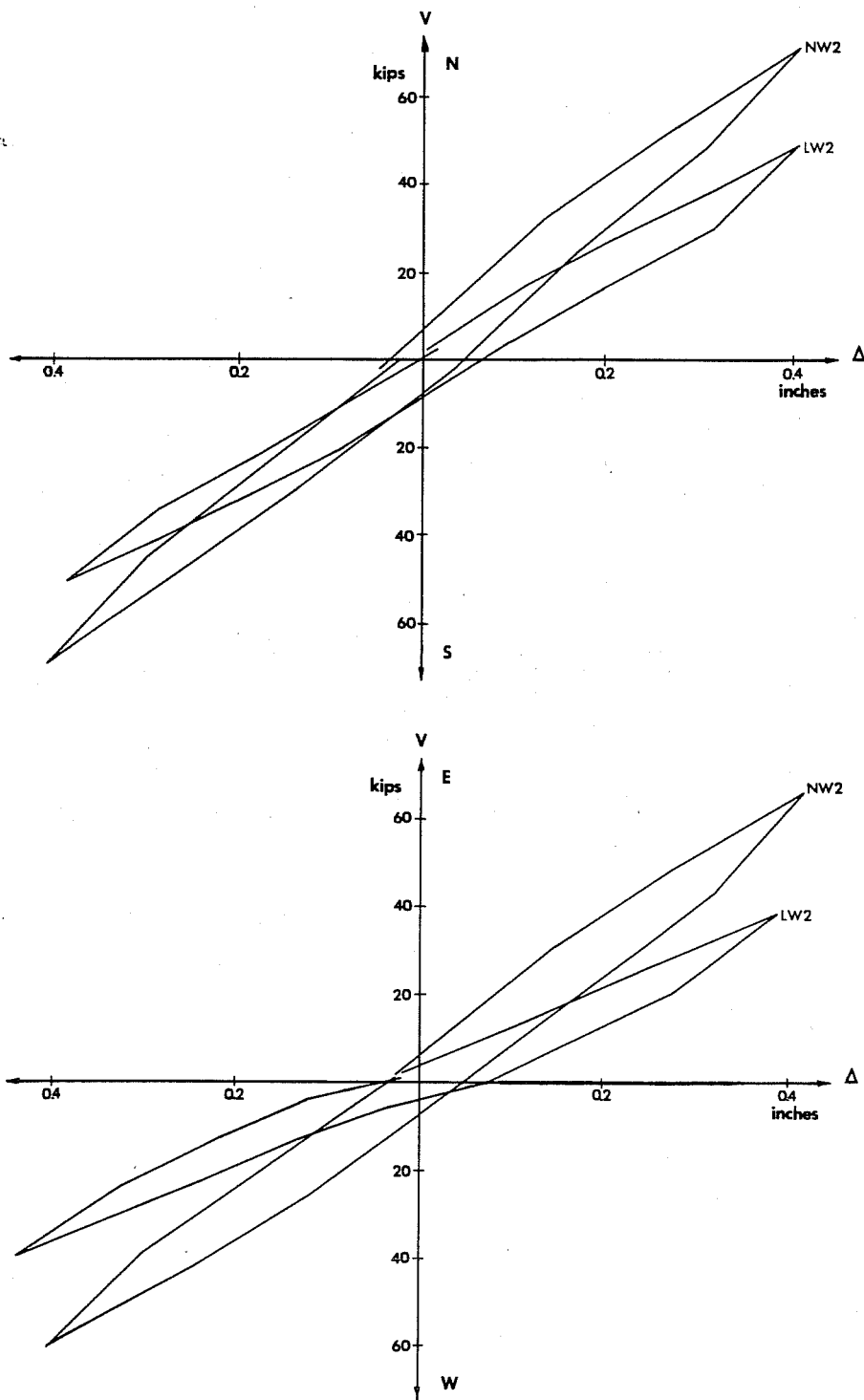


Fig. 5.9 Load deflection curves, tests LW2 and NW2, three cycles at $2\Delta_i$

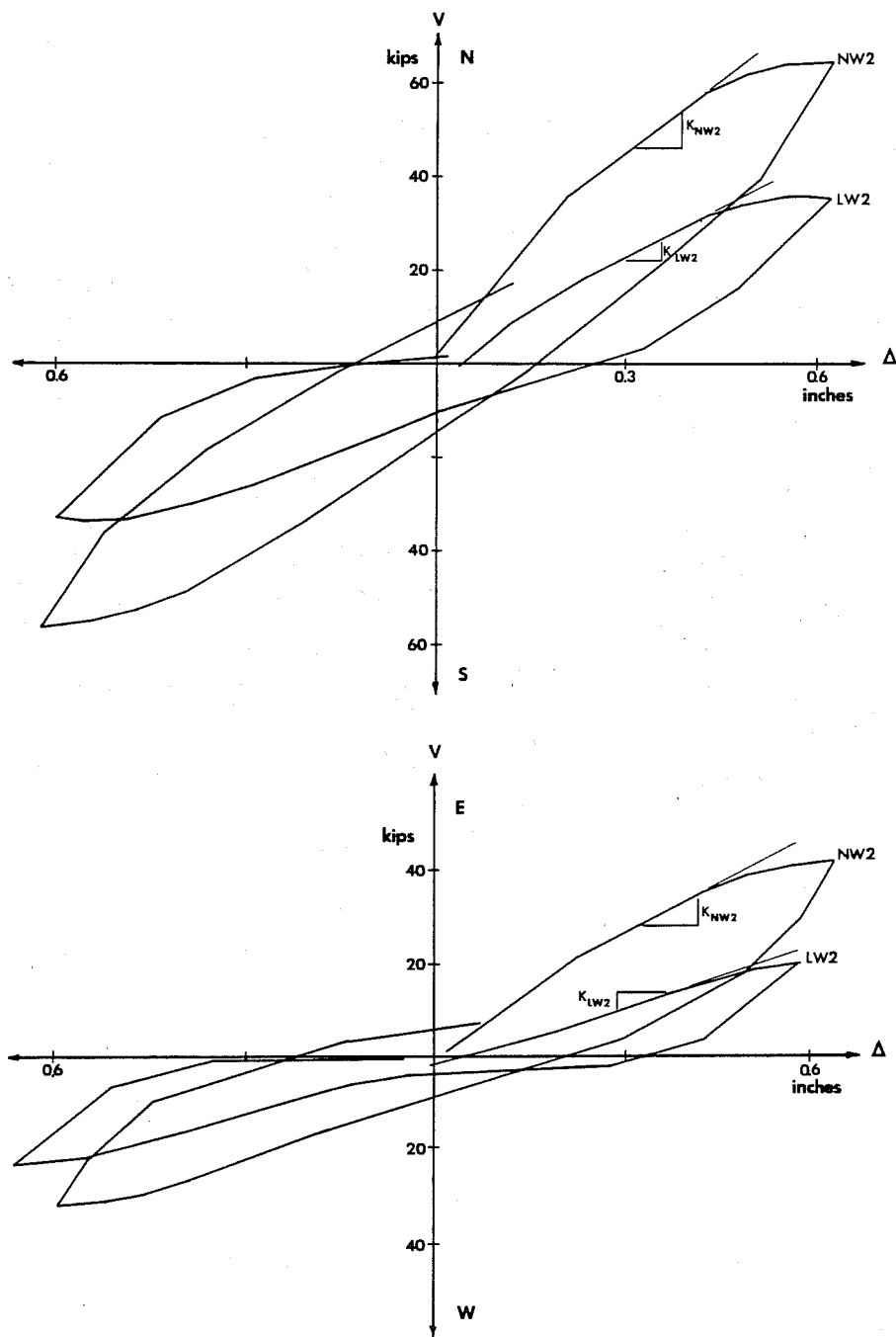


Fig. 5.10 Load deflection curves, tests LW2 and NW2, one cycle at $3\Delta_i$

5.2.2 Shear Strength and Deterioration due to Cycling.

Normalized shear strength versus deformation plots are shown in Figs. 5.11 and 5.12 for test specimens LW1 and NW1 (no axial load). Significant differences between the strength of NW1 and LW1 were observed at all levels of deformation. For deformations up to $2\Delta_i$ (0.40 in.), specimen strength variations are less than 20 percent for both first and third cycles at any deformation level. At a deformation of $3\Delta_i$ (0.60 in.), significant losses in specimen strength are observed for LW1 while only minor strength reductions are observed for NW1. For deformations greater than $3\Delta_i$, loss of specimen strength was observed for both LW1 and NW1. Figure 5.13 illustrates the rate of shear capacity deterioration for the tests with no axial load (LW and NW1).

Normalized shear strength versus deformation plots for test specimens LW2 and NW2 (axial load) are shown in Figs. 5.14 and 5.15. The strength of specimen NW2 was greater than LW2 for deformations up to $2\Delta_i$ (0.40 in.). The peak lateral load on NW2 occurred at a deformation $2\Delta_i$; after the specimen was cycled at a deformation level $2\Delta_i$ in the orthogonal direction. The peak lateral load for LW2 occurred in the first cycle at deformation $2\Delta_i$. Significant losses in strength were observed for both test specimens at deformations greater than $2\Delta_i$. Rapid strength degradation was observed to be a result of previous cycling in the orthogonal direction. Figure 5.16 illustrates the rate of shear capacity deterioration for tests with axial load (LW2 and NW2).

5.2.3 Crack Patterns. The crack patterns observed in tests LW1 and NW1 (no axial load) were similar for all levels of deformation. Initial diagonal cracking was observed near the end blocks of both tests at deformation $1\Delta_i$ (0.20 in.). The orientation of the initial diagonal cracking was approximately 45° . During the $2\Delta_i$ deformation cycle, both specimens continued to develop uniformly

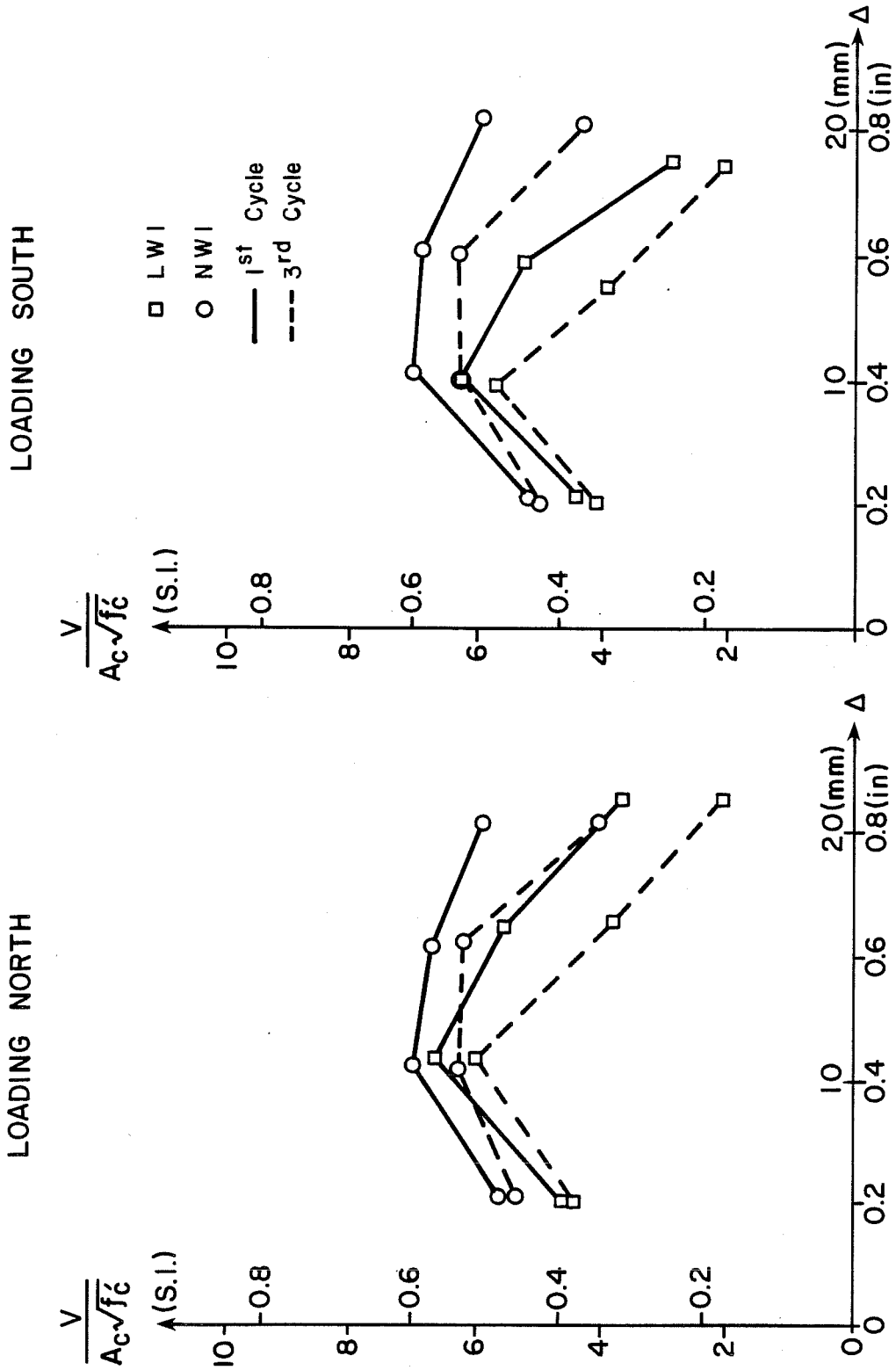


Fig. 5.11 Envelopes of load-deflection for LWI and NWI, N-S direction

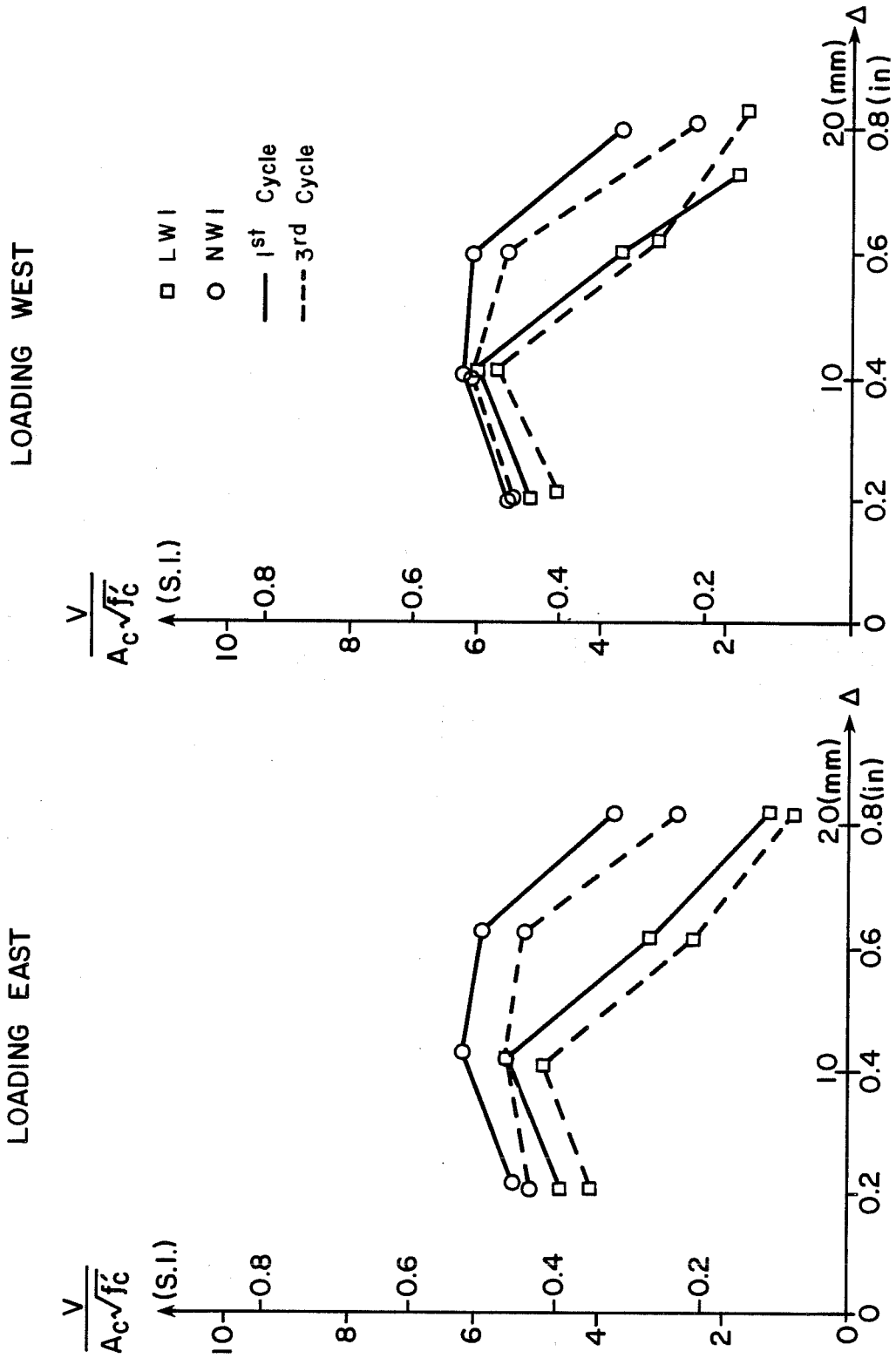


Fig. 5.12 Envelopes of load-deflection for LWI and NWI, E-W direction

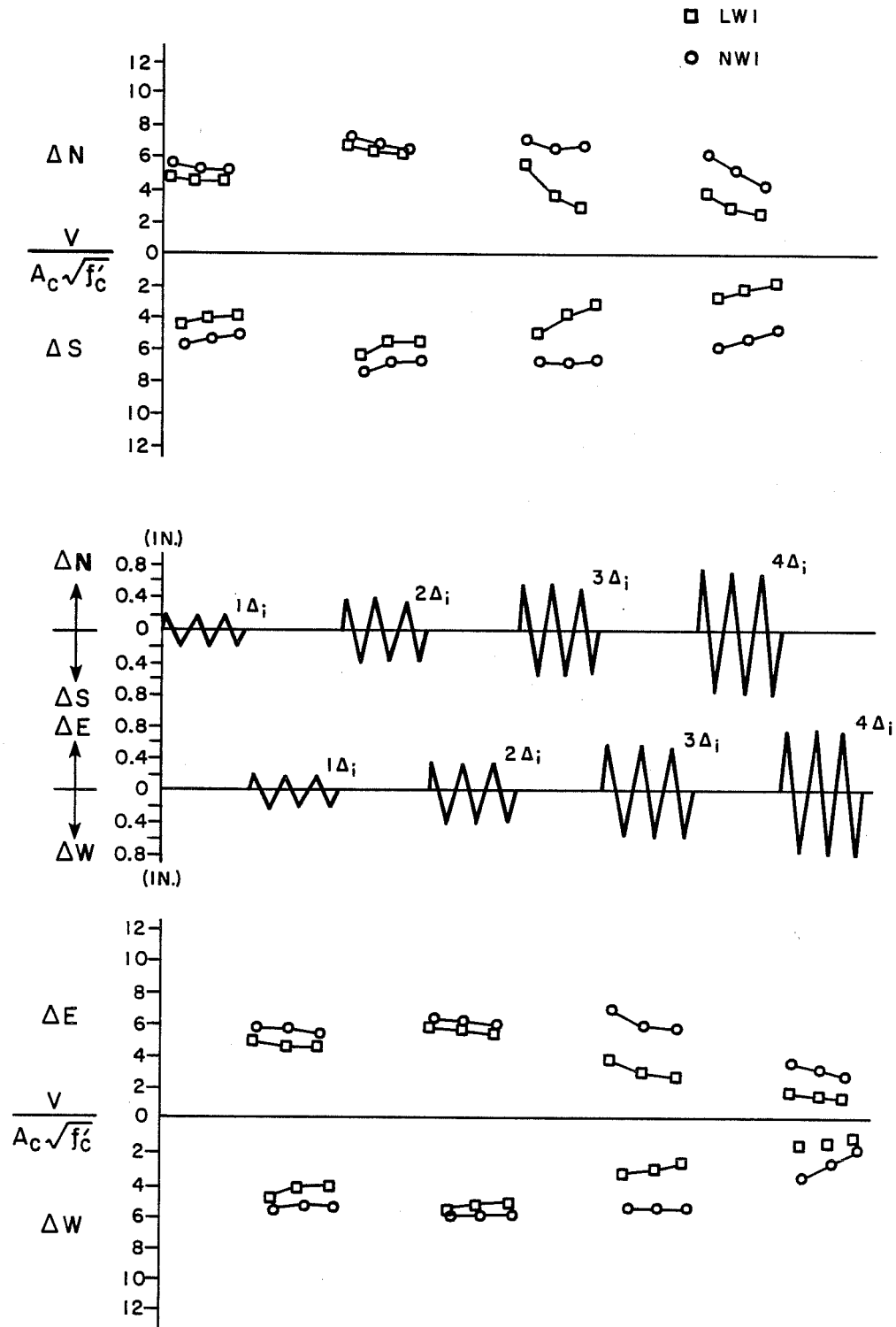


Fig. 5.13 Shear deterioration, tests LWI and NWI

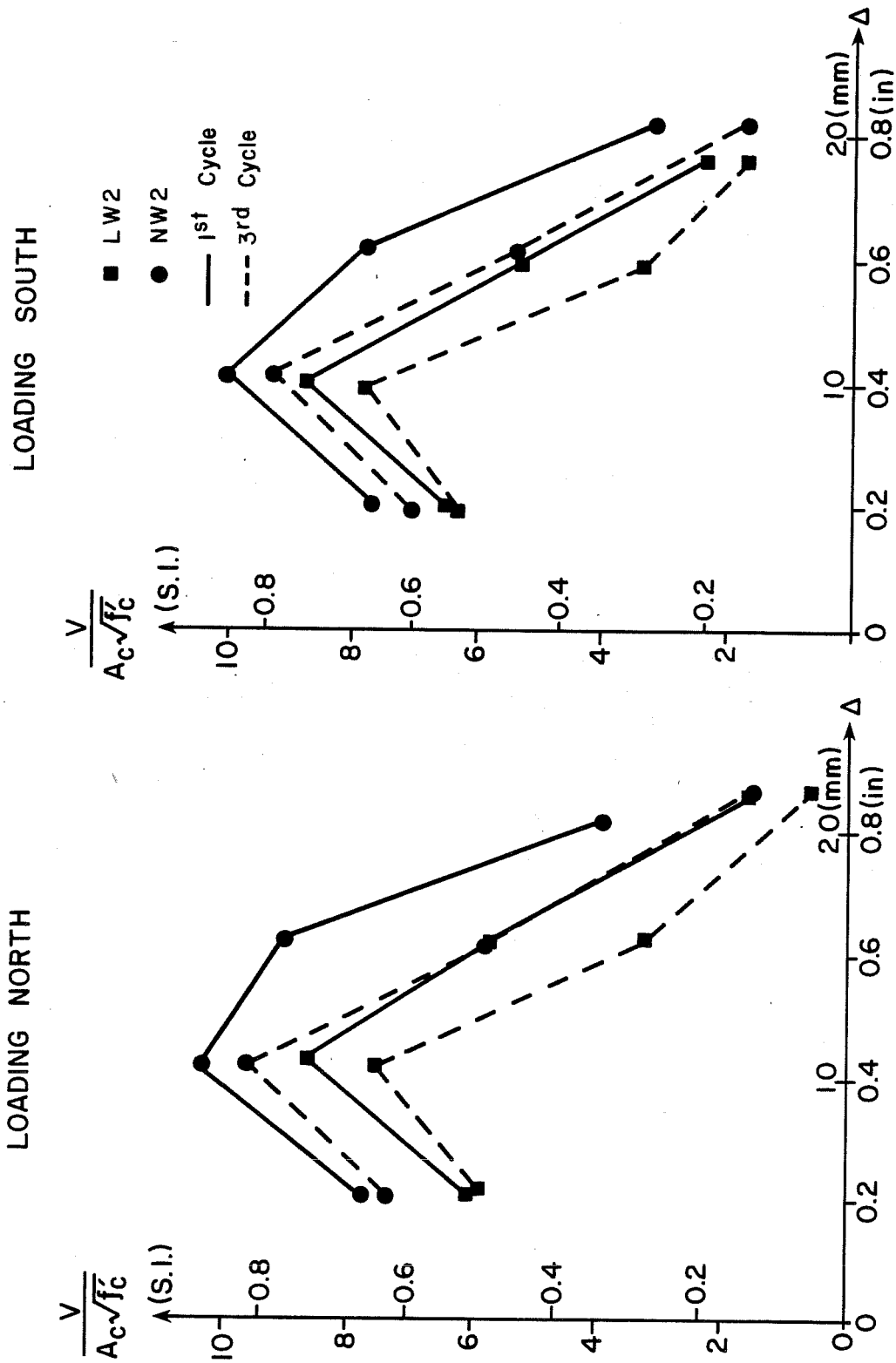


Fig. 5.14 Envelopes of load-deflection for LW2 and NW2, N-S direction

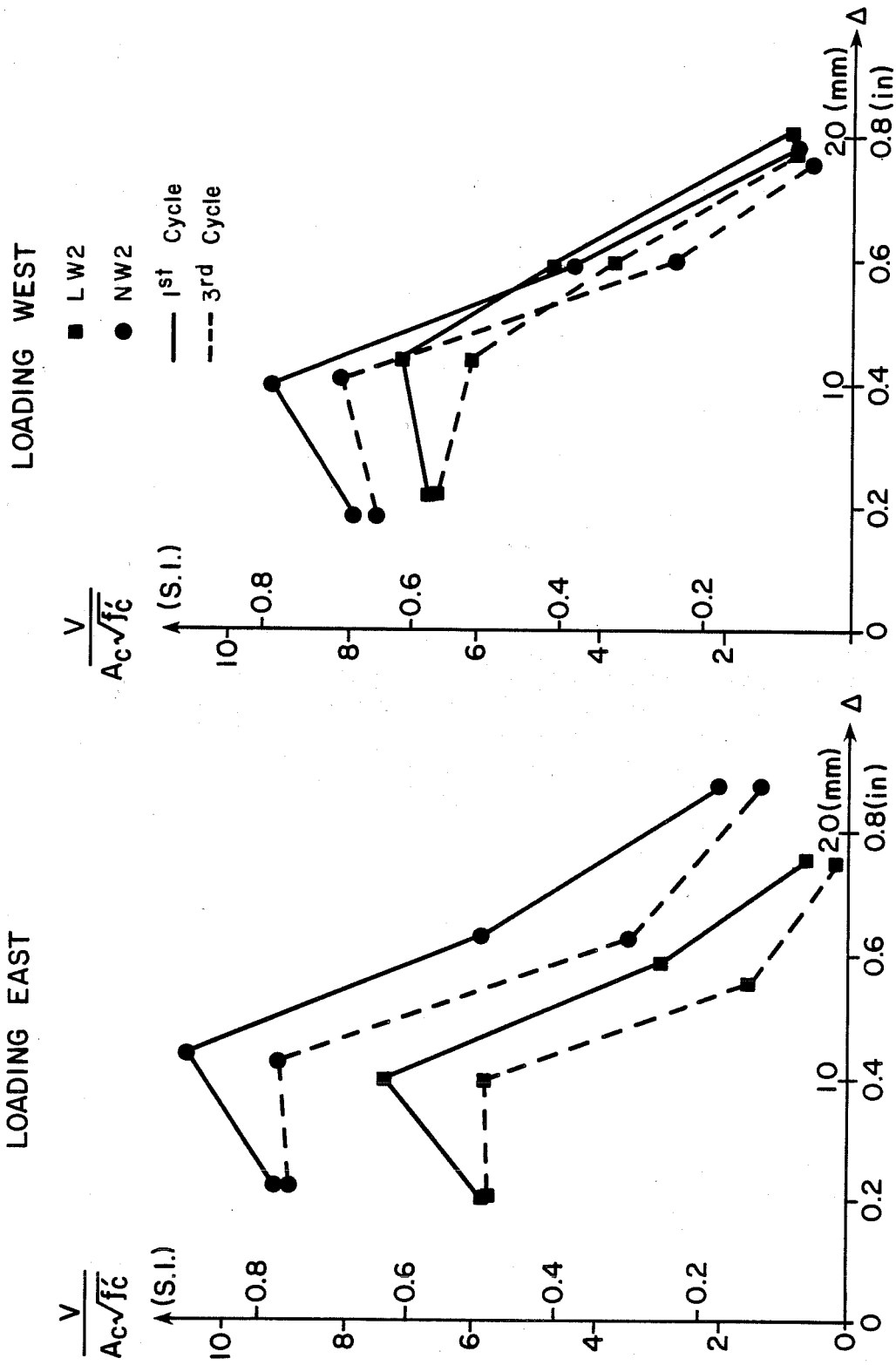


Fig. 5.15 Envelopes of load-deflection for LW2 and NW2, E-W direction

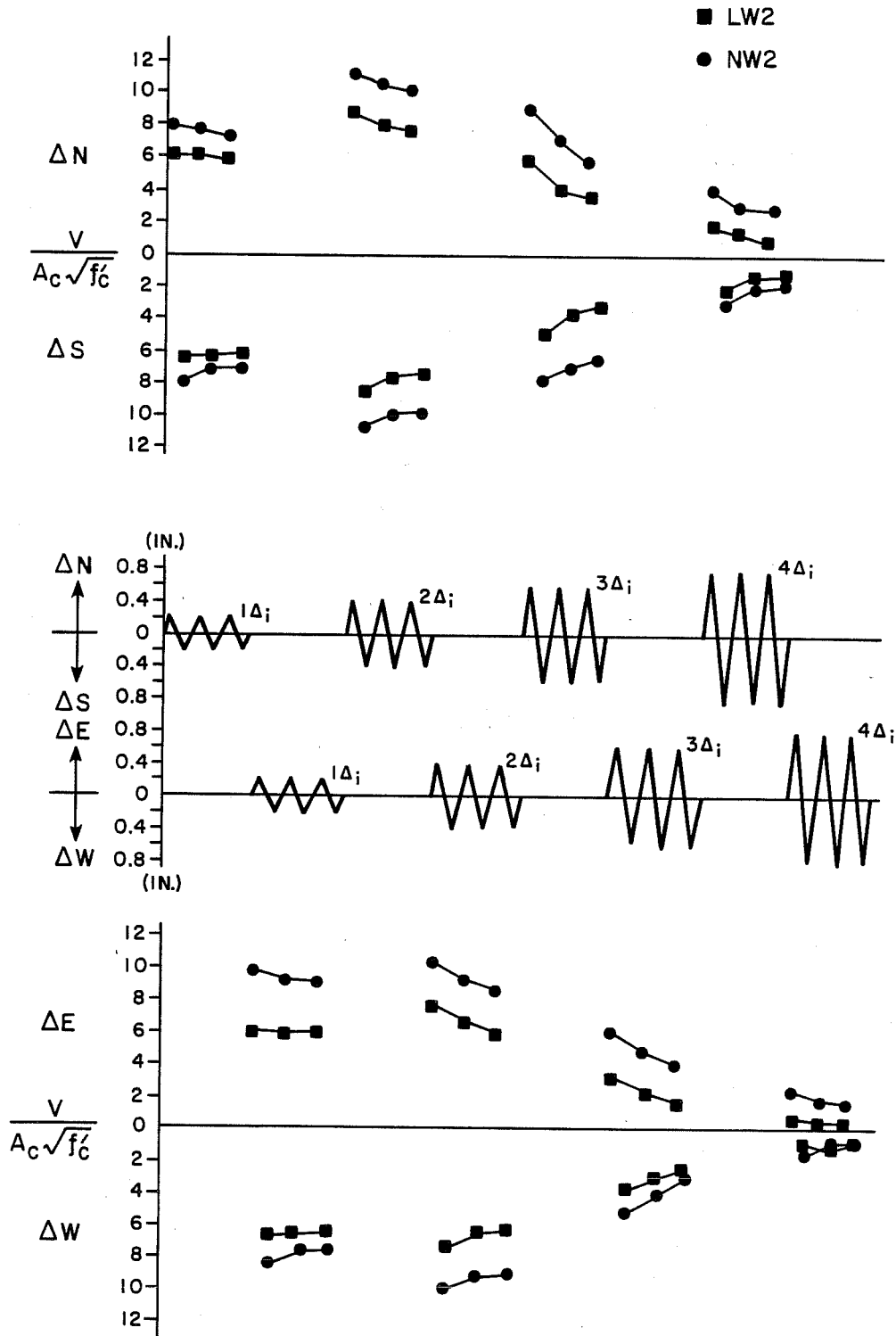


Fig. 5.16 Shear deterioration, tests LW2 and NW2

distributed cracking along the height of the specimen. Major diagonal cracking at approximately 30° was observed in test NW1 during the $3\Delta_i$ (0.60 in.) deformation cycle, while spalling of the concrete cover and severe diagonal cracking at 45° was observed in test LW1 (Fig. 5.17). At failure, both specimens were severely cracked. Surface spalling was recorded on all faces of LW1, but no spalling was observed in test NW1.

Test LW2 exhibited more severe cracking and spalling and at much earlier load stages than test NW2. Both specimens had only minor cracking near the end blocks after the $1\Delta_i$ (0.20 in.) deformation. At a deformation level $2\Delta_i$, large diagonal cracks orientated at 30° were observed in test LW2. Smaller and less severe cracking was recorded in test NW2. Specimen LW2 exhibited spalling of the concrete cover and continued diagonal cracking of the column core during deformation cycles at $3\Delta_i$ (0.60 in.). Large diagonal cracking but no spalling was observed in test NW2 at deformation $3\Delta_i$. At failure, $4\Delta_i$ (0.80 in.), severe spalling, buckling of the longitudinal reinforcement and crushing of the core area were observed in specimen LW2. Test NW2 exhibited severe cracking, but only minor spalling of the concrete cover at failure. Figure 5.18 illustrates the cracking pattern for specimens LW2 and NW2 at failure.

5.3 Discussion of Test Results

By comparing the results of the two lightweight concrete tests with the results of the two normalweight concrete tests significant differences in the behavioral characteristics are observed. The lightweight concrete specimens exhibited shear strength and stiffness properties lower than were observed in the associated normalweight concrete specimens. The lightweight concrete specimens experienced more rapid deterioration of shear

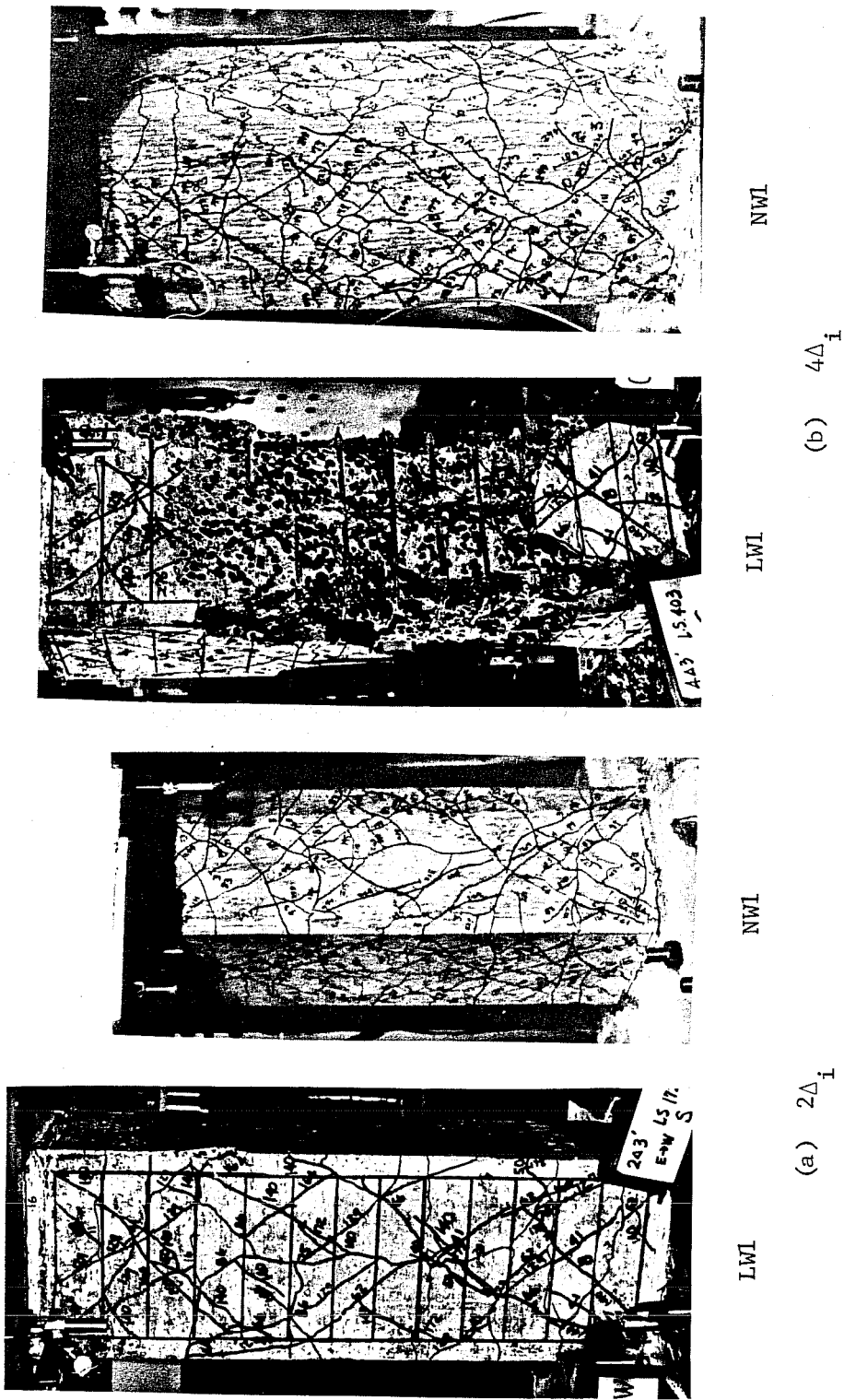


Fig. 5.17 Crack patterns, tests LWI and NWI

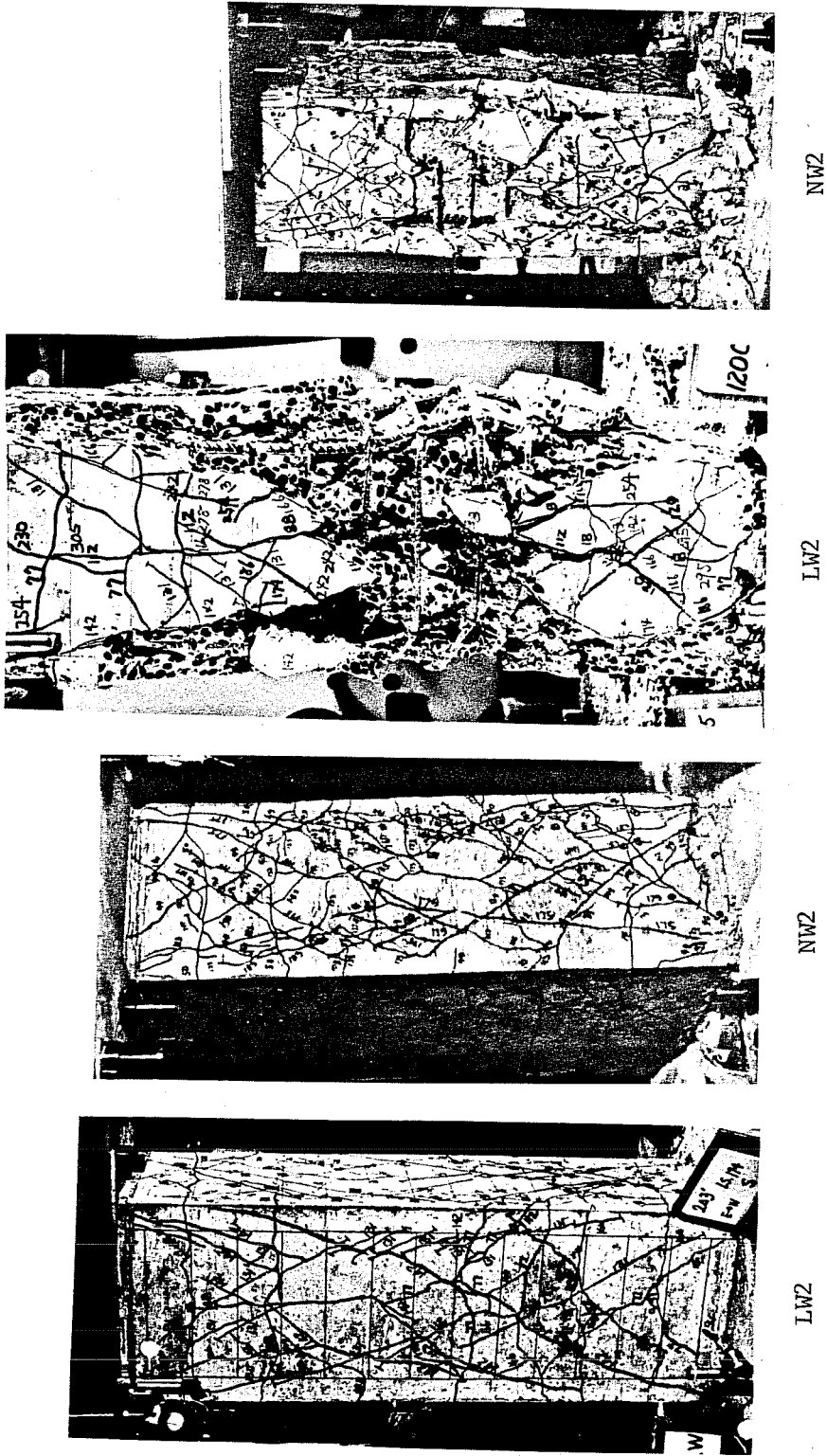


Fig. 5.18 Crack patterns, tests LW2 and NW2

capacity due to the cyclic loading history. More severe cracking and spalling was observed in the lightweight concrete tests as compared to the normalweight concrete specimens.

Since the modulus of elasticity of the normalweight concrete was substantially greater than for the lightweight concrete, the initial stiffness of the normalweight specimens was greater than the lightweight specimens. Table 5.1 summarizes initial stiffness values for all tests. Values of initial stiffness were obtained from plots of the individual load-deflection cycles (see Figs. 5.1 through 5.10). The initial stiffness of NW1 was 30 percent greater than the initial stiffness of LW1 at the $1\Delta_i$ (0.20) deformation level and 36 percent greater at the $2\Delta_i$ deformation level. Specimen NW2 had an initial stiffness 15 percent greater than the initial stiffness of specimen LW2 at $1\Delta_i$. At a deformation of $2\Delta_i$ (0.40 in.), the stiffness of NW2 was 20 percent greater than LW2. The stiffness values for the lightweight concrete specimens are greater than would be predicted by comparing the modulus of elasticity (see Section 2.4.1) for the normalweight concrete [4.47×10^3 ksi ($30.8 \times 10^3 \text{MP}_a$)] which was 77 percent greater than the modulus of elasticity for the lightweight concrete 2.51×10^3 ksi [$(17.3 \times 10^3 \text{MP}_a)$].

As cracking of the concrete and yielding of the longitudinal steel took place at higher levels of deformation, the stiffness of the specimens became more dependent on the steel reinforcement. Initial specimen stiffness, at low deformation levels, was affected by the different moduli of elasticity for the concrete; however, as the level of deformations was increased, the stiffness of the specimens was a function of variables other than concrete strength.

The shear strength of the lightweight concrete specimens was less than the normalweight concrete specimens for tests both with and without axial load. The present ACI 318-77 "Building Code Requirements for Reinforced Concrete" specifies a 15 percent reduction in allowable shear strengths when "sand-lightweight"

concrete is used. Table 5.2 summarizes the normalized peak lateral loads for all tests. The strength of specimen NW1 was 22 percent greater than LW1 in the first cycle at deformation $1\Delta_i$ (0.20 in.). At a deformation of $2\Delta_i$, the strength of NW1 was only 6 percent greater than LW1. In the tests conducted with an axial load applied, the strength of specimen NW2 was 29 percent greater than LW2 at $1\Delta_i$ and 19 percent greater at $2\Delta_i$. Although the reduction specified by ACI 318-77 does not directly apply to members subjected to cyclic loads, for deformation levels up to $2\Delta_i$ (0.40 in.), the effect of the cyclic loading pattern was small and the provisions of ACI 318-77 are applicable. At deformations greater than $2\Delta_i$, the application of cyclic deformations in orthogonal directions affects the lateral capacity of the specimens and comparing ratios of peak loads is beyond the scope of the provisions in ACI 318-77. For the tests conducted without axial load (LW1 and NW1), the 15 percent strength reduction factor for shear strength calculations recommended by Chapter 11 of ACI 318-77 is adequate in predicting the reduction in shear strength due to the use of "sand-lightweight" concrete. For the tests with axial load (LW2 and NW2) the 15 percent strength reduction factor does not adequately account for reductions in shear strength due to the use of "sand-lightweight" concrete.

Significant losses in shear strength were observed for both lightweight specimens after the peak lateral load was reached. The peak lateral load was reached in the first cycle at deformation $2\Delta_i$ (0.40 in.) for both tests. For specimen NW1 (no axial load) the lateral strength did not decrease significantly after the peak load was reached in the first cycle at deformation $2\Delta_i$. The peak lateral load of specimen NW2 occurred at deformation $2\Delta_i$; after the specimen was cycled at deformation $2\Delta_i$ in the orthogonal direction. Significant losses in lateral strength were recorded for NW2 after the peak load. Table 5.3 summarizes the normalized peak lateral loads for all tests and the changes in peak loads between deformation

TABLE 5.2 COMPARISON OF NORMALIZED PEAK LATERAL LOADS

Deformation Cycle	No Axial Load			120 kips Axial Load		
	Lightweight Concrete	Normalweight Concrete	V_{LW1}/V_{NW1}	Lightweight Concrete	Normalweight Concrete	V_{LW2}/V_{NW2}
1A1 N-S	4.64	5.68	0.817*	6.03	7.75	0.778*
1A1 E-W	4.64	5.42	0.856*	5.88	9.24	0.636*
2A1 N-S	6.65	7.04	0.945*	8.66	10.33	0.838*
2A1 E-W	5.57	6.23	0.894*	7.42	10.60	0.770*
3A1 N-S	5.57	6.77	0.823	5.57	8.98	0.620
3A1 E-W	3.25	5.96	0.545	3.09	5.85	0.528
4A1 N-S	3.71	5.96	0.622	1.55	3.94	0.393
4A1 E-W	1.39	3.79	0.367	0.62	2.17	0.286

* ACI 318-77 requires that $V_{LW}/V_{NW} = 0.85$.

TABLE 5.3 COMPARISON OF NORMALIZED PEAK HORIZONTAL SHEARS

	Peak Shear* $1\Delta_i$	% Change $1\Delta_i$ to $2\Delta_i$	Peak Shear* $2\Delta_i$	% Change $2\Delta_i$ to $3\Delta_i$	Peak Shear* $3\Delta_i$	% Change $3\Delta_i$ to $4\Delta_i$	Peak Shear* $4\Delta_i$
LW1 N-S	4.64	+43	6.65	-16	5.57	-33	3.71
NW1 N-S	5.68	+24	7.04	-4	6.77	-12	5.96
LW1 E-W	4.64	+20	5.57	-42	3.25	-57	1.39
NW1 E-W	5.42	+15	6.23	-4	5.96	-36	3.79
LW2 N-S	6.03	+44	8.66	-36	5.57	-72	1.55
NW2 N-S	7.75	+33	10.33	-13	8.98	-56	3.94
LW2 E-W	5.88	+26	7.42	-58	3.09	-80	0.62
NW2 E-W	9.24	+15	10.60	-45	5.85	-63	2.17

* Note: Peak lateral load at each deformation level is normalized as follows: $\frac{V}{A_c \sqrt{f'_c}}$

levels. Between cycles at $1\Delta_i$ and $2\Delta_i$ (0.40 in.), all test specimens exhibited increases in peak lateral loads. The largest increases (43 percent and 44 percent) were recorded for the lightweight specimens (LW1 and LW2). The peak load of specimen LW1 decreased 16 percent from the first cycle at $2\Delta_i$ to the first cycle at $3\Delta_i$ (0.60 in.). A 33 percent decrease in peak load was observed between the $3\Delta_i$ and $4\Delta_i$ deformation levels. The peak load of specimen NW1 decreased only 4 percent and 12 percent between the first cycles at $2\Delta_i$ and $3\Delta_i$, and $3\Delta_i$ and $4\Delta_i$, respectively. The peak load of specimen LW2 decreased 35 percent and 72 percent between the first cycles at $2\Delta_i$ and $3\Delta_i$, and $3\Delta_i$ and $4\Delta_i$, respectively while the peak load of specimen NW2 decreased 13 percent and 56 percent for the same deformation levels. For deformation levels greater than $2\Delta_i$ (0.40 in.) the peak lateral load for both lightweight specimens was significantly reduced due to the cyclic nature of the applied load. For both the lightweight and normalweight concrete specimens the degrading effects of the bidirectional loading were greatly accelerated by the axial load. With no axial load, the behavior of the normalweight specimen was not significantly affected by the bidirectional loading until a deformation of $4\Delta_i$ was reached. The lightweight specimen (LW1) exhibited large reductions in peak load due to the alternate application of deformations at $2\Delta_i$ (0.40 in.).

CHAPTER 6

SUMMARY AND CONCLUSIONS

6.1 Summary of Study

The shear strength and response of lightweight reinforced concrete short columns subjected to bidirectional lateral loads was studied. Primary objectives of the program were to study the effect of axial load on the strength and response characteristics of lightweight reinforced concrete short columns and to compare the behavior of lightweight columns to the behavior of similar short columns constructed with normalweight concrete. All test specimens had the same geometry and reinforcement. The specimens had a 12 in. (30 cm) square cross section with eight #6 bars (19 mm) for longitudinal reinforcement, #2 (6 mm) closed stirrups at 2.5 in. (65 mm) as transverse reinforcement and 1 in. (25 mm) cover. The specimen cross section was a two-thirds scale model of an 18 in. (46 cm) prototype column section. The shear span was 1.5 times the thickness of the cross section. The spacing of the transverse reinforcement was greater than required to prevent shear failure. The intent was to test short columns that might not perform satisfactorily under the imposed load histories, but would represent the practice of captive column design in seismic regions.

The lateral loading history was the same for all tests. The lateral loading was controlled by monitoring deformations. A unit deformation of 0.20 in. ($1\Delta_i$) was used as the loading increment. A lateral deformation of $1\Delta_i$ produced first yielding in the longitudinal reinforcement. Three cycles at each deflection level of $1\Delta_i$, $2\Delta_i$, $3\Delta_i$ and $4\Delta_i$ were used. For both the lightweight and

normalweight tests, one specimen was tested with no axial load (LW1 and NW1) and one was tested with an axial compression load of 120 kips ($0.12P_u$) (LW2 and (NW2)). During each test the applied forces, lateral deflection, strain in longitudinal and transverse reinforcing bars and rotation of the column ends were measured at each load stage. Cracks were marked at each peak deflection.

6.2 Summary of Test Results

6.2.1 Lightweight Concrete Specimens. Lightweight specimens LW1 (no axial load) and LW2 (axial load) exhibited similar hysteretic behavior for deformation levels less than $2\Delta_i$ (0.40 in.). The peak lateral capacity of specimen LW2 was greater than the peak lateral capacity of LW1. At deformations greater than $2\Delta_i$, rapid deterioration of shear capacity of both specimens was observed. Diagonal cracking orientated at 45° was observed on all faces of LW1 at deflection $2\Delta_i$. Concrete spalling and cracking extending into the column core were observed at $3\Delta_i$. At the end of cycling at $4\Delta_i$, most of the concrete cover was spalled off and diagonal cracking extending into the core was observed. Minor diagonal cracking was observed on specimen LW2 after cycling at $1\Delta_i$. At $2\Delta_i$, uniformly distributed diagonal cracks inclined at 30° were observed. Spalled concrete was observed at $3\Delta_i$. Diagonal cracking extending into the core section and major spalling of the concrete cover were observed at the end of $4\Delta_i$.

6.2.2 Normalweight Concrete Specimens. The lateral load associated with a given deformation was greater in NW2 (axial load) than NW1 (no axial load) for deformation levels to $2\Delta_i$ (0.40 in.) At deformations greater than $2\Delta_i$ (past the peak lateral capacity of each specimen), significant losses in specimen strength were observed in NW2. Diagonal cracking was observed in test NW1 at the end of cycling at $1\Delta_i$. At $2\Delta_i$, major diagonal cracks orientated at 30°

were observed. At $4\Delta_i$, diagonal cracks at 35° were dominant. Observed cracking in test NW2 was similar to the cracking patterns of test NW1.

6.2.3 Comparison of Lightweight and Normalweight Tests.

Comparison of behavioral characteristics between the lightweight and normalweight concrete specimens can be made in terms of specimen shear strength and stiffness and rate of shear capacity deterioration. For the tests without axial load, LW1 and NW1, the initial shear strength and stiffness of the lightweight concrete specimen was about 20 percent less than the normalweight specimen. The peak lateral capacity of both specimens occurred in the first cycle of $2\Delta_i$. For deformation levels up to $4\Delta_i$, the normalweight specimen demonstrated stable hysteretic behavior and had only minor losses of shear capacity. Once the peak lateral capacity of specimen LW1 was reached, rapid losses of both shear strength and stiffness were observed. For each deformation level more severe cracking was associated with the lightweight specimen.

The peak lateral capacity of specimens LW2 and NW2 (axial load) occurred in the $2\Delta_i$ cycle. Stable hysteretic behavior was observed in both tests for deformations less than $2\Delta_i$. Rapid losses in specimen strength and stiffness were observed in both tests at deformation levels greater than $2\Delta_i$. Similar cracking patterns were observed at each deformation level for both tests.

6.3 Conclusions

Based on the four tests compared in this study the following conclusions are made:

- (a) The shear capacity of columns constructed with normalweight concrete was 15 percent greater than the capacity of similar columns constructed with lightweight concrete. The application of a constant compression axial load

increased by 30 percent to 50 percent the shear capacity of both types of columns with respect to similar tests conducted with no axial load for low levels of deformation.

- (b) The stiffness of lightweight columns was 20 percent to 25 percent less than the stiffness of normalweight columns. For columns subjected to no axial load, lightweight columns exhibited rapid losses of strength and stiffness after the peak lateral load was reached, while normalweight columns exhibited stable hysteretic behavior and suffered only minor reductions in shear strength after the peak lateral load was reached.
- (c) Although the stiffness of the lightweight columns was 20 percent to 25 percent less than the stiffness of the normalweight columns, the reduction in stiffness was less than predicted by comparing the modulus of elasticity, determined in accordance with ACI 318-77, of lightweight and normalweight concrete.
- (d) For columns subjected to no axial load, the 15 percent reduction for shear calculations specified in Chapter 11 of ACI 318-77 was adequate. The shear capacity of the lightweight column was 6 percent less than the capacity of the normalweight specimen. For columns subjected to a constant axial compression, the 15 percent reduction was not adequate. The shear capacity of the lightweight column was 19 percent less than the normalweight column.
- (e) Although only two tests with lightweight concrete were conducted, the capacity of the lightweight columns to dissipate energy during bidirectional cyclic loadings was found to be poor.

A P P E N D I X A

APPENDIX A PEAK VALUES LW1

LOAD CYCLE	AXIAL LOAD (kips)	SHEAR (kips)	$\frac{V}{A_c \sqrt{f'_c}}$	DEFORMATION (in.)	
	1Δ1	0.0	30.0	4.64	0.200
	1Δ1'	0.0	29.0	4.49	0.210
1Δ _i	1Δ2	0.0	29.0	4.49	0.205
	1Δ2'	0.0	27.0	4.17	0.199
N-S	1Δ3	0.0	29.0	4.49	0.200
	1Δ3'	0.0	27.0	4.18	0.200
	1Δ1	0.0	30.0	4.64	0.200
	1Δ1'	0.0	33.0	5.10	0.200
1Δ _i	1Δ2	0.0	28.0	4.33	0.202
	1Δ2'	0.0	31.0	4.79	0.208
E-W	1Δ3	0.0	27.0	4.18	0.200
	1Δ3'	0.0	31.0	4.79	0.210
	2Δ1	0.0	43.0	6.65	0.430
	2Δ1'	0.0	41.0	6.34	0.400
2Δ _i	2Δ2	0.0	40.0	6.18	0.424
	2Δ2'	0.0	37.0	5.72	0.381
N-S	2Δ3	0.0	39.0	6.03	0.430
	2Δ3'	0.0	37.0	5.72	0.390
	2Δ1	0.0	36.0	5.57	0.410
	2Δ1'	0.0	39.0	6.03	0.410
2Δ _i	2Δ2	0.0	34.0	5.26	0.406
	2Δ2'	0.0	38.0	5.88	0.410
E-W	2Δ3	0.0	32.0	4.95	0.400
	2Δ3'	0.0	37.0	5.72	0.410
	3Δ1	0.0	36.0	5.57	0.640
	3Δ1'	0.0	34.0	5.26	0.590
3Δ _i	3Δ2	0.0	29.0	4.49	0.640
	3Δ2'	0.0	27.0	4.18	0.578
N-S	3Δ3	0.0	25.0	3.87	0.650
	3Δ3'	0.0	24.0	3.71	0.570
	3Δ1	0.0	21.0	3.25	0.620
	3Δ1'	0.0	24.0	3.71	0.600
3Δ _i	3Δ2	0.0	17.0	3.63	0.607
	3Δ2'	0.0	21.0	3.25	0.601
E-W	3Δ3	0.0	16.0	2.47	0.620
	3Δ3'	0.0	20.0	3.09	0.620
	4Δ1	0.0	24.0	3.71	0.850
	4Δ1'	0.0	19.0	2.94	0.750
4Δ _i	4Δ2	0.0	16.0	2.47	0.897
	4Δ2'	0.0	16.0	2.47	0.740
N-S	4Δ3	0.0	14.0	2.17	0.850
	4Δ3'	0.0	14.0	2.17	0.740
	4Δ1	0.0	9.0	1.39	0.810
	4Δ1'	0.0	12.0	1.86	0.730
4Δ _i	4Δ2	0.0	7.0	1.08	0.810
	4Δ2'	0.0	11.0	1.70	0.770
E-W	4Δ3	0.0	6.0	0.93	0.810
	4Δ3'	0.0	11.0	1.70	0.830

A P P E N D I X B

APPENDIX B PEAK VALUES LW2

LOAD CYCLE	AXIAL LOAD (kips)	SHEAR (kips)	$\frac{V}{A_c \sqrt{f'_c}}$	DEFORMATION (in.)	
1 Δ_i N-S	1 Δ_1	120.0	39.0	6.03	0.200
	1 Δ_1'	120.0	42.0	6.50	0.200
	1 Δ_2	120.0	39.0	6.03	0.210
	1 Δ_2'	120.0	41.0	6.34	0.195
	1 Δ_3	120.0	38.0	5.88	0.210
	1 Δ_3'	120.0	41.0	6.34	0.190
1 Δ_i E-W	1 Δ_1	120.0	38.0	5.88	0.200
	1 Δ_1'	120.0	44.0	6.81	0.220
	1 Δ_2	120.0	37.0	5.72	0.188
	1 Δ_2'	120.0	43.0	6.65	0.220
	1 Δ_3	120.0	37.0	5.72	0.190
	1 Δ_3'	120.0	43.0	6.65	0.220
2 Δ_i N-S	2 Δ_1	120.0	56.0	8.66	0.420
	2 Δ_1'	120.0	57.0	8.82	0.400
	2 Δ_2	120.0	51.0	7.89	0.416
	2 Δ_2'	120.0	52.0	8.04	0.392
	2 Δ_3	120.0	49.0	7.58	0.410
	2 Δ_3'	120.0	51.0	7.89	0.390
2 Δ_i E-W	2 Δ_1	120.0	48.0	7.42	0.390
	2 Δ_1'	120.0	47.0	7.27	0.440
	2 Δ_2	120.0	42.0	6.50	0.392
	2 Δ_2'	120.0	41.0	6.34	0.434
	2 Δ_3	120.0	38.0	5.88	0.390
	2 Δ_3'	120.0	40.0	6.19	0.440
3 Δ_i N-S	3 Δ_1	120.0	36.0	5.57	0.620
	3 Δ_1'	120.0	34.0	5.26	0.600
	3 Δ_2	120.0	25.0	3.87	0.624
	3 Δ_2'	120.0	26.0	4.02	0.594
	3 Δ_3	120.0	21.0	3.25	0.620
	3 Δ_3'	120.0	22.0	3.40	0.590
3 Δ_i E-W	3 Δ_1	120.0	20.0	3.09	0.580
	3 Δ_1'	120.0	24.0	3.71	0.660
	3 Δ_2	120.0	13.0	2.01	0.558
	3 Δ_2'	120.0	19.0	2.94	0.667
	3 Δ_3	120.0	10.0	1.55	0.550
	3 Δ_3'	120.0	17.0	2.63	0.680
4 Δ_i N-S	4 Δ_1	120.0	10.0	1.55	0.860
	4 Δ_1'	120.0	16.0	2.47	0.760
	4 Δ_2	120.0	7.0	1.08	0.845
	4 Δ_2'	120.0	12.0	1.86	0.766
	4 Δ_3	120.0	4.0	0.62	0.860
	4 Δ_3'	120.0	11.0	1.70	0.760
4 Δ_i E-W	4 Δ_1	120.0	4.0	0.62	0.750
	4 Δ_1'	120.0	7.0	1.08	0.810
	4 Δ_2	120.0	3.0	0.46	0.757
	4 Δ_2'	120.0	7.0	1.08	0.816
	4 Δ_3	120.0	1.0	0.16	0.750
	4 Δ_3'	120.0	2.0	0.31	0.820

A P P E N D I X C

APPENDIX C PEAK VALUES NW1

LOAD CYCLE	AXIAL LOAD (kips)	SHEAR (kips)	$\frac{V}{A_c \sqrt{f'_c}}$	DEFORMATION (in.)	
1 Δ_i N-S	1 Δ_1	0.0	42.0	5.687	0.210
	1 Δ_1'	0.0	39.0	5.281	0.210
	1 Δ_2	0.0	40.0	5.416	0.210
	1 Δ_2'	0.0	38.0	5.146	0.200
	1 Δ_3	0.0	40.0	5.416	0.210
1 Δ_i E-W	1 Δ_3'	0.0	37.0	5.010	0.200
	1 Δ_1	0.0	40.0	5.416	0.210
	1 Δ_1'	0.0	40.0	5.416	0.200
	1 Δ_2	0.0	39.0	5.281	0.210
	1 Δ_2'	0.0	41.0	5.552	0.200
2 Δ_i N-S	1 Δ_3	0.0	38.0	5.146	0.210
	1 Δ_3'	0.0	40.0	5.416	0.200
	2 Δ_1	0.0	52.0	7.041	0.420
	2 Δ_1'	0.0	52.0	7.041	0.410
	2 Δ_2	0.0	49.0	6.635	0.416
2 Δ_i E-W	2 Δ_2'	0.0	49.0	6.635	0.413
	2 Δ_3	0.0	47.0	6.364	0.410
	2 Δ_3'	0.0	47.0	6.364	0.400
	2 Δ_1	0.0	46.0	6.229	0.420
	2 Δ_1'	0.0	46.0	6.229	0.400
3 Δ_i N-S	2 Δ_2	0.0	45.0	6.093	0.412
	2 Δ_2'	0.0	46.0	6.229	0.394
	2 Δ_3	0.0	45.0	6.093	0.420
	2 Δ_3'	0.0	45.0	6.093	0.390
	3 Δ_1	0.0	50.0	6.770	0.610
3 Δ_i E-W	3 Δ_1'	0.0	51.0	6.906	0.610
	3 Δ_2	0.0	48.0	6.449	0.619
	3 Δ_2'	0.0	48.0	6.449	0.602
	3 Δ_3	0.0	46.0	6.229	0.620
	3 Δ_3'	0.0	46.0	6.229	0.620
4 Δ_i N-S	3 Δ_1	0.0	44.0	5.958	0.620
	3 Δ_1'	0.0	45.0	6.093	0.600
	3 Δ_2	0.0	41.0	5.552	0.614
	3 Δ_2'	0.0	43.0	5.823	0.602
	3 Δ_3	0.0	39.0	5.281	0.620
4 Δ_i E-W	3 Δ_3'	0.0	41.0	5.552	0.600
	4 Δ_1	0.0	44.0	5.958	0.810
	4 Δ_1'	0.0	44.0	5.958	0.820
	4 Δ_2	0.0	36.0	4.875	0.813
	4 Δ_2'	0.0	37.0	5.010	0.810
4 Δ_i E-W	4 Δ_3	0.0	30.0	4.062	0.810
	4 Δ_3'	0.0	32.0	4.333	0.810
	4 Δ_1	0.0	28.0	3.791	0.810
	4 Δ_1'	0.0	28.0	3.791	0.800
	4 Δ_2	0.0	24.0	3.250	0.817
4 Δ_i E-W	4 Δ_2'	0.0	22.0	2.979	0.804
	4 Δ_3	0.0	21.0	2.844	0.810
	4 Δ_3'	0.0	19.0	2.573	0.810

A P P E N D I X D

APPENDIX D PEAK VALUES NW2

LOAD CYCLE	AXIAL LOAD (kips)	SHEAR (kips)	$\frac{V}{A_c \sqrt{f'_c}}$	DEFORMATION (in.)	
1 Δ_i N-S	1 Δ_1	120.0	57.0	7.751	0.200
	1 Δ_1'	120.0	47.0	7.751	0.200
	1 Δ_2	120.0	56.0	7.614	0.200
	1 Δ_2'	120.0	53.0	7.207	0.190
	1 Δ_3	120.0	54.0	7.343	0.200
	1 Δ_3'	120.0	52.0	7.071	0.190
1 Δ_i E-W	1 Δ_1	120.0	68.0	9.246	0.220
	1 Δ_1'	120.0	59.0	8.023	0.190
	1 Δ_2	120.0	67.0	9.110	0.217
	1 Δ_2'	120.0	56.0	7.615	0.185
	1 Δ_3	120.0	66.0	8.975	0.220
	1 Δ_3'	120.0	56.0	7.615	0.190
2 Δ_i N-S	2 Δ_1	120.0	76.0	10.334	0.410
	2 Δ_1'	120.0	74.0	10.062	0.410
	2 Δ_2	120.0	73.0	9.926	0.411
	2 Δ_2'	120.0	71.0	9.654	0.408
	2 Δ_3	120.0	71.0	9.654	0.410
	2 Δ_3'	120.0	69.0	9.382	0.410
2 Δ_i E-W	2 Δ_1	120.0	78.0	10.606	0.430
	2 Δ_1'	120.0	69.0	9.382	0.400
	2 Δ_2	120.0	71.0	9.654	0.421
	2 Δ_2'	120.0	64.0	8.703	0.401
	2 Δ_3	120.0	67.0	9.110	0.420
	2 Δ_3'	120.0	61.0	8.295	0.410
3 Δ_i N-S	3 Δ_1	120.0	66.0	8.975	0.620
	3 Δ_1'	120.0	58.0	7.887	0.620
	3 Δ_2	120.0	51.0	6.935	0.605
	3 Δ_2'	120.0	46.0	6.255	0.605
	3 Δ_3	120.0	43.0	5.847	0.600
	3 Δ_3'	120.0	40.0	5.439	0.610
3 Δ_i E-W	3 Δ_1	120.0	43.0	5.847	0.630
	3 Δ_1'	120.0	33.0	4.487	0.590
	3 Δ_2	120.0	31.0	4.215	0.622
	3 Δ_2'	120.0	24.0	3.263	0.594
	3 Δ_3	120.0	26.0	3.535	0.620
	3 Δ_3'	120.0	21.0	2.856	0.600
4 Δ_i N-S	4 Δ_1	120.0	29.0	3.943	0.810
	4 Δ_1'	120.0	24.0	3.263	0.820
	4 Δ_2	120.0	20.0	2.719	0.812
	4 Δ_2'	120.0	17.0	2.312	0.818
	4 Δ_3	120.0	16.0	21.76	0.820
	4 Δ_3'	120.0	13.0	1.768	0.820
4 Δ_i E-W	4 Δ_1	120.0	16.0	2.176	0.870
	4 Δ_1'	120.0	9.0	1.224	0.760
	4 Δ_2	120.0	12.0	1.632	0.863
	4 Δ_2'	120.0	6.0	0.815	0.760
	4 Δ_3	120.0	11.0	1.496	0.870
	4 Δ_3'	120.0	5.0	0.680	0.760

B I B L I O G R A P H Y

1. Aoyama, H., and Sozen, M. A., "Dynamic Response of a Reinforced Concrete Structure with Tied and Spiral Columns," Proceedings, Fifth World Conference on Earthquake Engineering, Rome, 1973, Paper No. 15.
2. Karlsson, B. I., Aoyama, H., and Sozen, M. A., "Spirally Reinforced Concrete Columns Subjected to Loading Reversals Simulating Earthquake Effects," Proceedings, Fifth World Conference on Earthquake Engineering, Rome, 1973, Paper No. 93.
3. Aktan, A. E., Pecknold, D. A. W., and Sozen, M. A., "Effects of Two-Dimensional Earthquake Motion on a Reinforced Concrete Column" Civil Engineering Studies, Structural Research Series 399, University of Illinois, May 1973.
4. Pecknold, D. A. W., and Sozen, M. A., "Calculated Inelastic Structural Response to Uniaxial and Biaxial Earthquake Motions," Proceedings, Fifth World Conference on Earthquake Engineering, Rome, 1973, Paper No. 223.
5. Mahin, S. A., Bertero, V. V., Chopra, A. K., and Collins, R. G., "Response of the Olive View Hospital Main Building during the San Fernando Earthquake," Report No. EERC 76-22, Earthquake Engineering Research Center, University of California, Berkeley, October 1976.
6. Salna, L. G., Morrill, K. B., and Ersoy, O. K., "Shear Collapse, Elastic and Inelastic Biaxial Studies of the Olive View Hospital Psychiatric Day Clinic," Proceedings, U.S.-Japan Seminar on Earthquake Engineering, Berkeley, 1973.
7. Bertero, V. V., and Bresler, B., "Olive View Medical Center Materials Studies-Phase I," Report No. EERC 73-19, Earthquake Engineering Research Center, College of Engineering, University of California, Berkeley, 1973.
8. Manrique, M. A., Bertero, V. V., Popov, E. P., "Mechanical Behavior of Lightweight Concrete Confined by Different Types of Lateral Reinforcement," Report No. UCB/EERC-79/05, Earthquake Engineering Research Center, College of Engineering, University of California Berkeley, 1979.

9. Bertero, V. V., Bresler, B., Selna, L. B., Chopra, A. K., Koretsky, A. V., "Design Implications of Damage Observed in the Olive View Medical Center Building," Proceedings, Fifth World Conference on Earthquake Engineering, Rome, 1973.
10. Shideler, J. J., "Lightweight Aggregate Concrete for Structural Use," ACI Journal, Proceedings, V. 54, October 1957, p. 299; PCA Development Department Bulletin D17.
11. Hanson, J. A., "Shear Strength of Lightweight Reinforced Concrete Beams," ACI Journal, Proceedings, V. 55, September 1958, p. 387; PCA Development Department Bulletin D22.
12. Hanson, J. A., "Tensile Strength and Diagonal Tension Resistance of Structural Lightweight Concrete," ACI Journal, Proceedings, V. 58, July 1961, p. 1; PCA Development Department Bulletin D50.
13. Hanson, J. A., "Strength of Structural Lightweight Concrete under Combined Stress," ACI Journal, Proceedings, V. 5, No. 1, January 1963, p. 39-46; PCA Development Department Bulletin D61.
14. Hognestad, E., Elstner, R. C., Hanson, J. A., "Shear Strength of Reinforced Structural Lightweight Aggregate Concrete Slabs," ACI Journal, Proceedings, V. 61, June 1964, p. 643; PCA Development Department Bulletin D78.
15. Jirsa, J. O., Maruyama, K., and Ramirez, H., "Development of Loading System and Initial Tests--Short Columns under Bidirectional Loading," CESRL Report No. 78-2, Civil Engineering Structures Research Laboratory, The University of Texas at Austin, September 1978.
16. Maruyama, K., and Jirsa, J. O., "Shear Behavior of Reinforced Concrete Members under Bidirectional Reversed Lateral Loading," CESRL Report No. 79-1, The University of Texas at Austin, August 1979.
17. Ramiraz, H., and Jirsa, J. O., "Effect of Axial Load on Shear Behavior of Short RC Columns under Cyclic Lateral Deformations," PMFSEL Report No. 80-1, The University of Texas at Austin, June 1980.
18. Woodward, K. A., and Jirsa, J. O., "Behavior Classification of Short Reinforced Concrete Columns Subjected to Cyclic Deformations," PMFSEL Report No. 80-2, The University of Texas at Austin, July 1980.

19. Nielsen, N. N., and Nakagawa, K., "The Tokachi-Oki Earthquake, Japan, May 16, 1968: A Preliminary Report on Damage to Structures," International Institute of Seismology and Earthquake Engineering, Report No. 2, Tokyo Japan, June 1968.
20. ACI Committee 318, Building Code Requirements for Reinforced Concrete (ACI 318-77) American Concrete Institute, Detroit, 1977.
21. Umehara, H., "Shear Strength and Deterioration of Short Reinforced Concrete Columns under Cyclic Deformations," unpublished Ph.D. dissertation, The University of Texas at Austin, Texas, 1982.
22. ACI-ASCE Committee 426, "The Shear Strength of Reinforced Concrete Members," Journal of the Structural Division, ASCE, Vol. 99, No. ST6, Proc. Paper 9791, June 1973, pp. 1091-1187.

V I T A

Mark Edward Moore was born in Culver City, California, on March 30, 1957, the son of Tommy Lou English Moore and Vernon Edward Moore. After completing his work at Prospect High School, Mt. Prospect, Illinois, in 1975, he entered Purdue University. He received the degree of Bachelor of Science in Civil Engineering from Purdue University in May of 1979. During the following years he was employed as a structural engineer for Wiss, Janney, Elstner and Associates, Incorporated in Northbrook, Illinois. In September, 1980, he entered The Graduate School of The University of Texas at Austin.

Permanent address: 125 We Go Trail
Mt. Prospect, Illinois

This thesis was typed by Tina Robinson.